CHAIR FOR INDUSTRIAL ENVIRONMENTAL PROTECTION AND PROCESS TECHNOLOGY
Montan University of Leoben
Franz-Josef-Straße 18
vtiu.unileoben.ac.at
A-8700 Leoben

AUSTRIAN MARSHALL PLAN FOUNDATION
VIENNA | AUSTRIA

Marshall Plan Scholarship Research Report

Degradation of model reactants as a chemical probe for cavitation induced hot spots in water treatment devices

in cooperation with

arisdyne systems
The Power of Cavitation

Submitted by:
Daniel Vallant
0935407

Supervisors:
Ao. Prof. DI Dr. Christian Weiß
MSc Joe Chiarelli

Leoben, 1/27/16

EIDESSTATTLICHE ERKLÄRUNG

Ich erkläre an Eides statt, dass ich die vorliegende Masterarbeit/Bachelorarbeit selbständig und ohne fremde Hilfe verfasst, andere als die angegebenen Quellen und Hilfsmittel nicht benutzt und die den benutzten Quellen wörtlich und inhaltlich entnommenen Stellen als solche erkenntlich gemacht habe.

AFFIDAVIT

I declare in lieu of oath, that I wrote this thesis and performed the associated research myself, using only literature cited in this volume.

1/27/16

Daniel Vallant

ACKNOWLEDGMENT

Firstly, I would like to express my sincere gratitude to my advisor Prof. Christian Weiß for the continuous support, for his motivation and immense source of knowledge. His guidance helped me in all the time of research and writing of this thesis.

I would like to express my special appreciation and thanks to Dr. Tzahi Y. Cath, Colorado School of Mines, civil and environmental engineering department for the invitation to work at his department at the Colorado School of Mines, the access to the AQWATEC lab and for comments that greatly improved the manuscript.

My sincere thanks also goes to the team of Arisdyne Systems, especially Dr. Peter Reimers, MSc Joe Chiarelli, Dr. Oleg Kozyuk, Paul Mulhollem and Bill who provided me the opportunity to do this research, and who gave access to the laboratory and research facilities. Without their precious support and sharing their pearls of wisdom during the course of this research, it would have not been possible to conduct this thesis.

Besides my advisor, the team of Arisdyne Systems and the civil and environmental engineering department at MU - Leoben, I would like to thank the Austrian Marshall Plan Foundation for funding my research stay with a scholarship and the Chair for Process Technology and Industrial Environmental Protection for financial support.

Abstract

Degradation of model reactants as a chemical probe for cavitation induced hot spots in water treatment devices

Cavitation is the formation, growth and implosion of vapor bubbles in a liquid medium (Capocelli et al. 2014a, p. 2566) causing localized high temperature (1000 - 10000 K) and pressure (100 - 500 bar) for a few nanoseconds (Suslick 1990). A number of studies show that these so called “hot spots” lead to the generation of free radicals like $\dot{O}H$ and $\dot{H}$. They are produced through the homolytic dissociation of water and used to oxidize complex contaminants in waste water streams (Advanced Oxidation Process (AOP)). This is the point where in this thesis the term cavitation is strictly differentiated from the damaging event of cavitation. Two different kinds of cavitation are considered: The first, hydrodynamic cavitation (HC) is performed with the patented cavitation unit from Arisdyne systems Inc., which is implemented into a closed loop. The second is ultrasonic cavitation (UC) which is realized through an ultrasonic horn. To investigate the degradation and the existence of cavitation induced hot spots, three different model reactants are used for the experiments: The liberation of iodine (Weissler reaction), the oxidation of sulfite to sulfate and the metabolization of PNP (p-nitrophenol). Samples are prepared for photometric measurement (UV/VIS spectrometer) and the performance of the HC loop is compared with the UC setup. The HC is studied over the pressure range 1000 - 15000 psi and the results of all three model reactants demonstrate that an applied pressure of 1000 psi shows the biggest degradation effect. All HC results are compared with the UC under the same operating parameters like temperature and pH. On the one hand the findings of this study indicate the existence of cavitation induced hot spots through HC and on the other hand it provides a possibility to control them. Future investigation will be about the scale-up of the used HC system and if it is suitable for different applications like the cracking of long-chained hydrocarbons in the oil industry or the removal of persistent contaminants in waste water streams.

Kurzfassung

Chemischer Nachweis für durch Kavitation erzeugte Hot Spots in Wasserbehandlungsanlagen durch den Abbau von Modellreaktanten

Unter Kavitation versteht man die Formation, das Wachstum und die Implosion von Dampfblasen in einer Flüssigkeit und die damit verbundenen kurzzeitig (einige Nanosekunden) lokal auftretenden hohen Temperaturen (1000 - 10000 K) und Drücke (100 - 500 bar). Mehrere Studien im industriellen Umweltbereich zeigen, dass es bei diesen sogenannten „Hot Spots“ durch homolytische Dissoziation von Wasser (H_2O) zur Entstehung von freien Radikalen wie z.B. $\dot{O}H$ und $\dot{H}$ kommt, welche für die Reinigung von komplexen und mit herkömmlichen Mitteln schwer behandelbaren Abwässern eingesetzt werden. An dieser Stelle grenzt sich der in dieser Arbeit verwendete Begriff der Kavitation vom Schadensfall ab. Es werden zwei unterschiedliche Arten der Kavitation untersucht: Die hydrodynamische Kavitation (HC) wird durch die patentierte Kavitationseinheit von Arisdyne systems Inc. erzeugt, welche in einem vollkommen geschlossenen Kreislauf implementiert ist. Ultraschall Kavitation (UC) stellt die zweite Art dar und wird durch ein Ultraschallhorn erzeugt. Um die Effekte der Kavitationsarten zu untersuchen, werden drei unterschiedliche Modelreaktanten eingesetzt: Die Freisetzung von Jod (Weissler Reaktion), die Oxidation von Sulfit zu Sulfat und der Abbau von PNP (p-Nitrophenol). Die Proben werden photometrisch ausgewertet (UV/VIS Spektrometer) und die Ergebnisse des HC Kreislaufes mit denen des Ultraschallkavitations - Setups verglichen. Die HC wird in einem Druckbereich von 1000 - 15000 psi untersucht und die Ergebnisse zeigen, dass die Anwendung von 1000 psi die besten Abbauresultate erzielt. Unter gleichen Betriebsparametern wie pH und Temperatur werden die HC Ergebnisse mit den Ergebnissen der UC Tests verglichen. Einerseits deuten die Ergebnisse auf die Existenz der „Hot Spots“ hin und andererseits stellen sie eine Möglichkeit dar, diese kontrolliert einzusetzen. Zukünftige Untersuchungen werden zeigen, wie sich das angewendete System im Zuge eines Upscaling verhält und ob es z.B. für Anwendungen in der Ölindustrie wie das Cracken von langkettigen Kohlenwasserstoffen oder in der Reinigung von persistenten Schadstoffen in Abwasserströmen eingesetzt werden kann.

Content

Page

1 Introduction

The majority of people do not know the term “cavitation” because there are only a few fields that have to deal with that phenomenon. A field maybe nobody will think of the first time, is nature. A crab species called “mantis” uses self - made cavitation to stun their prey (Patek et al. 2004). Engineers who are designing pumps or ship’s propellers know “cavitation” because they want to avoid it at all costs. Bioengineers are using “cavitation” to control for example the growth of algae like M. aeruginosa (Li et al. 2014, p. 247). Generally there are only two points of view, the user wants cavitation or not. The mechanism to create cavitation is basically the same in both cases and is very important for this study.

The cavitational effect includes three steps, the **formation**, **growth** and **implosion** of **vapor bubbles in a liquid medium** (Capocelli et al. 2014a, p. 2566).

The phase change takes place at narrowly constant temperature which is quite the contrary to boiling (d'Agostino, Luca and Salvetti, Maria Vittoria 2007, p. 8).

Generally speaking there are four different types of cavitation based on the mode of its generation. Two modes which are rarely in use are optic cavitation where photons produced by high intensity light (e.g. laser) rupturing the liquid continuum, and particle cavitation where any other type of beam of elementary particles rupturing a liquid (bubble chamber) (Gogate 2002). The two most important forms of cavitation for this study are acoustic and hydrodynamic cavitation. If the cavitational effects are caused by the application of high frequency sound waves (e.g. ultrasound), then it is called acoustic or ultrasonic cavitation. Terms like “Sonochemistry” and “Sonoluminescence” base on this form of cavitation. Different pressures in the liquid stream due to a change in the geometry of the flowing system generates hydrodynamic cavitation (Li et al. 2015, p. 246). More detailed explanations can be found in chapter 3.1 and 3.2.

In both cases the implosion of the bubble creates a so called “hot spot” and products a dramatically increase of temperature and pressure inside the bubble. Early data referring to temperature and pressure is published by Suslick (1990). In his study, hot spots with intense local heating (1000 - 10000 K), high pressures (100 - 5000 bar) and very short lifetimes (few nanoseconds) are found. Other pertinent literature reports temperatures up to 14000 K and pressures between 10 and 25 kbar (14500 and 36000 psi), depending on the radius of the bubble (Leighton (1995)). The values of these parameters are responsible for the use of cavitation to enhance or boost chemical reactions.

This study strictly differentiated itself from the damaging event of cavitation.

Much research ((Capocelli et al., p. 2569), (Kalumuck)) in recent years has focused on waste water treatment using cavitation to remove different contaminants from the water. Numerous experiments have established that this energy is adequate to generate oxidizing species in form of radicals. A current focus in this field is to investigate the impact of this oxidizing species on chemical reactions and the upscaling to industrial applications.

2 Task

2.1 Actual technological issues

“Arisdyne systems Inc.”, a company from Ohio, Cleveland, is specialized in using cavitation for industrial applications. They successfully established their technology in several fields, like ethanol and biodiesel production, degumming of crude vegetable oil and waste water treatment. Several patents make it possible to control cavitation and avoid erosion. One very important property of cavitation itself, beside the generated energy, is the mixing and particle homogenization effect. Shear forces, created by cavitation, are able to disrupt agglomerates or lyse cells. In case of ethanol and biodiesel production, smaller particles mean higher surface areas. Through the application of controlled cavitation, the particle size distribution shows that particles with lager diameters gets smaller and small particles stay at the same size. In case of biodiesel production, it is possible to reduce the catalyst consumption by 25% and decrease the retention time which increases the capacity. Crude vegetable oils contain phosphatides or so-called gums and they have to be removed during the refining process. These contaminants lead to losses in oil yield and a high demand of acid and alkali. Arisdyne is using a compressing - decompressing jet atomization process (see also 3.2) which allows a reduction in chemical consumption and oil yield loss. A lot of customers have realized that this novel side-effect of cavitation works better than a stirrer for the applications mentioned above (Arisdyne Systems 2015).

Mixing, particle homogenization and atomization are not the only effects connected to cavitation. Evidence that the patented technology from Arisdyne is able to create the mentioned cavitation induced hot spots is non-existent. To get a foot into the waste water treatment field it is very important to prove that the application is able to boost chemical reactions. The generated oxidizing species should be able to treat waste water (e.g. pharmaceutical waste water). Another important aim of Arisdyne for the future is to cooperate with oil companies. An undisputed fact is that every oil distillation column produces oil residues which are collected as the bottom product. This oil residue is used for bitumen, asphalt or roofing. Further processing to increase the valuable output of crude oil like petrol for vehicles, jet fuel or diesel fuel, is beyond the economical limit of currently use technologies. A concept to be proven in the future is that the cavitation induced hot spots are strong enough to crack the long chained hydrocarbons in the residual to maximize the output stream of valuable products.

2.2 Objective

In the present study fundamental research plays an important role. To probe the existence of cavitation induced hot spots generated with the cavitation unit from Arisdyne[1], chemical model reactions are required. A model reaction has a simple and well known reaction mechanism and experimental data is available from previous work. The aim of this thesis is to prove the existence of controlled cavitation induced hot spots by using three model reactants.[2] For each model different concentrations of the contaminant in a defined volume are used. These model reactants are investigated under acoustic cavitation and hydrodynamic cavitation conditions.[3] The changing of several parameters like temperature, pressure, concentration and pH leads to a wide range of covered reaction conditions.

The thesis is organized as follows: Chapter 3 deals with the theory of the different forms of cavitation and introduces the 3 model reactants. The Methodology in chapter 4 provides specific and precise details about the model reactants and their reactions, used materials and instruments. Further it includes the basic calculation methods, result quantification and it describes and justifies the choices made referring to several parameters. Chapter 5 deals with the calculation of the results and the chemical explanations of specific results of every single model reaction. Every calculation is described on the basis of one randomly chosen input data set. At the end of each section, possible implications and open issues are discussed. Chapter 6 ends the thesis with a conclusion of the whole study. It analyses the achievement, lines out the limitations and gives an outlook for future work and applications.

[1] see Cavitation unit and retention time in 3.2.1 for more details

[2] see chapter 3 for more details

[3] see chapter 4 for the experimental approach

3 Theory

This thesis distinguishes two types of cavitation: Acoustic and hydrodynamic cavitation. In the following chapters (4-6) the acoustic cavitation is called ultrasonic cavitation (abbreviation UC) and the abbreviation of hydrodynamic cavitation is HC. It should be noticed that the reactor design, geometry of the cavitation unit and the kind of pollutant are very important parameters for the performance of cavitation (Gogate (2002, p. 335), Gogate et al. (2001, p. 2526), Gogate et al. (2011, p. 1066), Suslick, M. mdleleni, Millan and T. Ries, Jeffrey (1997, p. 9303). Kumar, P.S. and Pandit, A.B. (1999, p. 1017), Chand et al. (2007, p. 357)).

3.1 Ultrasonic cavitation, sonochemistry and sonoluminescence

Through the study of sonochemistry, scientists try to understand the effect of ultrasound in forming UC in liquids. As a result of ultrasound induced cavitation the chemical activity in the solution is increased. This proves the fact that the chemical effects of ultrasound do not come from a direct interaction with molecular species. The bubble collapse during cavitation is able to concentrate the diffuse energy of sound to a very small volume element in the liquid. This phenomenon is responsible for effects like sonochemistry and sonoluminescence (Suslick 1990). That means that it is not the ultrasound that changes the chemical activity in the solution, however, it is responsible for the creation, growth and implosion of the bubbles. The local energy release during bubble collapse changes the chemical properties in the solution. Another very interesting effect is sonoluminescence whereby a liquid excited by sound, emits short flashes of light from imploding bubbles. The effect can occur when a sound wave with sufficient intensity induces a gaseous cavity within a liquid to collapse quickly.

3.1.1 Formation of cavities through ultrasound (Suslick 1990)

The nucleation process for every cavitation event is the formation of cavities in liquids. The acoustic expansion wave has a negative and positive pressure half and both are combined to one acoustic cycle. Under typical laboratory conditions the theoretical tensile strength of a pure liquid is too high to simply form cavities from the negative pressure of an acoustic expansion wave. Weak points in the liquid are fundamental for the nucleation of bubbles, such as gas-filled crevices in suspended particles or from already existing microbubbles from prior cavitation events.

There are several different mechanisms for the bubble growth in an irradiated liquid. A small cavity or bubble may grow rapidly through inertial effects if high - intensity ultrasound is applied. If the rate of expansion is sufficiently fast, the bubble will not have enough time to recompress during the positive-pressure half of the acoustic cycle. Slow cavity growth can also occur at lower acoustic intensities and is called rectified diffusion. This kind of diffusion bases on the fact that the cavity's surface area is slightly greater during expansion than during compression and therefore, growth processes are slightly faster than shrinking processes. Simply said, over many acoustic cycles, the cavity will grow. If the cavity or bubble reaches a specific size (resonant size) it is able to efficiently absorb energy from the

sound field (acoustic wave). This size depends on the frequency of the ultrasound. In this study a frequency of 20 kHz is used and the critical size of the bubble is 170 µm in diameter. In phase with the sound field, such a cavity is able to grow rapidly in the course of one single expansion cycle. Once the cavity is too big, it can no longer efficiently absorb energy from the sound field and can no longer maintain itself. The cavity implodes as the surrounding liquid rushes in. In the moment of collapse free radicals are formed through the homolytic dissociation of water because of the aforementioned high temperature and pressure conditions. Especially the $\dot{OH}$ - radical is known to be a strongly oxidizing species.

3.2 Hydrodynamic cavitation

d'Agostino, Luca and Salvetti, Maria Vittoria (2007, p. 8) reported that a local pressure drop generated by the flow itself is required to initiate the formation and growth of bubbles. A local pressure drop is for example realized by a venturi nozzle (Figure 1). The transition from a larger to a small and again to a larger pipe diameter leads to a maximum velocity of the liquid flow at the constriction. According to the Bernoulli equation, the pressure is minimized at the throat and the chance to create cavitation is maximized, when the throat pressure is smaller than the vapor pressure of the liquid.

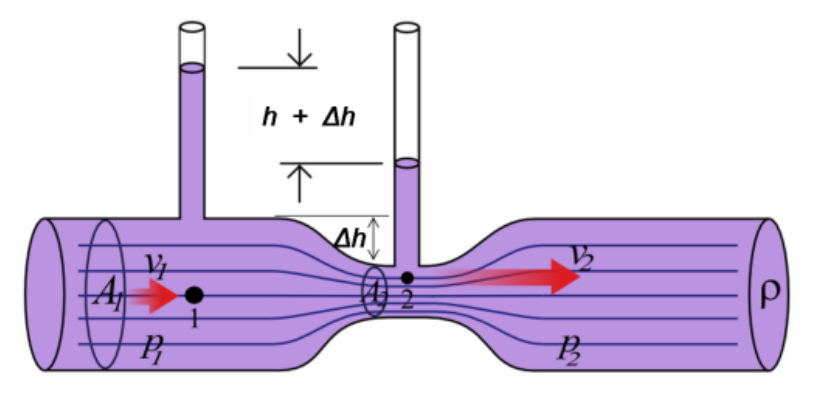

Figure 1: venturi effect[4]

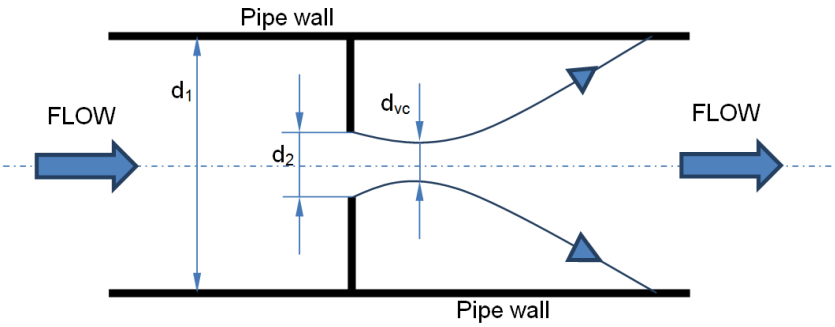

Figure 2: orifice - d_1 is the pipe diameter, d_2 the opening size and d_{vc} vena contracta diameter

[4] Wikipedia contributors. Venturi effect [Internet]. Wikipedia, The Free Encyclopedia; 2016 Jan 4, 16:56 UTC [cited 2016 Jan 9]. Available from: https://en.wikipedia.org/w/index.php?title=Venturi_effect&oldid=698201539.

Very important examples for this study are orifices (Figure 2). Through enough throttling the pressure around the area of *vena contracta* can fall below the threshold pressure of cavitation. When this is the case, an uncountable number of cavities are generated. The threshold pressure is the required pressure to create cavitation and is normally defined as the vapor pressure of the medium at the operating temperature. After that local pressure drop the liquid jet expands and the pressure recovers which leads to the implosion or collapse of the cavities. (Gogate et al. 2001). As reported for the UC, free radicals (oxidizing species) are formed at the time of implosion. In an earlier work, Kumar, P.S. and Pandit, A.B. (1999) reported two different applications referring to different inlet pressure: High inlet and recovered downstream pressure of the liquid through the venturi or orifice can be used to generate cavitation of higher intensity, necessary for influencing chemical reactions. Low inlet and recovered downstream pressure can be used to generate cavitation of low intensity required for applications, such as the removal of blue-green algae reported by Wu et al. (2012, p. 152).

3.2.1 Cavitation unit and retention time

As mentioned in the objective in 2.2, Arisdyne is using its own developed and patented cavitation unit. The company provides great flexibility by offering a range of different cavitation units in their product portfolio for miscellaneous applications. These cavitation or mixing units are following the principle technology of flow through orifices.

3.2.1.1 Orifice dimensions

Number 5a and 5b in Figure 3 represent the mentioned units. These units are available in different sizes. In this study size 6/8 and 8/12 are used. The dimensions are the opening sizes in thousandths of an inch for one chamber (1 inch = 25.4 mm). That means unit 5a has an opening size of for example 6 thousandths and unit 5b of 8 thousandths of an inch. A 12 means twelve thousands of an inch.

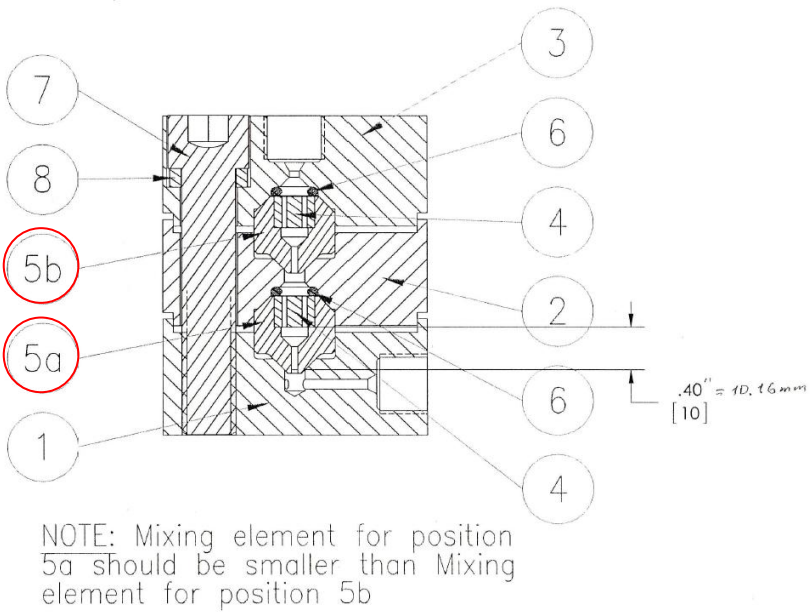

Figure 3: Original drawing of one cavitation chamber with two cavitation units. Each chamber consists of two mixing units (5a and 5b) and two baffles (4) with four channels.

3.2.1.2 Retention time

The retention time describes the time the solution is treated with HC. Compared to UC, where the solution is treated under static conditions (without any macro - motion of the fluid except the motion through the induced ultrasound waves) the fluid is in constant motion in the HC system because it is pumped through the loop. With the HC system the cavitation is only created in a very specific location in the cavitation unit. In case of the UC system the effective volume is limited by the surface area of the transducer which creates the ultrasound (ultrasonic horn, ultrasonic flow cell and other different types of reactors (Gogate et al. 2011, p. 1067)) and the fluid volume in the boundary layer at the transducer surface is always much bigger in comparison with the effective fluid volume in the HC system.

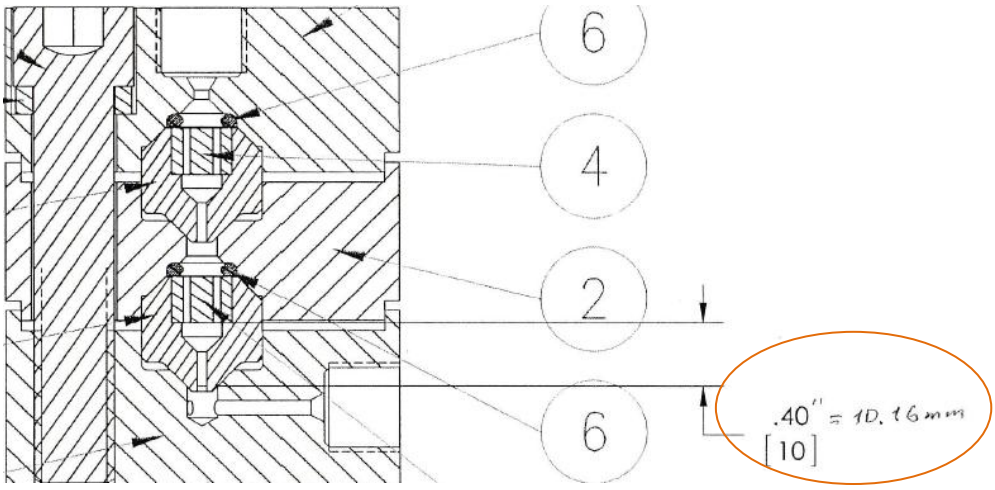

Figure 4: The marked value (h = 10.16 mm) indicates the length of the inlet channel

Table 1: calculated reactor volume (Equation 1) and retention time (Equation 2)

orifice dimension	diameter	area	reactor volume	reference pressure	reference pressure	volume flow	volume flow	retention time
thousans of an inch	d	A	VR	p	p	V_point	V_point	τ
-	m	m²	m³	psi	Pa	ml/min	m³/s	s
6	1.5E-04	1.8E-08	1.9E-10	2500	1.7E+07	142	2.4E-06	7.83E-05
				5000	3.4E+07	200.5	3.3E-06	5.55E-05
				10000	6.9E+07	283.5	4.7E-06	3.92E-05
				15000	1.0E+08	347.2	5.8E-06	3.20E-05
8	2.0E-04	3.2E-08	3.3E-10	2500	1.7E+07	142	2.4E-06	1.39E-04
				5000	3.4E+07	200.5	3.3E-06	9.86E-05
				10000	6.9E+07	283.5	4.7E-06	6.97E-05
				15000	1.0E+08	347.2	5.8E-06	5.69E-05
12	3.0E-04	7.3E-08	7.4E-10	1000	6.9E+06	167.3	2.8E-06	2.66E-04
				2500	1.7E+07	264.2	4.4E-06	1.68E-04

It should be noted that the values for the volume flow in Table 1 and Table 3 are for continuous flow and measured with new cavitation units (courtesy of Arisdyne). In this study a plunger pump[5] is used which means a pounding delivery of the liquid. These values can be used because the volume flow inside the cavitation chamber is the same in both cases. The same argument holds for the calculation of the cavitation number in 3.2.2.2. Table 1 presents the retention time for the HC system for one cavitation unit. According to Figure 3 and Figure 4 two units are used for the study, which results in a total retention time of $2.18 * 10^{-4}\ s$ for each pass and the stated example where a 6/8 chamber is used.

$$V_R = \frac{d^2 * \pi}{4} * h = \frac{(1.5 * 10^{-4}\ m)^2 * \pi}{4} * 1.02 * 10^{-2}\ m = 1.9 * 10^{-10}\ m^3 \qquad \text{Equation 1}$$

$$Retention\ time\ \tau = \frac{V_R}{\dot{V}} = \frac{1.9 * 10^{-10}\ m^3}{2.4 * 10^{-6}\ \frac{m^3}{s}} = 7.83 * 10^{-5}\ s \qquad \text{Equation 2}$$

On the whole the results show that the retention time is extremely short compared to the retention time in the UC system.

3.2.2 Cavitation number

3.2.2.1 Theory

The amount or intensity of cavitation is characterized by a non dimensional parameter, the cavitation number σ_c, defined by:

$$\sigma_c = \frac{(p_{ref} - p_v)}{(\frac{1}{2} * \rho * {v_{th}}^2)} \qquad \text{Equation 3}$$

[5] see Figure 10 in 4.3.2.1

In this expression, p_{ref} is a reference pressure taken at a given point in the liquid flow, v_{th} is a characteristic flow velocity, p_v is the vapor pressure and ρ the density of the liquid. The reference pressure and the flow velocity need to be precisely specified for each practical situation. Density and vapor pressure are temperature dependant parameters. Large values of the cavitation number imply a non cavitating flow. This is easy to understand because high reference pressures usually correspond to large values of the cavitation number but this is not the dominant parameter if the flow velocity is high enough. In the first case, it can be expected that the pressure will be everywhere above the vapor pressure of the liquid and the flow will remain free of cavitation. This number is a relevant scaling parameter only for cavitating flows and it measures the global extent of cavitation. Cavitation generally appears for a critical value of the cavitation number known as the incipient or beginning cavitation number σ_i. The point of cavitation inception can be reached either by decreasing the reference pressure or increasing the flow velocity which leads in both cases to smaller cavitation numbers. Any further decrease will lead to an additional development of cavitation. Increasing the reference pressure afterwards means that cavitation disappears for a critical cavitation number somewhat higher than σ_i. (d'Agostino, Luca and Salvetti, Maria Vittoria 2007, p. 9)

3.2.2.2 Calculation

One example (orifice dimension 6, pressure 2500 psi and temperature 20°C) for the calculation of the cavitation number is shown. The equations and explanations can be found below Table 3.

There are 4 assumptions for the calculation of the cavitation number:

1. constant volume flow through the mixing unit at the same point (Figure 5)
2. The data for vapor pressure and density are for water because of the low concentration of the model reactants in the initial solution (Table 2).

Table 2: vapor pressure[6] and density[7] of water at different temperatures

water temperature	vapor pressure	density water
T_w	p_v	ρ
°C	Pa	kg/m³
5	866.3	999.97
10	1221.2	999.70
20	2329.8	998.21
36	5927.2	993.69
42	8180.5	991.44
65	24949.1	980.55

3. point where hydrodynamic cavitation occurs (Figure 5)
4. pipe resistances are not considered

[6] http://www.endmemo.com/chem/vaporpressurewater.php; requested 1/5/2016

[7] http://www.internetchemie.info/chemiewiki/index.php?title=Wasser-Dichtetabelle; requested 1/5/2016

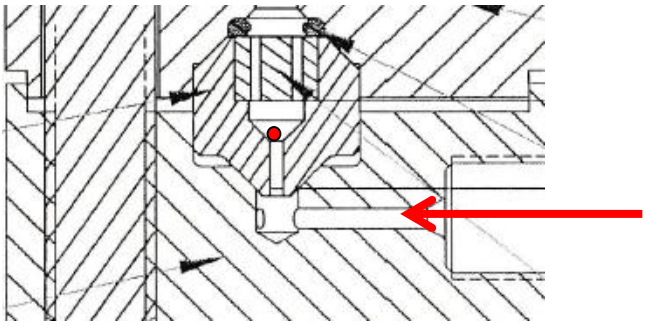

Figure 5: The red circle presents the relevant point for the calculation after the throat of the orifice where the smaller diameter changes to a bigger diameter. The red arrow shows the direction of flow.[8]

Table 3: calculated outflow velocity from the throat

orifice dimension	diameter	area	reference pressure	reference pressure	volume flow	volume flow	velocity
thousans of an inch	d	A	p	p	V_point	V_point	vth
-	m	m²	psi	Pa	ml/min	m³/s	m/s
6	1.5E-04	1.8E-08	2500	1.7E+07	142	2.4E-06	129.7
			5000	3.4E+07	200.5	3.3E-06	183.2
			10000	6.9E+07	283.5	4.7E-06	259.0
			15000	1.0E+08	347.2	5.8E-06	317.2
8	2.0E-04	3.2E-08	2500	1.7E+07	142	2.4E-06	73.0
			5000	3.4E+07	200.5	3.3E-06	103.0
			10000	6.9E+07	283.5	4.7E-06	145.7
			15000	1.0E+08	347.2	5.8E-06	178.4
12	3.0E-04	7.3E-08	1000	6.9E+06	167.3	2.8E-06	38.2
			2500	1.7E+07	264.2	4.4E-06	60.3

To calculate the flow velocity, the continuity equation (Equation 4) is transformed into Equation 6 ($\dot{V}$ is the volume flow, A is the cross-sectional area and v_{th} the flow velocity). The area of the throat is calculated with Equation 5 (d is the opening diameter). This calculation is made for each orifice dimension for the full range of the applied pressures (Table 3).

$$Continuity\ equation: \dot{V} = A * v_{th} \qquad \text{Equation 4}$$

$$A = \frac{d^2 * \pi}{4} = \frac{(1.5 * 10^{-4}\ m)^2 * \pi}{4} = 1.8 * 10^{-8}\ m^2 \qquad \text{Equation 5}$$

$$w = \frac{\dot{V}}{A} = \frac{2.4 * 10^{-6}\ \frac{m^3}{s}}{1.8 * 10^{-8}\ m^2} = 129.7\ \frac{m}{s} \qquad \text{Equation 6}$$

The experimental setup, the geometry of the cavitation unit and the high inlet pressures indicate the existence of a critical pressure and consequential a critical mass flux. For the calculation of the critical mass flux the model from the VDI Heat Atlas (2010, p. 1177) is

[8] For details about the cavitation unit from Arisdyne see Cavitation unit and retention time in 3.2.1

used. The cavitation number is calculated by Equation 7, whereas p_{ref} is the critical pressure, v_{th} the velocity out of the transformation of the critical mass flux and p_v the vapor pressure of water at 1000 psi.

$$\sigma_c = \frac{(p_{ref} - p_v)}{(\frac{1}{2} * \rho * {v_{th}}^2)} = \frac{(7.4 * 10^5 - 2329.8)\ Pa}{(\frac{1}{2} * 1001.29\ \frac{kg}{m^3} * (84.73\ \frac{m}{s})^2)} = 0.2046 \qquad \text{Equation 7}$$

As mentioned in 3.2.2.1, cavitation performance increases if the value for the cavitation number decreases. A cavitation number smaller than one means that HC occurs (Kalumuck 2000). The result indicates that the used cavitation unit reaches small cavitation numbers and the number increases by increasing the temperature and decreases by increasing the reference pressure. It should be noted that the value changes only slightly in both directions. The calculated velocities in Table 3 are theoretically true but the mass flow is limited and consequently the velocity changes. The trend of the cavitation number indicates that the increased inlet pressure has practically no influence on the cavitation performance. Generally speaking, the investigated cavitation unit creates cavitation in all applied settings.

3.2.3 High pressure and low pressure

In case of HC the operating parameter inlet pressure is very important. This is the pressure the liquid medium is pumped into the cavitation chamber and through the cavitation unit. Referring to the continuity equation (Equation 4) a pressure increase at the inlet as well as decreasing the cross-sectional diameter leads to a flow velocity increase. High values for the flow velocity results in a turbulence regime after the orifice at the point of *vena contracta* (Figure 2). To define the turbulence regime the dimensionless Reynolds number is needed (Equation 8). Re_{crit} in Equation 9 shows the transition range where the laminar flow changes to the turbulence. It turns out that cavitation only occurs in the turbulent flow regime.

$$Re = \frac{w * d * \rho}{\eta} \qquad \text{Equation 8}$$

$$Re_{crit} \approx 2400 \mp 10^9 \qquad \text{Equation 9}$$

An empirical look at cavitation shows that high inlet pressure and flow rates lower the bubble growth, the amount of captured vapor molecules and, as a consequent, the intensity of collapse but increases the number of cavities. The collapse intensity is affected because at higher pressure the flow rate increases, leaving less time for the bubble to grow and generating higher turbulence stresses which act against the expansion of the bubble. The increased number of cavities at higher p_{in} is the opposite of higher specific radical production at lower pressure. The relation between high and low pressure and the cavitation number is given in 3.2.2.1. The study from Capocelli et al. (2014a, p. 2569) introduces a slight dependence of radical production on initial radius of the bubble. In their study they stress that

[9] Avila et al. 2011

there is a strong dependence of the collapse bubble size on the turbulence intensity and, consequently, on p_{in}. The initial size of the bubble is of minor importance because the collapse is controlled by the inlet pressure at a fixed geometry of the bubble.
Higher inlet pressure induces more cavities but less production of radicals. Lower inlet pressure leads to an increased production of free radicals and the number of cavities is smaller, however the bubbles size is bigger (more vapor molecules).

3.3 The energy of cavitation

As mentioned in the Introduction, UC and HC cause high temperature and high pressure. In both cases this energy release is high enough for the dissociation of vapors trapped in the cavitating bubbles (Parag R. Gogate and Abhijeet M. Kabadi (2009)) and can therefore be used to provide extremely reactive species like $OH^{\cdot}$-,$O^{\cdot}$- and $HOO^{\cdot}$- radicals (Suslick 1990, (Saharan et al. 2012, p. 1981)). This finding has been implemented as an Advanced Oxidation Process (AOP) (Capocelli et al. 2014a, p. 2566). AOP can be defined as the process that involves formation and following attack of free radicals, which are capable of oxidizing organic compounds and attacking inorganic molecules. Beside cavitation, Saharan et al. (2012, p. 1981) reports alternative types of AOPs like photocatalytic oxidation (using UV light/sunlight in the presence of semiconductor catalyst), Fenton chemistry (using reaction between Fe - ions and hydrogen peroxide), and chemical oxidation (use of ozone and hydrogen peroxide).

3.4 Comparison between acoustic and hydrodynamic cavitation

The main differences between UC and HC referring to generation and flow mechanism are explained in 3.1 and 3.2. From the energy efficiency point of view, HC represents a cheaper and more energy efficient method for generating cavitation than UC (Capocelli et al. 2014b, p. 17). Kalumuck (2000, p. 466) and Gogate (2002) reports that the equipment used for generating HC is more simple, flexible and the maintenance effort of such systems (loop and reactor) is very low. Pertinent literature also outlines the good scale - up properties from HC contrary to the corresponding problems with UC (Gogate et al. 2011, p. 1067).

3.5 Three model reactants

This chapter is about the choice, applicability and limitations of the three model reactants and associated reactions used in this study[10].

3.5.1 Inorganic reactions

One inorganic model reactant that is suitable for this study is used by Gogate et al. (2001). In their study they investigate the *Weissler*[11] reaction to prove cavitation. Free radicals, formed under cavitating conditions, attack the KI (Potassium Iodide) and liberate iodine. The

[10] chemism of the model reactions is explained in detail in chapter 4

[11] Named after A. Weissler, H.W. Cooper, S. Snyder, J. Am. Chem. Soc. 72 (1950) 1769–1775.

liberated iodine reacts, after a series of intermediate steps, to the tri-iodide complex I_3^-. Morison, K. and Hutchinson, C. (2009, p. 176) established limitations of the Weissler reaction referring to the comparability of UC and HC. They argue that this reaction is inappropriate because the I_3^- - complex may form during hydrodynamic flow, with and without cavitation. The potential limitations of this reaction led to the conclusion that a second inorganic model reaction is required. From a search for a suitable reaction system the oxidation from sulfite to sulfate as a model reaction turned out as a candidate. Free radicals, again formed under cavitating conditions, form hydrogen peroxide (H_2O_2) which is an oxidizing agent capable oxidize sulfite to sulfate. This expected theoretical mechanism needs evidence. To the knowledge of the author of this thesis, currently no reference exists that describes the oxidation of sulfite forced by UC or HC.

3.5.2 Organic reactions

Beside the inorganic reactions it is very important to investigate the behavior of organic reactions under cavitating conditions. The third model reactant for this thesis is converted by an organic reaction and has been chosen from several authors like Capocelli et al. (2014a, p. 2568) and Kalumuck (2000, p. 467). They used the degradation of PNP (Para Nitrophenol) or 4-Nitrophenol for their study. In this case the free radicals form an oxidizing agent and this agent oxidizes the PNP to several products which are less harmful compared to the reactant.

4 Methodology

The purpose of this work is to prove the existence of cavitational hot spots. HC and UC are tested by the performance of three different model reactions.

4.1 Chemical model reactions

A radical is an atom, ion or molecule that has unpaired valency electrons. Equation 10 shows the decomposition of water into hydrogen and hydroxyl radicals. Through a process called homolysis, which requires a certain amount of energy (homolytic bond dissociation energies), covalent bonds break. The break of the covalent bond can be realized by any process that puts enough energy into the water molecule (parent molecule). Previous work, for example from Kalumuck (2000), shows that the energy created by cavitation is enough to form free radicals.

$$H_2O \rightarrow \dot{H} + \dot{OH} \qquad \text{Equation 10}$$

The majority of the radicals are highly reactive towards themselves or other substances. Hydrogen peroxide, which is a strong oxidizing agent, is formed by hydroxyl radicals (Equation 11).

$$\dot{OH} + \dot{OH} \rightarrow H_2O_2 \qquad \text{Equation 11}$$

Because of their high reactivity the free radicals attack other substances. This form of “attack” is used in all three model reactions used in this thesis.

4.1.1 Inorganic reactions

The fundamental chemism in 4.1 is a central step for the conversion of all model reactants and therefore should be kept in mind as basis for the following sections.

4.1.1.1 Iodine liberation

Equation 12 presents the Weissler reaction which has been used for many years to indicate the presence of oxidizing species.

$$H_2O_2 + 2I^- \rightarrow I_2 + 2OH^- \qquad \text{Equation 12}$$

Alternatively, the free radicals attack the potassium iodide and liberate iodine (Equation 13). The complex I_3^-- is formed after several steps (Equation 14, Equation 15 and Equation 16) and is responsible for the yellow and brown color of the samples. A high concentration of this complex is associated with a high intensity of the brown color in the solution.

$$\dot{OH} + I^- \rightarrow OH^- + I \qquad \text{Equation 13}$$

$$I + I^- \rightarrow OH^- + I_2^- \qquad \text{Equation 14}$$

$$2I_2^- \rightarrow I_2 + 2I^- \qquad \text{Equation 15}$$

$I_2 + I^- \rightarrow I_3^-$ Equation 16

When starch (Table 5) is added to the solution, a blue colored complex is formed. This blue color makes a photometric measurement[12] possible for concentrations as low as 2×10^{-5} mole/l at 20°C.[13] The mechanism of this reaction is not fully clarified, but scientists think that the iodine (I_3^- and I_5^- ions) fit inside the coils of amylose. The charge transfers between the iodine and the starch, and the level of energy spacings in the resulting complex, correspond to the absorption spectrum in the visible light region.

4.1.1.2 Sulfite oxidation

Hydrogen peroxide reacts with the sulfite and oxidizes it to sulfate (Equation 17). This model reaction should prove the existence of cavitation induces hot spots generated in the cavitation unit.

$SO_3^{2-} + H_2O_2 \rightarrow SO_4^{2-} + H_2O$ Equation 17

The necessary reactant for the oxidation from sulfite to sulfate is an oxidation agent like hydrogen peroxide or oxygen[14]. Air consists of 21 % atmospheric oxygen. This oxygen has an impact on the reaction and accelerates the oxidation in an uncontrolled way. To avoid the contact, the whole process must be purged with an inert gas, for example nitrogen[15].

4.1.2 Organic reaction

4.1.2.1 Para - Nitrophenol

Reaction mechanism and removal pathway of PNP. The advanced oxidation process (AOP) with pseudo-first order kinetics works better in an acidic environment but ions like $\boldsymbol{HCO_3^-}$, $\boldsymbol{NO_3^-}$ and $\boldsymbol{Cl^-}$ slow down the degradation. Intermediate products are hydroquinone, 1,2,4 - trihydroxybenzene, 4-nitropyrogallol and 4 - nitrocatechol. (Zhang et al. (2003, p. 788)). Two different possible ways are proposed by Zhang et al. (2003, p. 793) where $\boldsymbol{\dot{O}H}$ radicals attack different positions in the benzene ring to form the mentioned hydroxylated compounds of PNP. One path describes a forming of molecules with no nitrogen ($\boldsymbol{NO_2}$- release through the free radical attack). The second one leads to small molecules which contain nitrogen. In both ways the PNP is subsequently oxidized by ring cleavage to yield compounds with and without nitrogen. This model reaction should again prove the existence of cavitation induced hot spots and the ability of the used system to remove organic contaminants from water.

[12] see chapter 4.2 for analytical procedure

[13] Wikipedia contributors. Iodine test [Internet]. Wikipedia, The Free Encyclopedia; 2015 Dec 2, 16:35 UTC [cited 2016 Jan 9]. Available from: https://en.wikipedia.org/w/index.php?title=Iodine_test&oldid=693443633.

[14] It should be noticed that a free radical like $\dot{H}$ or $\dot{OH}$ is completely different compared to the cation H^+ or anion OH^-. For example is the OH^- ion not a free radical because the unpaired electron is resolved by the addition of an electron.

[15] see chapter 4.3 for experimental setup

Handling and application of PNP. PNP normally occurs as a yellow powder and is a intermediate in the synthesis of paracetamol which is used in medication to reduce fever (Ellis 2002). This medication respectively the intermediates, get into the water circuit through the metabolism and finally excretion. PNP irritates the eyes, skin, and respiratory tract. It may also cause inflammation of those parts. It has a delayed interaction with blood and forms methaemoglobin which is responsible for methemoglobinemia, potentially causing cyanosis, confusion, and unconsciousness (Agency for Toxic Substances and Disease Registry U.S. Public Health Service 1992). As a solution it is used as a pH indicator. In a neutral state the solution is pale yellow and the intensity increases by increasing the pH. Under acidic conditions the solution turns into water clear appearance.

4.2 Analytical procedure

A calibration chart is required for each model reaction to calculate the concentration of the contaminant after HC and UC. The calibration charts base on the photometric measurement, realized by a UV/VIS spectrometer at different wavelengths for different contaminants. The calibration was established at Colorado School of Mines (Golden, Colorado, USA), Department for Civil- and Environmental Engineering (CEE), Coolbaugh Hall, AQWATEC[16] lab number 323. Table 4 shows the used instruments and lab equipment. The weighting is realized through a scale with high accuracy. Weighting papers and ships are used to put the chemicals into the beaker. An electronic digital pipette from RAININ is used for the small volumes from 0.01 to 4 ml. The manual pipette from HACH is used for volumes up to 10 ml. The beakers and any other glassware are covered with a stopper or PARAFILM to avoid contamination through the air. It should be noted that the samples from Arisdyne are mailed from Cleveland, Ohio to the CEE department.

Table 4: instruments and lab equipment for all three model reactants with manufacturer's data

UV/VIS - Beckman Coulter DU 800 Spectrometer; computer program: DU 800 Spec
Scale - Mettler AE 163 (accuracy of 4 digits after the decimal point)
Electronic digital pipette 1000µl (edp RAININ)
pH meter accumet AB 81209951 (Fisher Scientific) with a VWR probe
Florence flasks 10, 50, 100, 250 ml from PYREX and VWR
Beakers 50, 250, 500 ml from PYREX, VWR and KIMAX
small glassware
Pipette Hach 10 ml - TenSette Pipette
washing bottle
spatula
Bunsen burner
Cuvettes
funnel

[16] http://aqwatec.mines.edu/

weighting paper
DI water creation device Ultrapure (Type1) water from Synergy UV-R (18,2 MΩ.cm 25°C)
PARAFILM

Each model reactant needs special chemicals for the calibration (Table 5). The reason the iodine solution with the expiration date 2000 has though been used needs a more detailed explanation. Oxidizing materials which could have contaminated the solution by mistake could decompose the iodine which is unlikely in relevant amount. A leaking bottle through wrong storage could lead to an evaporation of iodine and is also excluded because of the original sealing of the reagent bottle. The author and the supervisors of this thesis accepted the use of this iodine solution.

Table 5: Specific chemicals for the model reactions

Liberation of iodine	Oxidation of sulfite	Degradation of PNP
Iodine solution 0.2 N (0.1 mole/l) Fisher Scientific SI106-1 UN2920 (Expiration date 2000)	DTNB (Ellman's reagent (5,5'-dithiobis-(2-nitrobenzoic acid))	4-Nitrophenol, 98% (SIGMA - ALDRICH, 425753-1KG, CAS 100-02-7)
Starch (potato starch flour from SWAN)	HOAc (acetic anhydride 99 % Aldrich 320102)	Sodium Hydroxide, Pellet (MACRON - Fine Chemicals, 500 g, Batch No: 0000026134)
	Na_2CO_3 (sodium carbonate anhydrous Fisher Scientific S263-3)	
	Na_2SO_3 (Sodium sulfite anhydrous Fisher Scientific S 447-3)	

4.2.1 Calibration method: Liberation of iodine

4.2.1.1 Stock solution from the standard solution

The standard solution with a concentration of $0.1\ \frac{mole}{l}$ is used to prepare a stock solution. 3.94 ml (Equation 18 and Equation 19) from the standard solution are pipetted into a 100 ml flask and filled up with DI water to generate the stock solution with $\frac{100\ mg}{100\ ml}$.

$$C_{standard} = MW_{I_2} * C_{I_2} = 253.81\ \frac{g}{mole} * 0.1\ \frac{mole}{l} = 25.38\ \frac{g}{l} \qquad \text{Equation 18}$$

MW_{I_2} is the molar weight of iodine and c_{I_2} is the given concentration from the manufacturer.

$$V_{standard} = c_{wanted} * V_{wanted} * \frac{1}{C_{standard}} = \frac{100\ mg}{100\ ml} * 100\ ml * \frac{1000\ ml}{25380.9\ mg} = 3.94\ ml \qquad \text{Equation 19}$$

$c_{standard}$ is the calculated standard concentration from Equation 18, $V_{standard}$ the necessary volume, c_{wanted} the defined concentration and V_{wanted} the wanted amount of the standard solution. To get a solution with 1 $\frac{mg}{l}$, 10 µl of the stock solution are pipetted into a 10 ml flask

and filled up with DI water. This procedure works up to $1000\ \frac{mg}{l}$, where $10000\ \mu l$ are pipetted into a 10 ml flask.

4.2.1.2 Preparation of solutions for the calibration

For the analysis of the samples 10 ml of each solution is pipetted into small glassware (approx. 50 ml). To use the UV/VIS for the analysis it is necessary to add 4 ml of starch solution to each 10 ml sample[17]. The starch solution with a concentration of $\frac{1\ g}{100\ ml}$ is boiled for approx. 15 minutes on a hot plate (Gogate et al. 2001, p. 2528). A filtration of the jelly and milky looking solution is necessary. After pipetting the starch solution to the samples the solution changes its color from copper brown to blue or purple. The intensity depends on the concentration. The last step is to fill it into the cuvette. The cuvette is the same for every test. After every test the cuvette is cleaned with two or three rinses of DI water. It is very important to keep the cuvette clean and not touch it without gloves.

4.2.1.3 Measuring with the UV/VIS

For this calibration 10 solutions (Table 6) with different concentrations plus one blank (starch solution) are measured at a wavelength of 353 nm. The results are shown in Table 6 and the calibration chart in Figure 6.

Table 6: liberation of iodine: concentration and extinction of the calibration solutions

concentration	extinction
mg/l	-
50	0.3573
45	0.3379
40	0.306
35	0.2854
30	0.2346
25	0.1908
20	0.181
15	0.1698
10	0.1505
5	0.1393
0	0.127

[17] see 4.1.1.1 for more details about starch chemistry

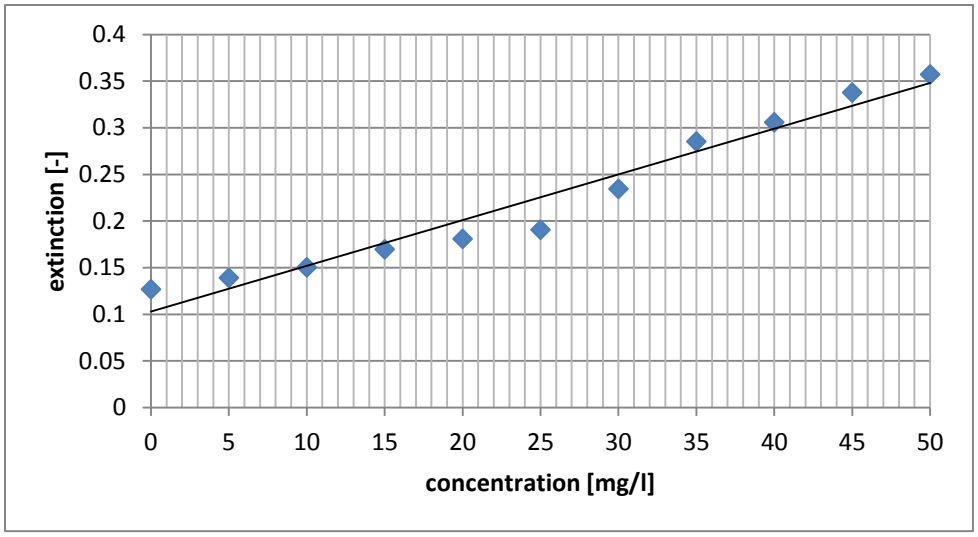

Figure 6: liberation of iodine: calibration chart

A linear regression (Equation 20) with a correlation coefficient (Equation 21) is made.

$$y = kx + d = 0.0049 * x + 0.1028$$ Equation 20

$$R^2 = 0.9557$$ Equation 21

4.2.1.4 Measuring method for samples

For the analysis of the samples 10 ml of each solution is pipetted into small glassware. To use the UV/VIS for the analysis it is necessary to add 4 ml of starch solution to each 10 ml sample. The rest of the procedure is the same as explained in 4.2.1.2

$$\frac{y-d}{k} = x \rightarrow C_{hc} = \frac{0.3573 - 0.1028}{0.0049} = 51.94\ \frac{mg}{l}$$ Equation 22

Equation 22 where y is the extinction, is used to calculate the concentration x of the iodine complex I_3^- of the samples. The samples from Arisdyne are measured the exact same way.

4.2.2 Calibration method: Oxidation of sulfite

4.2.2.1 Acetate - puffer pH 6

7 ml of 99 % $HOAc$ are pipetted and 5.3 g of Na_2CO_3 are weighted into a 500 ml beaker and filled up with DI water. The filling with DI water should be done under the airflow because of the exothermic reaction of Na_2CO_3 with H_2O. Probably some more of the Na_2CO_3 is needed to get a pH of 6. The pH of 6 is measured by an electronic pH meter.

4.2.2.2 DTNB - Solution 10^{-3} mole/l

99 mg of the DTNB powder are weighted into a 250 ml flask and then 8 ml of the acetate puffer is added. The function of the puffer is to dissolve the DTNB. At first, the flask is not completely filled up to the mark with DI water because swinging of it leads to an acceleration of the dissolution. If there is no solid particle left in the solution the flask is filled up to the mark with DI water.

4.2.2.3 Preparation of samples

2 ml of the DTNB solution and 4 ml of the acetate puffer are pipetted into small glassware (20 ml) for each calibration sample.

4.2.2.4 Preparation of solutions for the calibration

Table 7 shows the chosen target concentrations for the calibration and the associated extinction. For example the solution with a concentration of 35 mmole/l, is prepared through weighing 1.10285 g of Na_2SO_3 (Equation 23) into a 250 ml flask.

$$m_{Na_2SO_3} = c_{SO_3^{2-}} * MW_{Na_2SO_3} * V$$
$$= 35 * 10^{-3} \frac{mole}{l} * 126.04 \frac{g}{mole} * 0.25l$$
$$= 1.10285\, g = 1102.85\, mg$$

Equation 23

The wanted volume of the solution V multiplied with the molar weight of sodium sulfite $MW_{Na_2SO_3}$ and the wanted sulfite concentration $c_{SO_3^{2-}}$, results in the weight of sample taken $m_{Na_2SO_3}$.

After putting the powder with a funnel carefully into the flask, the flask is filled up to the mark with DI water after a complete dissolution. It is the same method and calculation for every other concentration in Table 7. To minimize the exposure time to the atmospheric oxygen, the samples are prepared previously (see 4.2.2.3). 10 µl of each sample to measure is pipetted into one of the small glassware. At this point, the sulfite is bound as a complex and there is no further oxidation to sulfate. The last step is to fill the light yellow solution into the cuvettes. The cuvette is the same for every test. Previous experiments showed that it is essential to measure the prepared samples right after the filling into the cuvettes. After 2 hours there is a crucial different in the color of the solution. After every test the cuvette is cleaned with two or three rinses of DI water. It is very important to keep the cuvette clean and not touch it without gloves.

4.2.2.5 Measuring with the UV/VIS

For this calibration 4 different solutions plus one blank (acetate puffer and DTNB solution) were measured at a wavelength of 430 nm. The results are shown in Table 7 and the calibration chart in Figure 7.

Table 7: Oxidation of sulfite: concentration and extinction of the calibration solutions

concentration	extinction
mmole/l	-
35	0.9633
30	0.8578
25	0.6596
20	0.5728
0	0.0185

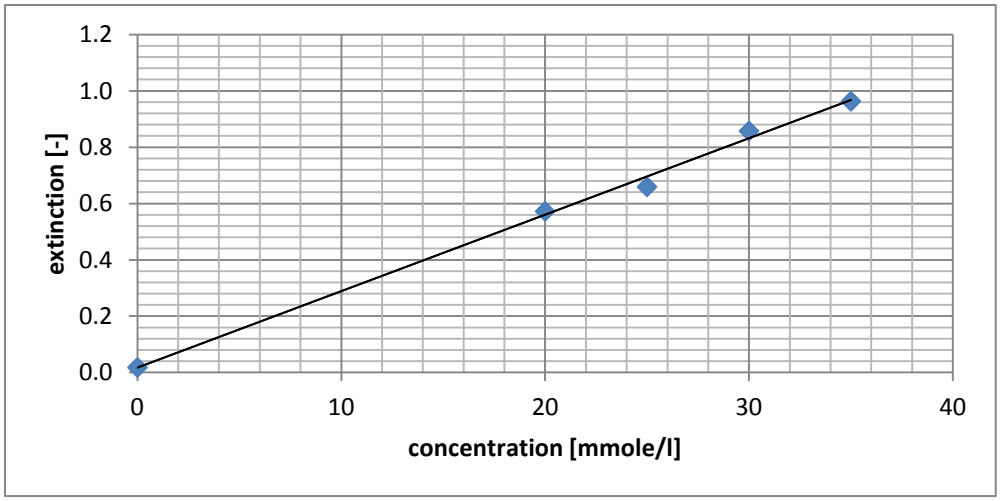

Figure 7: Oxidation of sulfite: Calibration chart

A linear regression is made. The linear equation is $y = 0.0271 * x + 0.0173$. The coefficient of determination is $R^2 = 0.996$.

4.2.2.6 Measuring method for samples

The samples from Arisdyne are prepared the exact same way as explained in 4.2.2.3. After that, 10 µl of the sample is pipetted into the previous prepared small glassware (4.2.2.4, paragraph 3).The previously created calibration chart (Figure 7) with the related linear equation is used for calculating the concentration of the sulfite in the samples.

4.2.3 Calibration method: Degradation of PNP

4.2.3.1 5% NaOH solution

To change the pH (see 4.2.3.3) 5% NaOH solution is used. This solution is created with NaOH - pellets (Table 5). 12.5648 g of the pellets are weighted into a 250 ml flask and filled up to the mark with DI water. To accelerate the dilution of the pellets a magnetic stirrer is in action. The concentration of 5 % was high enough to set the pH in an adequate time.

4.2.3.2 Preparation of the stock solution

A stock solution with a concentration of $500\ \frac{\mu mole}{l}$ is prepared to produce the concentrations for the calibration (Table 8).

$$m_{PNP} = c_{PNP} * MW_{PNP} * V$$
$$= 500 * 10^{-6}\ \frac{mole}{l} * 139.11\ \frac{g}{mole} * 1\ l$$
$$= 0.06956 g = 69.56\ mg$$

Equation 24

Equation 24 leads to m_{PNP} (the weight of sample taken) whereas c_{PNP} is the wanted PNP concentration, MW_{PNP} the molar weight of PNP and V the wanted volume. The slight

difference between $m_{target} = 0.06956\ g$ and $m_{being} = 0.06948\ g$ is due to the inaccuracy of the manual weighing.
0.06948 g are weighted into a beaker and filled up to approx. 250 ml with DI water. To be sure that all of the PNP powder is dissolved, the solution is mixed with a magnetic stirrer. After that, the solution from the beaker is poured into a 1 l flask and filled up to the mark. Out of this stock solution, 8 solutions were made through dilution. One example, whereby V_2 is the wanted volume to fill up to the target volume V_1, c_1 is the target concentration and c_2 the concentration of the starting solution, is given by Equation 25.

$$V_2 = V_1 * \frac{c_1}{c_2} = 250\ ml * \frac{25\ \frac{\mu mole}{l}}{500\ \frac{\mu mole}{l}} = 12.5\ ml$$

Equation 25

12.5 ml of the stock solution are pipetted into a 250 ml flask and filled up to the mark with DI water. This solution has then a concentration of 25 $\frac{\mu mole}{l}$. It is the same method, with other target concentrations, for the rest of the dilution series.

4.2.3.3 Preparation of solutions for the calibration

The pH of the solution after the complete dissolution depends on the concentration. For the measuring approx. 100 ml are poured into a beaker and a pH increase > 11((Kalumuck 2000, p. 467), (Hua et al. 1995, p. 2336)) is realized by carefully adding 5% NaOH solution with a pipette (18 - 90 µl). During this the solution is mixed with a magnetic stirrer. The last step is to fill it into the cuvette. The cuvette is the same for every test. After every test the cuvette is cleaned with two or three rinses of DI water. It is very important to keep the cuvette clean and not touch it without gloves.

4.2.3.4 Measuring with the UV/VIS

For this calibration 8 different solutions plus one blank (DI water) are measured at a wavelength of 400 nm. The results are shown in Table 8 and the calibration chart in Figure 8.

Table 8: degradation of PNP: concentration and extinction of the calibration solutions

concentration	extinction
µmole/l	-
0	0
1	0.0183
5	0.0851
10	0.1823
15	0.2759
20	0.3693
25	0.4599
30	0.5529
50	0.9267

4.2.3.5 Calibration chart

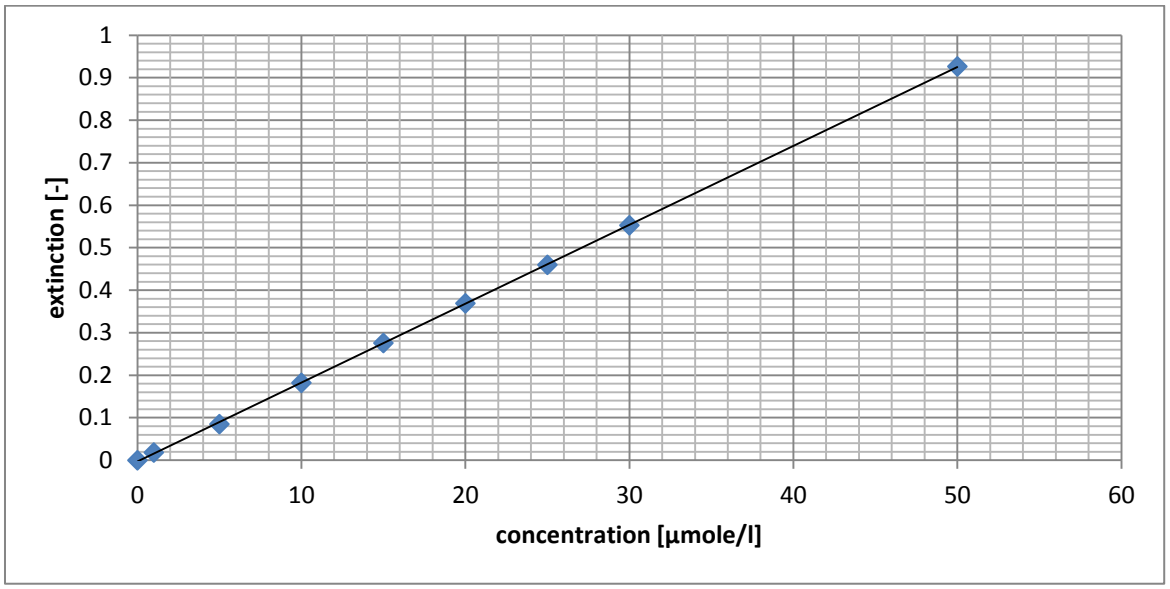

Figure 8: Degradation of PNP: calibration chart

A linear regression is made. The equation is $y = 0.0186 * \mathrm{x} - 0.0028$. This equation is used to calculate the concentration. The coefficient of determination is $R^2 = 0.9999$.

4.2.3.6 Measuring method for samples

For the analysis of the samples from Arisdyne the whole sample volume, approx. 50 ml, is used. A pH increase > 11 is realized by carefully adding 5% NaOH solution with a pipette. The added amount (90 to 1700 µl) depends on the pH of the starting solution. The pH of each sample is measured before and after adding the base. The solution is mixed with a magnetic stirrer during adding NaOH. To be as accurate as possible the pH probe and the stirrer are rinsed with DI water after every sample. The last step is to fill up the cuvette and measure it with the UV/VIS at a wavelength of 400 nm.

4.3 Experimental approach

Basically there are two different experimental setups. The system for the UC is realized through an ultrasonic horn and a flow cell (Figure 9). For the HC system a completely closed cavitation loop is created (Figure 10 and Figure 11). The possibility to apply different temperature conditions is realized with a chiller or an oil heater. Table 9 displays the data about the used units for both systems.

Table 9: List of used units

Unit	Manufacturer	Details
Plunger pump	Five Stars Technologies	CP300 (300 means a maximum pressure of 30000 psi)
Ultrasonic horn	Sonics & Materials Inc.	VC750, 750 W, 20kHz, 120 VAC, 15 A, Serial number: 52172Y
Water chiller	Thermo Electron	115V, 60Hz, 13.2 A
Oil heater	Ogden Manufacturing Co.	4500W, 240V, Phase 3,
Thermometer	Oakton - Eutech Instruments	Temp JKT

4.3.1 Ultrasonic cavitation

Under assembled condition the UC system shows a small surface which is in contact with air. To avoid a longer impact in case of the sulfite oxidation the ultrasonic cell is again purged with N_2 through the gas valve in Figure 9. A relief valve is installed to secure safe operation conditions. The gas supply is not required for the other model reactants. The possibility to apply different temperature conditions is realized with a chiller or an oil heater. 50 ml glass vials are used to store the samples (Figure 9- sample valve). To exclude contamination from previous runs, tab water and DI water are used to rinse the loop after every test.

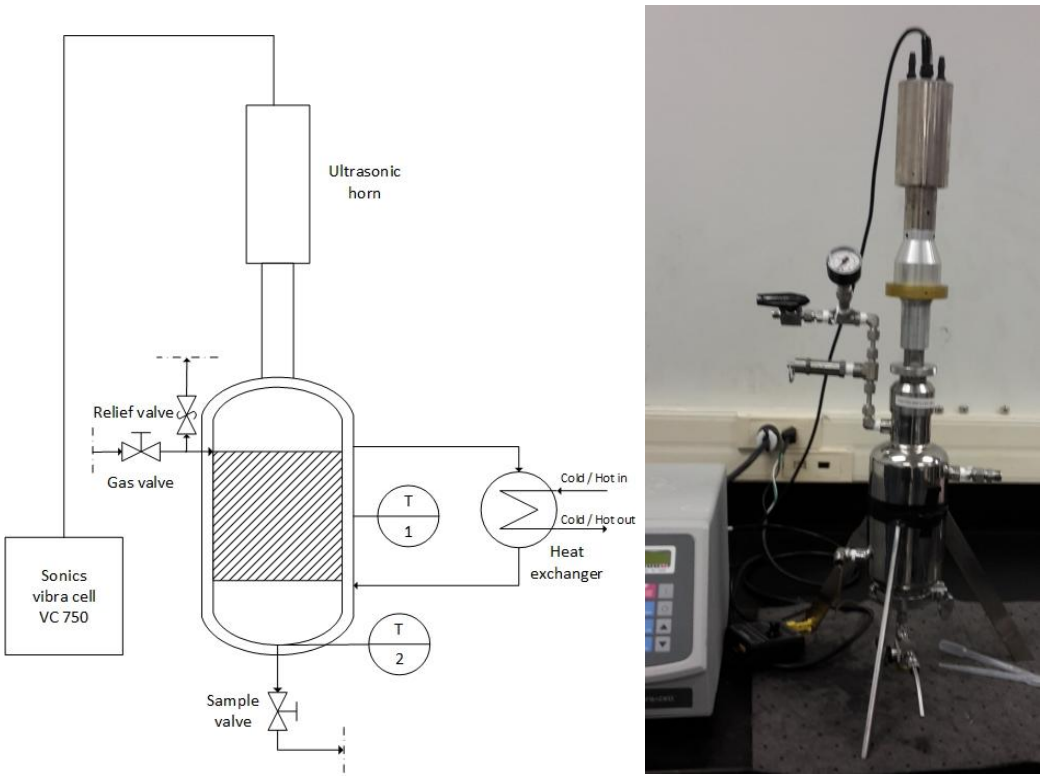

Figure 9: Flow chart and UC construction for all experiments

4.3.2 Hydrodynamic cavitation:

4.3.2.1 Liberation of iodine and degradation of PNP

At the beginning of every test, the initial solution is poured into the hopper. A completely with N_2 purged hydrodynamic cavitation loop is not required for these reactions (Figure 10 - gas valve is not used for these tests). The air compressor provides the plunger pump with the necessary air pressure.

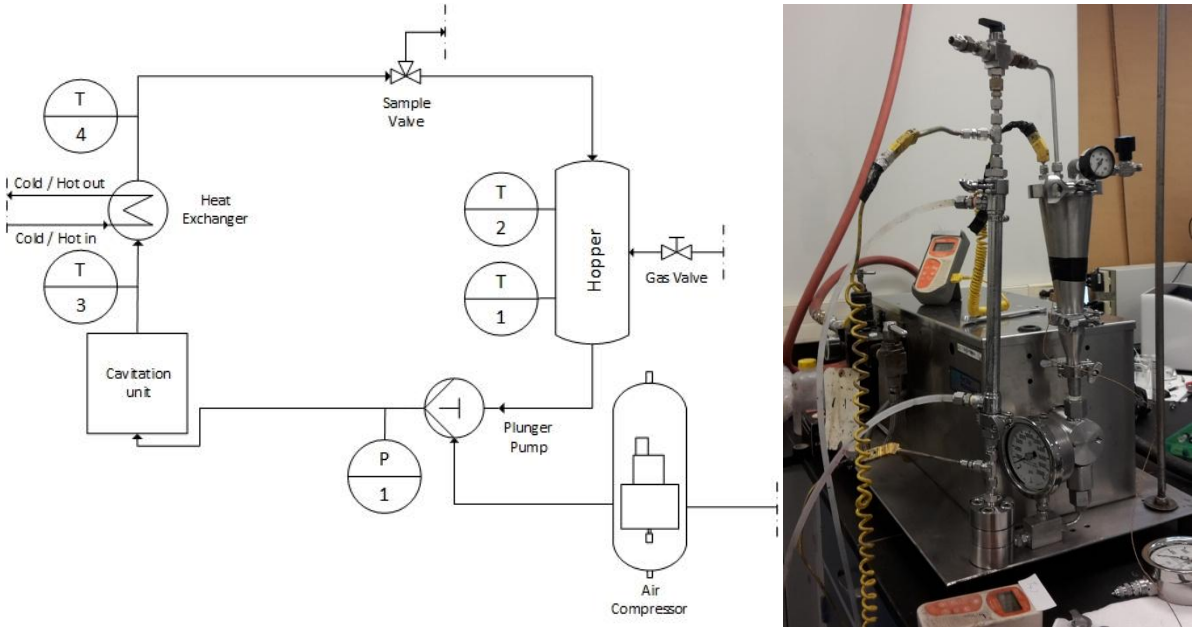

Figure 10: Hydrodynamic cavitation loop for the liberation of iodine and degradation of PNP

A tubular heat exchanger provides constant temperature conditions inside the hopper. The samples are taken and stored in 50 ml glass vials.

4.3.2.2 Oxidation of sulfite

At the beginning of every test, the initial solution is again poured into the hopper. A completely with N_2 purged HC loop is created to avoid the contact with the atmospheric oxygen (Figure 11). Every time a prepared sulfite solution has to be stored, the air above the surface is also driven out by N_2.

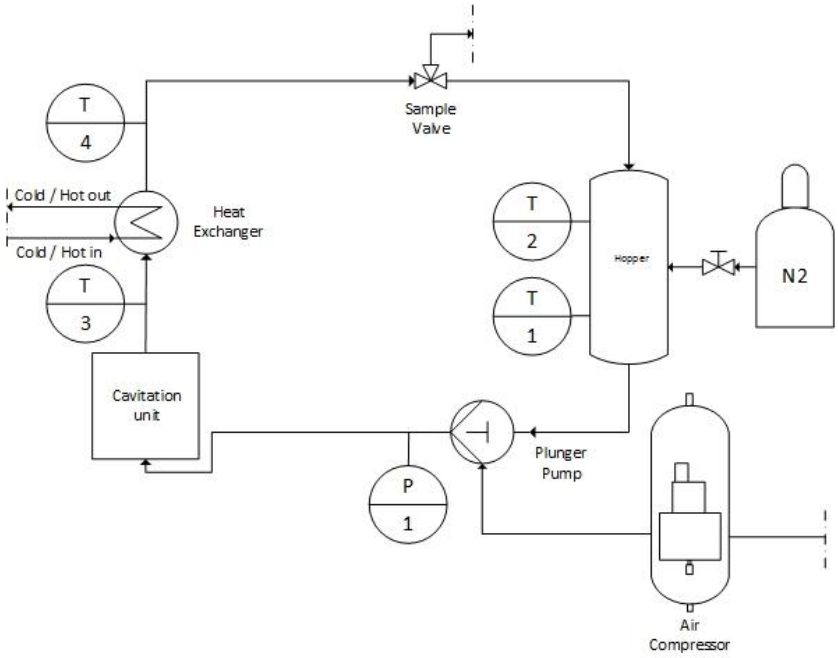

Figure 11: Hydrodynamic cavitation loop for the oxidation of sulfite to sulfate

20 ml glass vials are used to store the samples (Figure 11- sample valve). The same step includes the use of a crimp tool to seal the vials with a stopper against the impact of atmospheric oxygen. Previous tests show that the sealing is adequate. To exclude contamination from previous runs, tab water and DI water are used to rinse the loop after every test.

4.4 Result Quantification

The most important question this study has to answer is the existence of hot spots on the one hand and on the other hand how much energy input is required to ensure a proper conversion of the reactants. To compare the UC with the HC system the exactly same parameters are used for a specific experiment for both systems. All experiments with the different settings are tested on both systems. Appropriate care and effort was taken to accurately establish always the same conditions. Time is the basic parameter for the UC. The number of passes[18] whereby one pass means one pass of the initial volume through the whole loop, provides a more understandable and workable parameter for the HC system. Basically passes are just converted time, which is important for the comparison of the two systems. Additional to passes and time the other working parameters are pressure for the HC, temperature and pH for the UC. The applied pressure stages are 15000, 10000, 5000, 2500 and 1000 psi (Suslick, M. mdleleni, Millan and T. Ries, Jeffrey 1997, p. 9303). The different values for the temperature and the pH are explained in the Results section.

[18] see chapter 5 for a more detailed explanation

5 Results

5.1 Liberation of iodine

5.1.1 Liberation of iodine: Calculation scheme HC

The test with the number 1.6 - 4.6.has been chosen as one example to show the calculation of the different parameters. The explanation and the associated equations for quantification of the parameters is separately shown below each table.

Table 10: settings

number. series	initial concentration, mass and volume				passes	inlet pressure	orifice dimension
	C_0	sample m_{0s}	sample real m_{0Sr}	sample real corr. V_{0src}	Ω	p_i	thousandths of an inch
	g/l	g	g	ml	-	psi	-
1.6	50	400	400.4	387.77	5	2500	6/8
2.6		350	350.9	339.83	15		
3.6		300	301.1	291.60	25		
4.6		250	251.1	243.18	35		

5.1.1.1 number.series

The first number changes always from 1 to 4, whereas 1 means after 5, 2 after 15, 3 after 25 and 4 after 35 passes. The second number is for the same series always identical. In this case, 6 mean it is the sixth series with the HC system.

5.1.1.2 Initial concentration, mass and volume

The concentration for the initial solution C_0 is $50\ \frac{g}{l}$ and has been adopted from the work of Gogate et al. (2001, p. 2534). To use 400 g for the initial mass is due to the capacity of the hopper. “sample m_{0s}“ is the wanted sample mass, “sample real m_{0Sr}” the real mass after the measuring with the scale and “sample real corr. V_{0src}” is the conversion from mass into volume considering the density (Equation 26). To measure the density of the initial solution, 25 g are weighted into a 500 ml flask and filled up to the mark with DI water. Equation 27 shows the calculation of the density, where m_s is the mass of the solution, V_s the volume of the solution, ρ_{KI} the density of the solution, m_f the mass of the full flask and m_e is the mass of the empty flask.

$$V_{0src} = \frac{m_{0sr}}{\rho_{KI}} = \frac{400.4\ g}{1.03258\ \frac{g}{cm^3}} = 387.77\ ml \qquad \text{Equation 26}$$

$$m_s = V_s * \rho_{KI} \rightarrow \rho_{KI} = \frac{m_f - m_e}{V_s} = \frac{(681.81 - 168.52)\ g}{500\ ml} = 1.03258\ \frac{g}{cm^3} \qquad \text{Equation 27}$$

5.1.1.3 Passes

The range of passes is based on the time which is used in previous literature (Morison, K. and Hutchinson, C. 2009, p. 176). It was not possible to bring the samples back into the loop after the analysis because the analytic with the UV/VIS took place in the AQWATEC lap at CSM in Golden[19].

5.1.1.4 Inlet pressure

The inlet pressure presents the pressure the liquid medium is entering the cavitation chamber. The influence of pipe friction is not considered. The maximum pressure of 15000 psi (approx. 1034 bar) based on the work from Suslick, M. mdleleni, Millan and T. Ries, Jeffrey (1997, p. 9303) where the range of I_3^- - production was investigated over the range 100 - 1500 bar. The minimum pressure is limited with 1000 psi (approx. 70 bar) because of the plunger pump's specification and the used pressure display.

Table 11: calculated time and measured temperature

min/pass	time	time real	time accumulated	T1 (vessel)	T2 (vessel skin)	T3 (after cav. unit)	T4 (after heat ex)
t/Ω	t	t_r	t_{acc}	T11/T12	T21/T22	T31/T32	T41/T52
min/pass	min	h:mm:ss	min	°C	°C	°C	°C
3.58	17.88	00:17:52	17.88	21.3/20.5	21.8/20.9	24.0/23.3	chiller 20°C
3.13	31.33	00:31:20	49.21	20.5/20.4	20.9/20.7	23.3/23.3	
2.69	26.88	00:26:53	76.09	20.4/20.2	20.7/20.7	23.3/23.4	
2.24	22.42	00:22:25	98.51	20.2/20.2	20.7/20.7	23.4/23.4	

5.1.1.5 min/pass, time, time real, time accumulated

To quantify the minutes per pass in Table 11, Equation 28 with the data from Table 12 is used. The data in Table 12 is created through the manual determination of the strokes per minute, executed by simply counting and a stopwatch, and the ml per stroke, realized by catching the volume per stroke with a measuring cylinder.

Table 12: used orifice design and specific data of the plunger pump

6/8					
1000	psi	19	strokes/min	3.5	ml/stroke
2500		32		3.5	
5000		42		3.9	
10000		54		4.3	
15000		63		4.2	
8/12					
1000	psi	30	strokes/min	4	ml/stroke
2500		46		4.1	
5000		61		4.4	
10000		78		4.6	

[19] see 4.2 for more details about the analytical procedure

Because of the changing volume it is essential to use the difference of the passes. A certain volume needs certain strokes to get through the loop one time. Per stroke a certain volume is moved by the plunger pump. With Equation 29 the time t is calculated and the difference of passes is considered. t_r is t in a more clearly format and t_{acc} is the accumulated time of all passes. That means it takes 98.51 minutes for the entire series with a pressure of 2500 psi.

$$\frac{t}{\Omega} = \frac{V_{osrc}}{\frac{strokes}{min} * \frac{ml}{stroke}} = \frac{387.77\ ml}{32\ \frac{strokes}{min} * 3.5\ \frac{ml}{stroke}} = 3.58\ \frac{min}{pass} \quad \text{Equation 28}$$

$$t = \frac{t}{\Omega} * \Delta\Omega = 3.58\ \frac{min}{pass} * (5\ passes - 0\ passes) = 17.88\ min \quad \text{Equation 29}$$

5.1.1.6 Temperature T1 - T4

T1 to T4 are the temperatures at different locations in the loop (Table 11). “T4 (after heat ex)” is not always measured because after some runs it appears that the temperature after the heat exchanger is the same as the temperature inside the hopper (“T1 (vessel)”).

Table 13: measured results extinction and precipitation

sample taken at Arisdyne	pH at CSM	extinction (without filtration)	extinction (after filtration)	volume to filter	filter paper weight - unused	filter paper weight - used	produced precipitation and concentration		sample weight at CSM
m_{sAr}	pH	ζ_{wf}	ζ_{af}	V_f	m_{fpun}	m_{fpus}	m_p	m_{pc}	m_{sCSM}
g	-	-	-	ml	g	g	g	mg/ml	g
49.5	7.69	0.3573	0.4195	35	0.0869	0.1039	0.0170	0.49	
49.8	7.98	0.3497	0.4136	36	0.0877	0.1044	0.0167	0.46	48.2
50	8.05	0.3341	0.3987	35	0.0878	0.1024	0.0146	0.42	47.6
50	8.16	0.307	0.3802	39	0.0887	0.1052	0.0165	0.42	50.98

5.1.1.7 Sample weight

Table 13 (Table 21 for the UC system) shows a difference between the sample taken at Arisdyne and the sample weight at CSM. The reason is that at Arisdyne a scale with a maximum weight of 20 kg and 1 digit and at CSM an analytical scale with a maximum of 160 g and 4 digits is used. The deviation is due to the higher accuracy of the analytical scale.

5.1.1.8 Excursion: Observed precipitation

Some kind of black precipitation appears in every sample after some time. This precipitation gets visible through its sedimentation to the ground of the sample glass. The first thought that the precipitation are iodine crystals turned out false because no color change to purple is observed after pouring some droplets of carbon tetrachloride (CCl_4) or chloroform ($CHCl_3$) on the dried filtration residue. Tests with different kind of acids like HNO_3, HCl, H_2SO_4 and H_3PO_4 failed because no decomposition occurs. After an intensive cleaning session of the HC loop with several rinses with DI water, a replicant test was performed (All equipment was cleaned with acid before the start of the experiments). The black precipitation still appears and this indicates that the black flakes come from the only possible source left, the seal of the plunger pump. This seal is a graphite ring. This conclusion is confirmed by the fact that

no precipitation is found in the samples created with the UC system. In the following, the short excursion discusses the relation between carbon, activated surfaces and free radicals.
Liberation of iodine: The produced radicals during the cavitation process attack the potassium iodide (KI) and the graphite seal of the plunger pump (Boehm 2012, p. 3154). The high pressure seems to be an additional factor but no carbon is found in the samples of the other two model reactions. In this case, mainly hydrogen and oxygen radicals are responsible for the activated carbon surface referring to cavitation (Xu et al. 2007, p. 1365). It is already known that due to their strongly oxidizing properties, free radicals enhance the intercalation of many products into the carbon (Schlögl, R. and Boehm, H.P. 1988). Lau et al. (1986, p. 103) showed that there is an adsorption sequence at pH 7 of $\mathrm{rH}^+ > r\mathrm{K}^+ > r\mathrm{Li}^+ > r\mathrm{I}^- > r\mathrm{NO}_3^- > r\mathrm{OH}^-$, where r is the adsorption density in $\frac{\mathrm{mole}}{\mathrm{m}^2}$. The produced radicals are strong enough to intercalate the potassium ion. The potassium ion catalyzed the decomposition of the graphite surface (Billinge et al. 1984, p. 85). An immediate color change is not observed, because the iodide ion is also bound on the active surface of the carbon. After a specified time (weekend) these ions get dissolved in water and create the I_3^- complex which is responsible for the color change. It depends on the oxidizing properties of the produced radicals how active the surface is and, later, how high the concentration of the dissolved I_3^- complex is. **Oxidation of sulfite:** In this system the same radicals are created but no carbon precipitation occurs. No hint was found in the literature that sodium or sulfite is a catalyst like the potassium ion. An active carbon surface is also present but there is no decomposition because neither the Na^+ - ions nor the SO_3^{2-} ions are absorbed by or have any other impact on the graphite. There is no potassium or any other ion from the sequence mentioned above in the sulfite/sulfate - system. That suggests that different salts have different impacts on the graphite seal.

5.1.1.9 Extinction without and after filtration

To investigate if the carbon flakes influence the concentration, a measuring of the extinction with and without the precipitation is required. This means a measuring before and after the filtration. The values in Table 13 show that there is a difference between the extinctions in this example. The extinction before filtration was taken on a Friday and also the filtration has been taken place on this day. The measuring of the second extinction was performed on the Monday after. The filtration caused an additional activation (additional liberation of iodine through radicals from the carbon) of the carbon after the weekend. This is just a theory and additional investigations are needed. The measuring of all the other samples was executed on the same day and they show slightly different values before and after the filtration.

5.1.1.10 Produced precipitation and concentration

To quantify the existing amount of carbon flakes, Equation 30 is used. The used filter paper is dried in an oven for 30 minutes by 50°C. 30 minutes are enough because tests with a drying time up to 2 hours showed no difference in the weight of the filter residue. Generally the concentration increases by increasing the pressure. Weighing of the filter paper before

and after the filtration is required. To avoid contamination, it is absolutely necessary to handle the filter paper only with gloves and a forceps.

$$m_{pc} = \frac{m_{fpus} - m_{gpun}}{V_f} = \frac{(0.1044 - 0.0877) * 10^{-3} g}{36\ ml} = 0.46 \frac{mg}{ml}$$ Equation 30

5.1.1.11 pH at CSM

The pH can be excluded as an influence factor for the occurring precipitation because all samples show a pH around 8.

Table 14: measured concentration and calculated production of the tri-iodide (I_3^-) complex

concentration CCl_4	concentration I_3^-		I_3^- production	I_3^- production total	rate of I_3^- production	rate of I_3^- production
C_h	C_{hc}	C_{af}	n_p	n_{ptot}	n_p/Ω	n_p/t
g/l	mg/l	mg/l	µmole	µmole	µmole/pass	µmole/s
	51.94	64.6	25.89	69.77	5.18	2.41E-02
	50.39	63.4	20.56		2.07	1.10E-02
	47.20	60.4	14.75		1.48	9.15E-03
	41.67	56.6	8.48		0.85	6.30E-03

5.1.1.12 Concentration Carbon tetrachloride (CCl_4)

The column "concentration CCl_4" in Table 14 is empty because no CCl_4 is added in this series. 0.324 g CCl_4 /l are added to those solutions which are used for the investigation of the impact of haloalkanes to cavitation[20].

5.1.1.13 Blanks

Table 15 shows the results of the blank tests of the initial solution. There is a certain amount of the I_3^- complex formed in these solutions without HC or any other treatment. The concentration of the initial solution C_{blank} for all samples is defined with 20.1 $\frac{mg}{l}$ and represents the measurement directly after creating the solution. This is very important for further calculations.

Table 15: different blanks

number.series	initial concentration, mass and volume			extinction without filtration	concentration CCl_4	concentration I_3^-	I_3^- production
	C_0	sample m_{0s}	sample real corr. V_{0src}	ζ_{wf}	C_h	C_{blank}	$n_{p,blank}$
	g/l	g	ml	-	g/dm³	mg/l	µmole
5.3 Blank	50	400	387.38	0.2367		27.33	27.81
KI Blank			**387.38**	**0.2013**		**20.10**	**20.45**
KI Blank			387.38	0.2623		32.55	33.12
KI Blank			387.38	0.2643	0.324	32.96	33.54

[20] see 5.1.3.2 for more details

5.1.1.14 I_3^- - production and I_3^- - production total

To calculate the I_3^- production (Table 14 and Table 15), Equation 31 is used. The total I_3^- production is the summation of the produced amount of substance per volume or after 35 passes (Equation 32).

Equation 31

$$n_p = \mu mole\ sample - \mu mole\ initial\ solution =$$

$$\frac{C_{hc} * (V_{0src} - \frac{m_{sAr}}{\rho_{KI}})}{MW_{I_3^-}} - \frac{C_{blank} * V_{0src}}{MW_{I_3^-}}$$

$$= \left(\frac{\left(51.49 * 10^{-3}\frac{g}{l} * \left(387.77 - \frac{49.5}{1.03258}\right) * 10^{-3} l\right) - \left(20.10 * 10^{-3}\frac{g}{l} * 387.77 * 10^{-3} l\right)}{380.71\ \frac{g}{mole}} \right)$$

$$* 10^6 \mu mol = 25.89\ \mu mole$$

Equation 32

$$n_{ptot} = n_{p,5passes} + n_{p,15\ passes} + n_{p,25\ passes} + n_{p,35\ passes}$$
$$= (25.89 + 20.65 + 14.75 + 8.48)\mu mole$$
$$= 69.77\ \mu mole$$

5.1.1.15 Rate of I_3^- - production

Equation 33 and Equation 34 are used to quantify the rate of I_3^- - production in $\frac{\mu mole}{pass}$ and $\frac{\mu mole}{s}$.

Equation 33

$$\frac{n_p}{\Omega} = \frac{25.89\ \mu mole}{5\ passes} = 5.18\ \frac{\mu mole}{pass}$$

Equation 34

$$\frac{n_p}{t} = \frac{25.89\ \mu mole}{17.88 * 60\ s} = 2.41 * 10^{-2}\ \frac{\mu mole}{s}$$

Table 16: efficiency and energy

flow rate	power consumption P=Q*ΔP	power consumption total	energy density	oxidation efficiency	oxidation efficiency total	enhancement of liberation	energy	energy costs
Q	P	P_{tot}	ρ_e	O_e	O_{etot}	-	-	11.2 ¢/kWh
m³/s	W	W	J/ml	µmole/J	µmole/J	%	kWh	¢
1.81E-06	31.16	124.65	86.19	7.75E-04	9.47E-05	341.1	0.2	2.29
			172.38	3.53E-04				
			172.38	2.94E-04				
			172.38	2.02E-04				

5.1.1.16 Power consumption

Equation 35 describes the power consumption for a certain volume flow when a certain pressure is applied and Equation 36 calculates the flow rate. $1\ psi$ is equal to approx. $6895\ Pa$. It should be noted that the flow rate for 15 passes represents the flow rate for 10

passes with the associated volume (Equation 37). The same is valid for 25 and 35 passes which results in the same power consumption after each stage.

$$P = \dot{Q} * \Delta p = 1.81 * 10^{-6} \frac{m^3}{s} * 2500 * 6895\ Pa = 31.16\ W$$ Equation 35

$$\dot{Q}_{5\ passes} = \frac{\Omega * V_{0scr}}{t} = \frac{(5\ passes * 387.7710^{-6}\ m^3)}{17.88 * 60\ s} = 1.81 * 10^{-6}\ \frac{m^3}{s}$$ Equation 36

$$\dot{Q}_{15\ passes} = \frac{\Omega * V_{0scr}}{t} = \frac{((15\ passes - 5\ passes) * 339.83 * 10^{-6}\ m^3)}{31.33 * 60\ s} = 1.81 * 10^{-6}\ \frac{m^3}{s}$$ Equation 37

The total power consumption over the full range of passes (35 passes) is the summation of the consumption per stage.

5.1.1.17 Energy density

Equation 38 is used to calculate the energy density in $\frac{\mathrm{J}}{\mathrm{ml}}$. It describes, how much power is drawn per volume of the initial solution (Koh et al. 2014).

$$\rho_e = \frac{P * t}{V_{0scr}} = \frac{31.16\ W * 17.88 * 60\ s}{387.77\ ml} = 86.19\ \frac{J}{ml}$$ Equation 38

5.1.1.18 Oxidation efficiency or cavitational yield

$$Y(t) = \frac{moles\ degraded\ per\ second}{power\ consumption} = \frac{\dot{Q} * (C_t - C_0)}{\dot{Q} * \Delta P} * \frac{10^3}{MW}$$ Equation 39

where $\dot{Q}$ is the flow rate and ΔP is the system pressure drop, C_t and C_0 are the reagent concentration at time t and initial time, respectively (Capocelli et al. 2014a, p. 2570).

The cavitational yield, here practically oxidation efficiency (Equation 40) is calculated as $\frac{\mu\mathrm{mole}}{\mathrm{J}}$ for a certain pressure and volume. Oxidation efficiency total in Equation 41 is defined for a certain pressure and over the full range of passes (35 passes). Series 1.1 - 3.1 and 1.2 - 3.2 with pressures of 2500 and 5000 psi are performed without constant temperature conditions. It is not possible to run the system without heat control at higher pressure because of the occurring high temperatures in the cavitation unit. The calculation of the energy efficiency by using the calorimetric method is only possible for these two HC series but all UC tests and is explained in 5.1.1.20 and 5.1.2.3.

$$O_e = \frac{n_p}{P * t} = \frac{32.43\ \mu mole}{31.16\ W * 17.88 * 60s} = 7.75 * 10^{-4}\ \frac{\mu mole}{J}$$ Equation 40

$$O_{etot} = \frac{n_{ptot}}{P_{tot} * \Sigma t} = \frac{94\ \mu mole}{264.87\ W * 98.51 * 60s} = 9.47 * 10^{-5} \frac{\mu mole}{J}$$ Equation 41

5.1.1.19 Enhancement of liberation and energy

The "enhancement of liberation" describes how much more of the I_3^- complex is formed because of the cavitation. 100 % is the amount of I_3^- in µmole in the samples without cavitational or any other treatment (Table 15, $n_{p,blank}$).
There is an increase of the liberated amount of about 340% (Equation 42) for the given example with 2500 psi. Through cavitation 3.4 times more I_3^- ions are formed.

$$enhancement = \frac{100\ \%}{20.45\ \mu mole} * 69.77\ \mu mole = 341.1\ \%$$ Equation 42

The very important question of how much energy is needed for the given degradation, is answered by Equation 43 and Equation 44. The costs for the increased liberation of iodine are calculated with Equation 45. The specific electricity price for Colorado and Ohio is $11.2 \frac{¢}{kWh}$.[21]

$$1\ kWh = \ 1000\ Wh = 1000\ \frac{J}{s} * 3600\ s = 3600000\ J$$ Equation 43

$$Ee = \frac{124.65\ W * 98.51 * 60\ s}{3600000\ J} = 0.2\ kWh$$ Equation 44

$$¢ = 0.2\ kWh * 11.2 \frac{¢}{kWh} = 2.29\ ¢$$ Equation 45

5.1.1.20 Power dissipated into the liquid (calculation scheme for HC and UC)

HC series 1.1 - 3.1 and 1.2 - 3.2 and UC series 1.1 - 4.1[22] are performed without constant temperature conditions. Calorimetric calculations are used to determine the dissipated power into the liquid. Table 17 shows the settings for the HC series whereas here the time is the main parameter.

Table 17: settings

number. series	initial concentration, mass and volume				time	inlet pressure	orifice dimension	passes
#	C_0	sample m_{0s}	sample real m_{0Sr}	sample real corr. V_{0src}	t	p_i	thousandths of an inch	Ω
-	g/l	g	g	ml	min	psi	-	-
1.1	50	400	400.3	387.67	10	2500	6/8	2.80
2.1		350	400.3	387.67	20			5.60
3.1		300	400.3	387.67	30			8.40

[21] http://www.npr.org/sections/money/2011/10/27/141766341/the-price-of-electricity-in-your-state reviewed 1/8/2016

[22] Only for the UC test the temperature of the solution decreases and the temperature of the vessel skin increases. The cavitation generated condensation heat has to be dissipated to the outside.

1.2	50	400	400.2	387.57	10	5000	6/8	4.10
2.2		350	351.4	340.31	20			8.19
3.2		300	302.6	293.05	30			12.29

Because of measuring the temperature inside the vessel before and after the treatment it is possible to calculate the power dissipated into the liquid for the named HC series and for every UC series. A temperature increase at every measuring point can be observed from Table 18.

Table 18: measured temperature

temp. T1.1 (vessel)	**temp. T1.2 (vessel)**	**temp. T2.1 (vessel skin)**	**temp. T2.2 (vessel skin)**	**temp. T3.1 (after cav unit)**	**temp. T3.2 (after cav unit)**
T11	T12	T21	T22	T31	T32
°C	°C	°C	°C	°C	°C
22	26.2	22.4	27.2	23.2	28.1
26.2	28.6	27.2	30.1	28.1	31.1
28.6	30.6	30.1	32.4	31.1	32.8
23	34.4	23.2	36.9	28.4	39.9
34.4	40.2	36.9	43.7	39.9	47.1
40.2	44.6	43.7	49.1	47.1	53

The heat capacity for the KI solution is determined by Novikov (2014, p. 3). For the heat capacity of the sodium sulfite and PNP solution the heat capacity of water (4.186 J/gK at 20°C) is used. It is assumed that the low concentrations of the model reactants have no influence on the heat capacity.

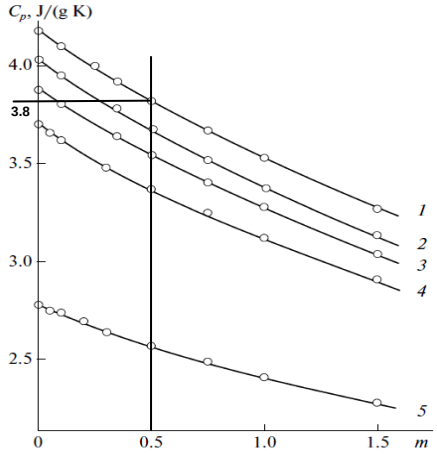

Figure 12: Concentration dependences of the specific heat capacities of potassium iodide solutions in water and mixed MP (N-methylpyrrolidone) - H_2O solvent at 298.15 K and different values of xMP: (1) 0, (2) 0.025, (3) 0.05, (4) 0.10, (5) 0.33;

$$C_p = 3.8 \frac{J}{g * K}$$

$$P = C_p * m * \frac{dT}{dt} = 3.8\ \frac{J}{g * K} * 400.3\ g * \frac{(26.2 - 22.0)K}{10 * 60s} = 10.65\ W$$ Equation 46

Equation 46, where C_p is the heat capacity, m the mass of the solution, dT the temperature difference and dt the time difference, is used to calculate the dissipated power.

Table 19: calculated calorimetric and enhancement of liberation

Power dissipated in the liquid	**Power dissipated in the liquid**	**energy efficiency**	**energy efficiency total**	**enhancement of liberation**
P_{diss}	$P_{disstot}$	E_e	E_{etot}	-
W	W	%	%	%
10.65	19.73	34.14	24.19	322.01
5.33		19.51		
3.75		16.26		
28.89	50.23	31.69	20.91	376.64
12.91		16.12		
8.43		12.23		

The positive values for the power dissipated into the liquid in Table 19 indicate that the cavitational process increases the temperature of the solution with increasing the treatment time.

5.1.2 Liberation of iodine: Calculation scheme UC

Basically, the calculation is the same as for the HC system but with some important differences. The declaration of the test series is the same as for the HC system and the example for the calculation scheme is the series 1.2 - 4.2. There is no counting of passes with the ultrasonic horn and the main parameter is time. The settings related to an amplitude of 25% and a pulse of 4 seconds on, 2 seconds off, are based on the previous work from Chakinala et al. 2008, p. 166).

Table 20: settings and measured temperature

number .series	initial concentration, mass and volume			time	temp. 11 (jacket)	temp. 12 (jacket)	temp. 21 (inside)	temp. 22 (inside)
	C_0	sample m_{0s}	sample real corr. V_{0src}	t	T11	T12	T21	T22
	g/l	g	ml	min	°C	°C	°C	°C
1.2	50	300.0	290.53	5	20	20	24.4	24.8
2.2		249.7	241.82	10			25.3	27
3.2		300.2	290.73	20			25.1	27.8
4.2		250.6	242.69	30			27.8	30

After pouring the 300 g solution with a concentration of 50 g KI per liter into the ultrasonic cell, the horn is fixed by tighten the bolt. 300 g are chosen for the starting volume because of the limited space in the ultrasonic cell. For the first series a sample after 5 and 10 minutes is taken (second run with 5 minutes). The rest of the solution is drained through the valve at the bottom of the cell and the cell and horn are rinsed two times with DI water. The second series also consists of 300 g solution, with the only difference that the sample is taken after 20 and 30 minutes (second run with 10 minutes). That leads to a total runtime of 40 minutes for each series (Table 20). Table 20 also shows the location and the temperatures of the different measuring points at the ultrasonic cell. The temperature is measured and noted before and after the treatment. T11 and T12 are the same because of constant cooling. T21 and T22 are the temperatures inside the cell before and after the treatment[23]. They are measured with a thermo element on the bottom of the cell. m_{sAr} presents the weight of the sample which was taken at Arisdyne.

Table 21: measured concentration

sample taken at Arisdyne	pH at CSM	extinction	sample weight at CSM	concentration CCl_4	concentration after ultrasonic
m_{sAr}	pH	ζ_{uc}	m_{sCSM}	C_h	C_{uc}
g	-	-	g	g/l	mg/l
50.3	6.95	0.3101	48.3092		42.31
50.1	7.06	0.3467	47.7735		49.78
49.6	7.01	0.3853	47.6932		57.65
49.7	7.06	0.4282	51.4015		66.41

[23] see 4.3.1 for the flow chart

There is no significant increase or decrease of the pH after storage and shipping (Table 21). The procedure for measuring the extinction with the UV/VIS and calculating the concentration is the same for both systems.[24] The column "concentration CCl_4" is again empty because no CCl_4 is added in this series as well. 0.324 g CCl_4 /l are added to those solutions which are used for the investigation of the impact of haloalkanes to ultrasonic cavitation.

Table 22: calculated tri-iodide (I_3^-) production

I_3^- production	**I_3^- production total**	**rate of I_3^- production**
n_p	n_{ptot}	n_p/t
µmole	µmole	µmole/s
11.53	24.04	3.84E-02
12.50		2.08E-02
21.40	42.52	1.78E-02
21.12		1.17E-02

As already mentioned, a certain amount of the I_3^- complex is formed in these solutions without any kind of cavitation or treatment. To calculate the I_3^- production, Equation 31 is used. Table 22 shows the I_3^- production after 5, 10, 20 and 30 min. The total I_3^- production is the summation of the produced amount of substance after 10 and 30 minutes. Equation 34 is used to get the rate of the I_3^- production in $\frac{\mu mole}{s}$.

5.1.2.1 Power consumption

The use of a temperature regulating device (water chiller or oil heater) leads to positive values for the power dissipated into the liquid because of a constant temperature regime in the cell (Table 23, column 1). The calculation of the power dissipated into the liquid is explained in 5.1.1.20.

Table 23: calculated power demand and enhancement

Power dissipated into the liquid	**total power dissipated into the liquid**	**power consumption total**	**energy density**	**enhancement of liberation**
P_{diss}	$P_{disstot}$	P_{tot}	ρ_e	-
W	W	W	J/ml	%
1.52	6.90	84.21	86.96	118
5.38		84.21	104.47	
2.57	6.06	84.05	173.47	208
3.49		84.11	207.93	

To get the energy efficiency, the electrical power consumption has to be calculated. The pulse of the horn causes a longer total runtime (Table 24). If the timer is set to for example 5

[24] see Measuring method for samples in 4.2.1.4

minutes, the total runtime is 7 minutes and 28 seconds because of the pause of 2 seconds. The 5 minutes represents the effective time of treatment. During the additional 2 minutes and 28 seconds power is only needed for the instruments.

Table 24: runtime ultrasonic horn

effective ultrasonication (timer)	**pause**		**total runtime**	
t_{eff}	t_p		t_{tot}	
min	min	sec	min	sec
5	2	28	7	28
10	4	58	14	58
20	9	58	29	58

Equation 47 shows the needed electrical power for the ultrasonic horn.

$$P = \frac{U * I_{run} * t_{eff} + U * I_0 * t_p}{t_{tot}} =$$

$$\frac{120\,Vac * 0.9\,A * 5 * 60\,s + 120\,Vac * 0.3\,A * (2 * 60 + 28)\,s}{(7 * 60 + 58)\,s} = 84.21\,W$$

Equation 47

$U \ldots Voltage\ alternating\ current$
$P \ldots total\ power$
$I_{run} \ldots ampere\ when\ running$
$I_0 \ldots ampere\ for\ the\ instruments$

5.1.2.2 Energy density and enhancement of liberation

Applying Equation 38 shows nearly the same energy density in all series. The slight difference occurs because always a little different volume of the initial solution is used and also the weight of sample taken is not always exactly the same. The enhancement of the liberation caused by UC is explained in 5.1.1.19 and calculated with Equation 42.

5.1.2.3 Energy efficiency

Energy efficiency (Equation 48) examines the question of how much of the energy is effectively dissipated into the system. This fraction of the total energy is used for the generation of cavitation and should be as high as possible (Gogate et al. 2001).

Table 25: calculated energy and efficiency

energy efficiency	**energy efficiency total**	**oxidation efficiency**	**oxidation efficiency total**	**energy**	**energy costs**
E_e	E_{etot}	O_e	O_{etot}	-	11.2 ¢/kWh
%	%	µmole/J	µmole/J	kWh	¢
1.15	5.22	4.28E-04	4.52E-04	0.02	0.08
4.07		2.38E-04			
1.94	4.59	1.81E-04	2.45E-04	0.07	0.25
2.65		1.24E-04			

$$E_e = \frac{P_{diss}}{P_{tot}} = \frac{1.52\ W}{132\ W} * 100\% = 1.15\ \%$$ Equation 48

$$E_{etot} = \frac{P_{disstot}}{P_{tot}} = \frac{6.90\ W}{132\ W} * 100\% = 5.22\ \%$$ Equation 49

Equation 49 is the total energy efficiency after 10 and 30 minutes. Equation 40 and Equation 41 are used for the calculation of the oxidation efficiency after 5, 10, 20 and 30 minutes. The total oxidation efficiency is calculated after 10 and 30 minutes, in other words, after every new initial solution. The total power consumption and consequently the energy demand and the arising costs are the same for every series. (Table 25 and Equation 43, Equation 44, Equation 45,).

5.1.3 Liberation of iodine: Results

The following results and discussion belong to the HC test series. The results of the UC tests are included in the comparison between HC and UC in 5.1.4. It should be kept in mind that the leading parameter of all the HC experiments is passes. After one pass the starting volume is pumped through the loop back into the hopper. The assumed range over passes is 5, 15, 25 and 35. The first sample is taken after 5 and the second after additional 10 passes, which consequently means after 15 passes. The same procedure applies for the samples after 25 and 35 passes.

5.1.3.1 Different pressure

The different pressures, temperatures and orifice designs used for the HC tests are given in Table 26. The reason to change the orifice dimension from 6/8 to 8/12 bases on the shorter total runtime for 35 passes.

Table 26: parameters; without CCl_4

pressure	orifice dimension	temperature
p_i	-	T1
psi	thousandths of an inch	°C
15000	6/8	20
10000	6/8	20
5000	6/8	20
2500	6/8	20
1000	8/12	5/20

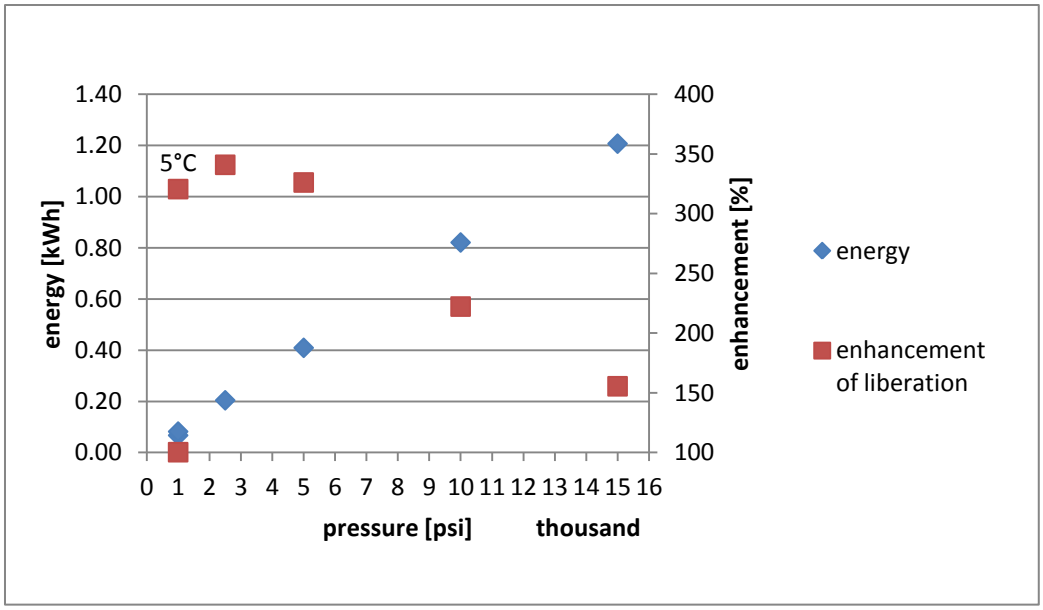

Figure 13: 50 g KI /l; different pressure; 20°C (except 1000 psi and 5°C); without CCl_4;

In general the results in Figure 13 display an increased enhancement by decreasing the pressure. The results of the tests with 1000 psi and different temperatures require a more detailed explanation. With 5°C the enhancement is an approx. 3.5 - fold and with 20°C no increase in production of I_3^-. This lower enhancement is due to the fact that the liberation of iodine and the following generation of the I_3^- - complex is chemically described as an oxidation. An oxidation is an exothermic reaction and decreasing the temperature ships the equilibrium to the products. High inlet pressure generates a large number of cavities and the comparison of the test with 2500 psi and 20°C with the 1000 psi and 20°C indicates that the liberation of iodine requires a pressure between 2500 and 5000 psi ($2500 \leq p_i < 5000$).The energy demand increases by increasing the pressure. It should be noticed that the displayed energy data point for the test with 1000 psi and 5°C does not consider the cooling energy.

5.1.3.2 Different pressure and carbon tetrachloride (CCl_4)

Chakinala et al. (2008, p. 170) investigated how the use of haloalkanes impacts the cavitational effect whereas the use of CCl_4 shows the most promising effect. In a next series different pressures are applied and a small amount of CCl_4 is added to each starting solution (Table 27).

Table 27: parameters; with CCl_4

pressure	orifice dimension	temperature	concentration CCl_4
p_i	-	T1	C_h
psi	thousandths of an inch	°C	g/l
15000	6/8	20	0.324
10000	6/8		
5000	6/8		
1000	8/12		

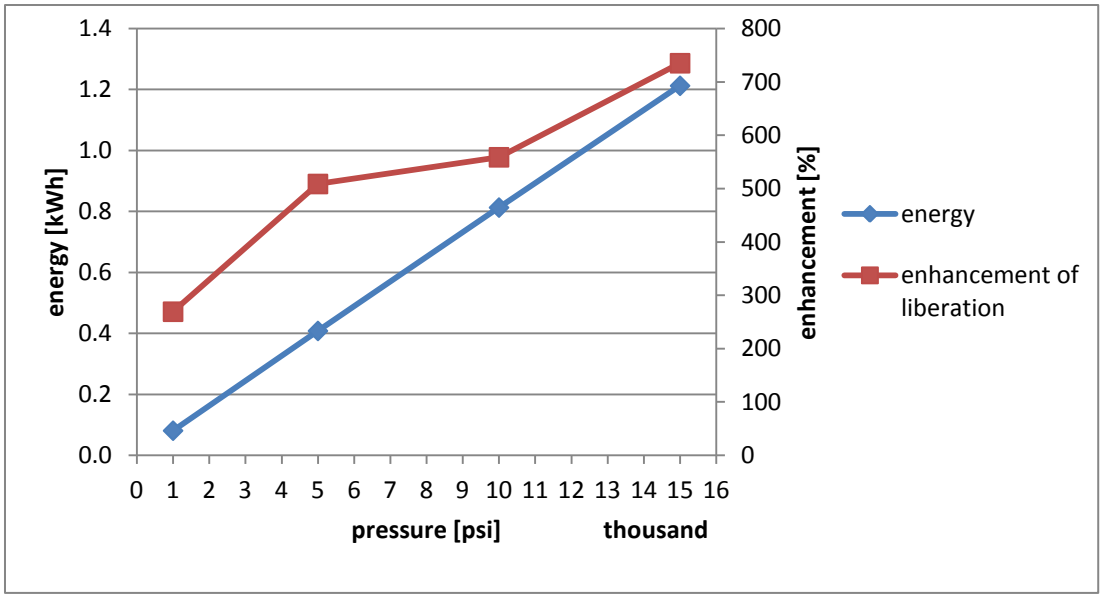

Figure 14: 50 g KI /l; different pressure; 20°C; with CCl_4;

By adding a small amount of CCl_4, the enhancement shows a peak at 15000 psi (Figure 14). In agreement with Suslick (1990), the current study found out that adding CCl_4 results in an increased output of the I_3^- - complex. Comparing the enhancement in Figure 13 and Figure 14, the adding of CCl_4 doubles the enhancement from a 3.5-fold to a 7-fold increasing production of I_3^-. Cavitational induced hot spots lead to additional generation of $\dot{C}l$ radicals. These additional radicals, beside $\dot{O}H$ and $\dot{H}$, also attack the KI and further increase the intensity of I_3^- - production. By undergoing several series of recombination reactions, oxidizing agents like Cl_2 and HOCl are formed. These agents are much more stable than the free radicals and so they cause an additional overall intensification effect on the oxidation rates (Chakinala et al. 2008, p. 166).

Considering pressure, the results in Figure 13 and the findings of this series are the complete opposite. Through adding CCl_4, a high pressure results in an increased enhancement. The same phenomenon was observed by Chakinala et al. (2008, p. 167). In their study the increased rates of oxidation are attributed to the higher inlet pressure which leads to higher intensity of cavitation (Gogate, Parag R. and Pandit, Aniruddha B. 2000). Higher intensity cavitation means enhanced degradation of the chloroalkanes generating higher amounts of the oxidizing agents (Cl, Cl_2 and HOCl). The results indicate a changed performance of HC at high pressure and by adding CCl_4. The high pressure is needed to create the more stable oxidizing agents. This correlation of pressure and enhancement inevitably leads to higher energy costs.

5.1.3.3 Different pressure plus low pH

The idea to decrease the pH of the starting solution bases on the homolytic dissociation of water. Because of the decreased pH, hydrogen radicals should increase the liberation of iodine. Through adding a few drops of 10 % citric acid ($C_6H_8O_7$) the pH is set to 3.3. To increase the pH is excluded for the HC loop because of Figure 20 “UC pH 12.5”. The settings for this series are shown in Table 28.

Table 28: parameters; low pH

pressure	orifice dimension	temperature	acid	pH
p_i	-	T1	-	-
psi	thousandths of an inch	°C	-	-
5000	6/8	20	citric acid	3.3
2500	8/12			
1000	8/12			

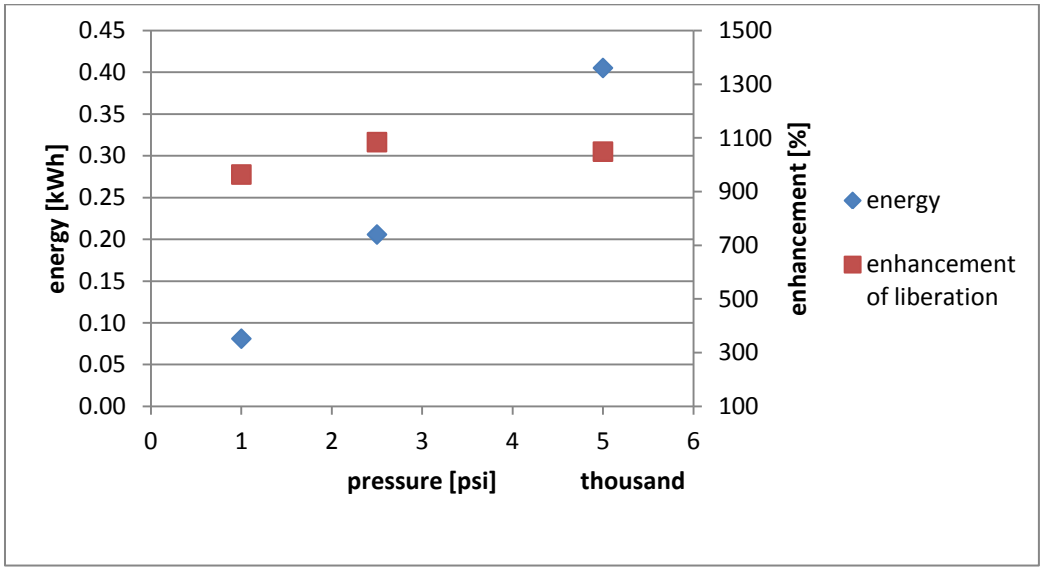

Figure 15: 50 g KI /l; different pressures; 20°C, pH 3.3;

Figure 15 presents that a decrease of the pH to 3.3 results in a 11-fold increase of I_3^- - production at an applied pressure of 2500 psi because the additional OH- and H+ - ions lead to an increased amount of the formed strong oxidizing agent H_2O_2. In general the series with the low pH showed even at 1000 psi a better enhancement than the best result of the series where CCl_4 is added.

5.1.3.4 Efficiency

Figure 16 shows the development of the efficiency (Equation 39) in µmole/J over the range of 35 passes. The parameter efficiency describes how many µmole I_3^- are formed per Joule.

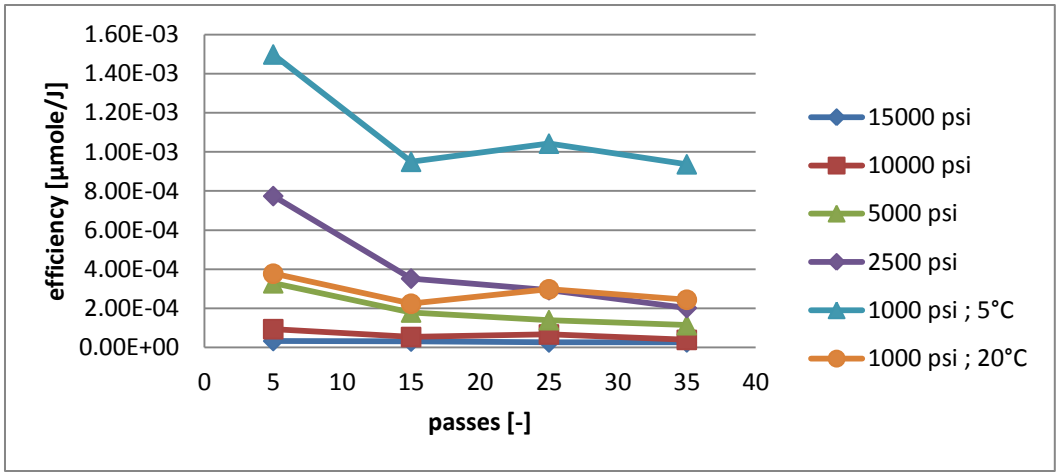

Figure 16: 50 g KI /l; different pressures; 20°C (except 5°C at 1000 psi);

The efficiency decreases from 5 to 35 passes because a high number of passes requires more electrical power. As mentioned before the additional energy for the cooling for the test with 1000 psi is not considered.

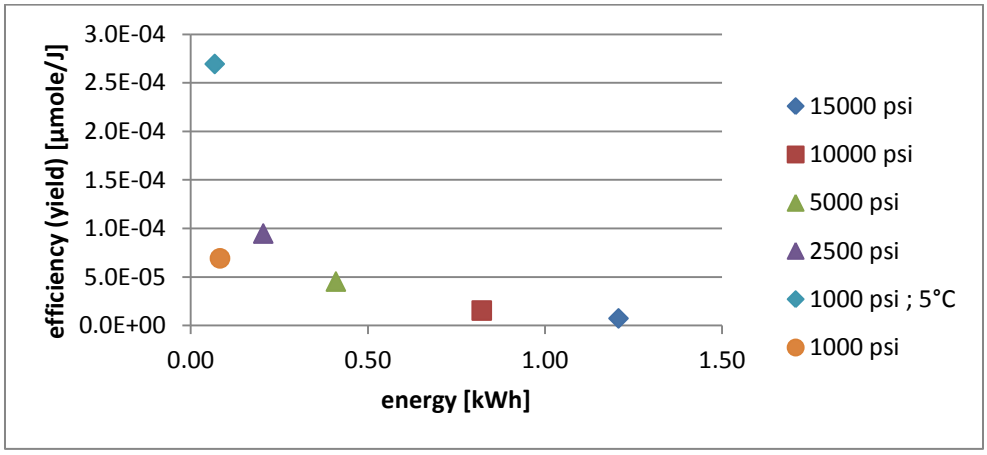

Figure 17: efficiency vs. energy at 20°C

By comparing the efficiency (yield) with the spent electrical energy (Figure 17), the results in Figure 16 are confirmed. Through decreasing the pressure the efficiency increases.

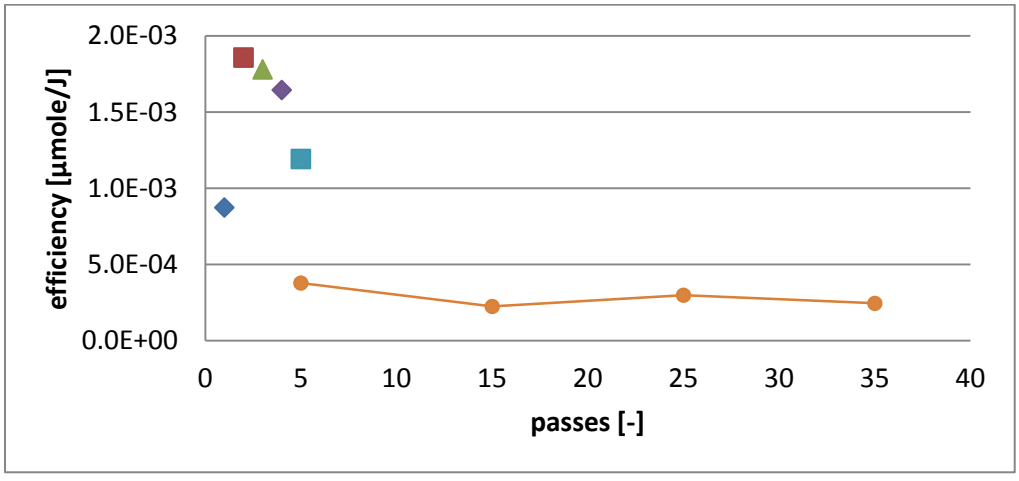

Figure 18: 50 g KI /l; 1000 psi; 20°C; 1-5 passes

A closer look to the big gap from zero to five passes is given in Figure 18. The efficiency increases from the first to the second pass which indicates also the most efficient point of operation. From the third to the fifth pass the efficiency decreases. A reasonable explanation for the gap between the two points at 5 passes is the difference of the starting volumes (450 ml instead of 400 ml). Figure 18 examines the question of how much µmole I_3^- per ml are created over the range of passes and shows a steep increase from the first to the second pass. The HC liberates approximately the same amount of iodine per ml after the second pass as after the fifth pass. From five to 25 passes the generation per ml increases and slightly decreases from 25 passes to 35 passes.

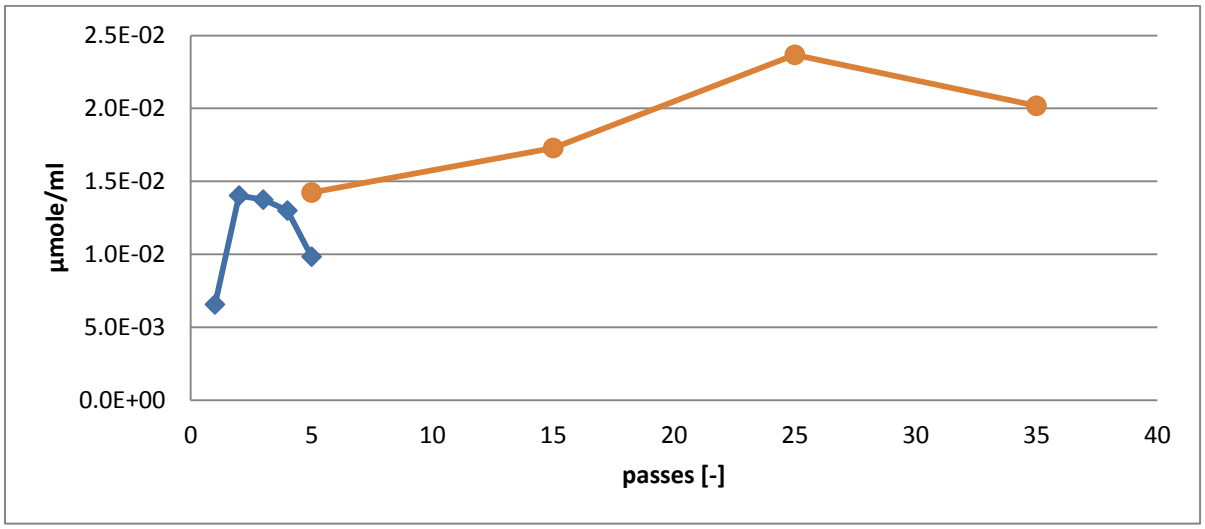

Figure 19: 50 g KI /l; 1000 psi; 20°C;

5.1.4 Liberation of iodine: Comparison HC with UC

Figure 20, Figure 22 and Figure 24 are diagrams for comparing the two different cavitation systems. The following comparison and discussion includes the results of the UC tests. A filled symbol (for example a circle or rectangle) indicates HC. A crossed symbol belongs to UC. The same indication is also applied for Oxidation of sulfite: Comparison HC and UC in 5.2.4 and Degradation of PNP: Comparison HC and UC in 5.3.5.

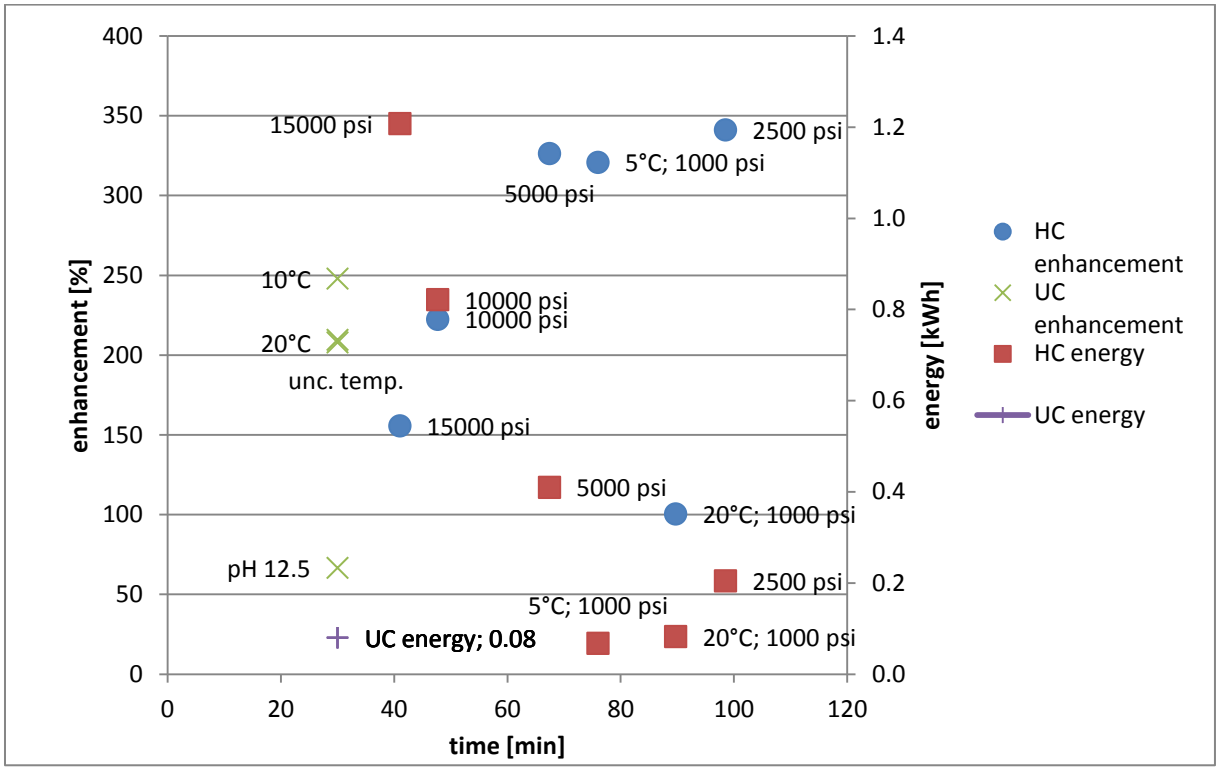

Figure 20: HC vs. UC; without CCl_4; number of passes for the HC data points is converted to treatment time acc. to explanation in section 5.1.1;

The results for the UC tests indicate that the enhancement increases by decreasing the temperature. This effect has already been observed with the HC system. The HC tests with a pressure of 2500 and 5000 psi are performed at 20°C and present a higher enhancement than the UC test with the same temperature. At higher pressure and 20°C the enhancement decreases comparing to the UC test with 20°C. HC tests with high pH are because the UC test with a pH of 12.5 shows practically no enhancement. The energy for all UC tests is the same because of the constant settings for the ultrasonic horn and the time for the sample collection.

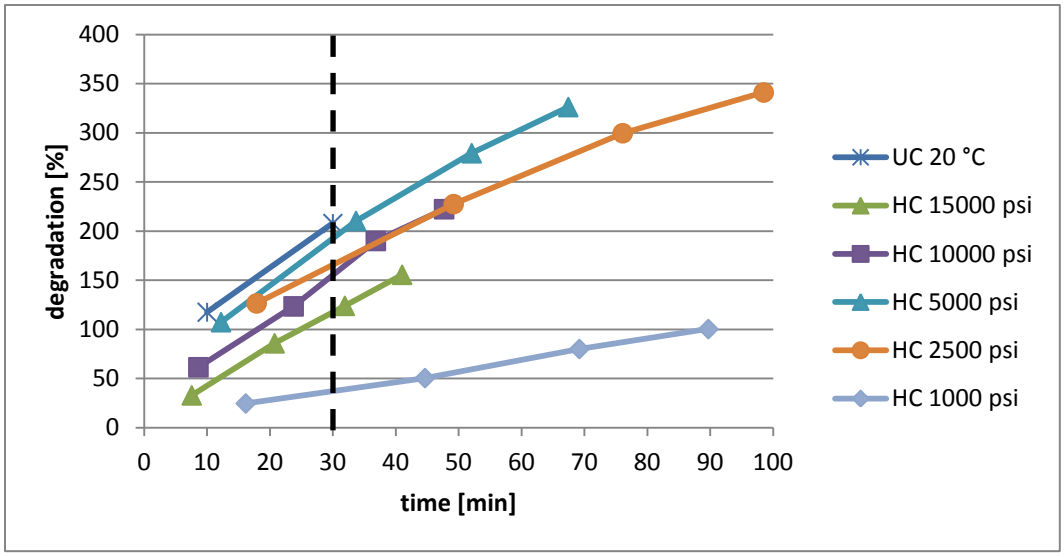

Figure 21: HC vs. UC (all HC tests at 20°C)

The black dotted line in Figure 21 highlights the fact that the UC test shows a better enhancement after 30 minutes than all HC experiments. This could be caused on the one hand by the short retention time in case of HC or on the other hand by the high energy input through the ultrasonic horn.

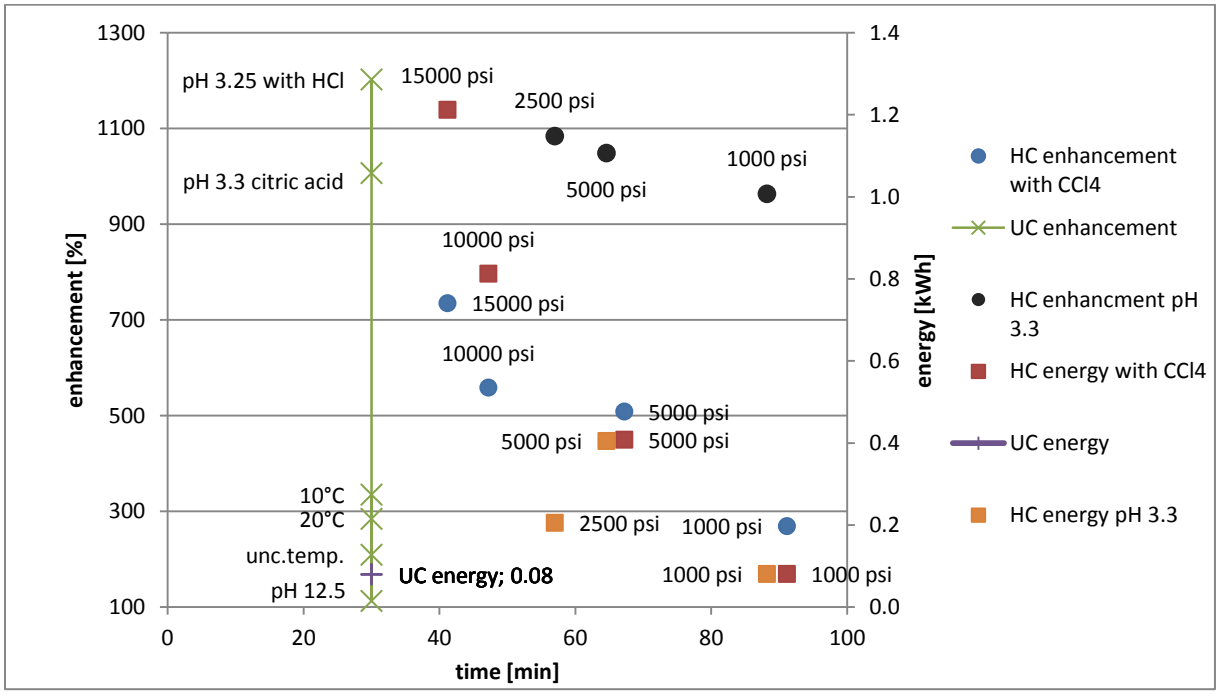

Figure 22: HC vs. UC (with CCl_4 and different pH)

A very interesting fact is represented by Figure 22. The enhancement in case of the low pH, set through citric acid, is for both systems approximately the same. The optimum for the HC system was found with a pressure of 2500 psi. The HC low pH (citric acid) shows an approx. 3 to 4 times better enhancement than at 15000 psi where CCl_4 is added. The discussion referring to UC test with a pH 3.25 (with HCl) can be found on page 52. The adding of CCl_4

or any other chemical in the applied low concentrations does not influence the energy demand. The deviation is due to the slightly different used starting volumes.

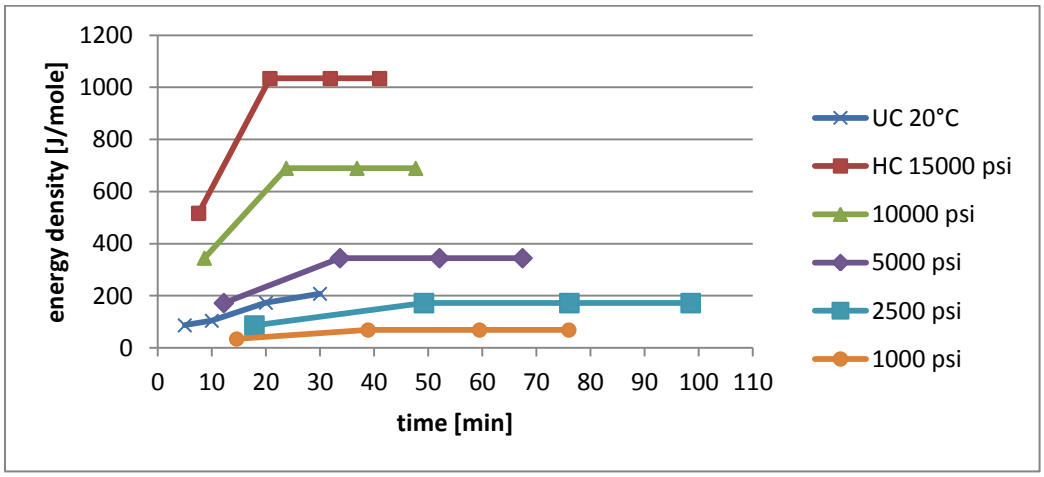

Figure 23: HC vs. UC; energy density

The energy follows the already determined rule, the higher the pressure, the higher the energy density and the costs. The energy density of the UC test is positioned between the HC test with 2500 and 5000 psi. The energy input during the UC test increases much steeper over time than observed with the HC tests with 1000 and 2500 psi. This finding confirms the literature (Capocelli et al. 2014b, p. 17).

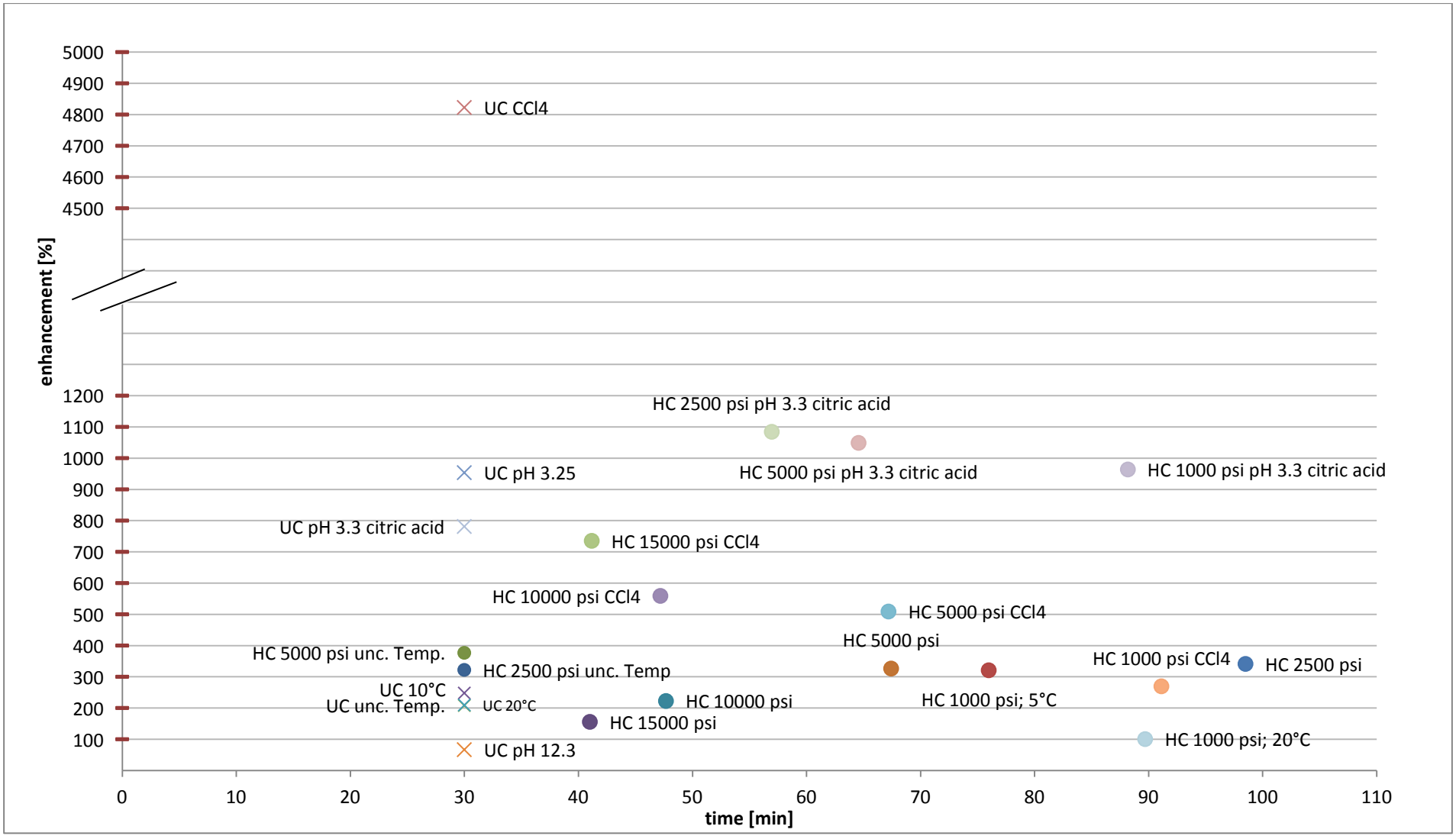

Figure 24: UC vs. HC

An exception is pictured in Figure 24: The pH of 3.25 for the UC test is set through 0.1 M HCl. The use of HCl is not representative because it is a very strong acid and causes concentration gradients in the solution. Beside the supply of H^+ - ions the hydrochloric acid also provides Cl^- - ions, which forms strong radicals under cavitational conditions.[25] Through cavitation chloride radicals are formed which are attacking the potassium iodide to liberate iodine. It should be noticed that the adding of 0.1 M HCl to the starting volume causes a formation of the I_3^- - complex without any cavitation. The effect with 10% citric acid is also given, but the concentration is 3-times smaller which is due to the weaker acid. The coloring increases in both cases with time. A 20-fold increase of I_3^- - production was determined by Suslick (1990) after adding liquid CCl_4 to the solution until saturation. The diagram in Figure 24 is required because of the UC test with CCl_4. It shows that this experiment stands alone with a 48-fold increase of I_3^- - production.

5.2 Oxidation of sulfite

To understand the analytic behind this calculation, it is important to know that the UV/VIS always measures the sulfite (SO_3^{2-}) concentration. The difference between the initial mole of sulfite and the mole of sulfite after the treatment, based on passes or time, are the mole of sulfate (SO_4^{2-}), respectively the oxidation output. The data of the parameters is given below (Table 29 - Table 32) for the series 1.9 - 4.9. The explanation of the identical parameters and calculated values are explained in 5.1. Parameters which are calculated in a different way are explained below the tables.

5.2.1 Oxidation of sulfite: Calculation scheme HC

Table 29: settings

number. series	initial concentration				passes	inlet pressure	orifice dimension	min/ pass	time	time real	time accumulated
	C_0	sample m_{0s}	sample real m_{0Sr}	sample real corr. V_{0src}	Ω	p_i	-	t/Ω	t	t_r	t_{acc}
	mmole /l	g	g	ml	-	psi	thousandths of an inch	min/pass	min	h:mm:ss	min
1.9	25	300	301.4	301.47	5	5000	6/8	1.84	9.2	00:09:12	9.2
2.9		280	280.8	280.87	15			1.71	17.2	00:17:09	26.35
3.9		260	259.3	259.36	25			1.58	15.8	00:15:50	42.18
4.9		240	238.3	238.36	35			1.46	14.6	00:14:33	56.74

[25] see Different pressure and carbon tetrachloride (CCl_4) in 5.1.3.2 for more details

Table 30: measured temperature and concentration

T1 (vessel)	T2 (vessel skin)	T3 (after cav. unit)	T4 (after heat ex)	sample taken at Arisdyne	extinction	concentration SO_3^{2-}	SO_3^{2-} - moles per sample
T11/T12	T21/T22	T31/T32	T41/T42	m_{sAr}	ζ_{HX}	C_{HC}	$n_{SO_3^{2-}}$
°C	°C	°C	°C	g	-	mmole/l	µmole
21.3/20.4	22.2/20.9	29.5/27.4	chiller 20°C	20.6	0.4123	14.58	4093.82
20.4/20.4	20.9/20.9	27.4/27.1		21.5	0.4224	14.95	3877.03
20.4/20.4	20.9/20.9	27.1/27.0		21	0.4475	15.87	3783.81
20.4/20.4	20.9/20.9	27.0/27.1		21.8	0.4487	15.92	3447.25
						25	7536.81

The text “chiller 20°C” in Table 30 (column “T4 (after heat ex)”) means, that a chiller for constant temperature conditions is used. At Arisdyne a scale with a maximum of 20 kg and 1 digit was used to weigh the samples. At CSM an analytical scale with a maximum of 160 g and 4 digits was in action. No back weights were made at CSM. The extinction is realized through measuring the absorbance of the samples with the UV/VIS at a wavelength of 430 nm.[26] The last two rows represent the initial concentration and multiplied with the starting volume, the moles of SO_3^{2-} of the reference solution.

5.2.1.1 SO_3^{2-} - moles per sample

The column “SO_3^{2-} - moles per sample” in Table 30 describes the amount of mole in each sample after certain passes (Equation 50 and Equation 51).

$$n_{SO_3^{2-},initial} = C_0 * V_{0src} = 25 * 10^3 \frac{\mu mole}{l} * 0.30147\ l = 7536.81\ \mu mole \quad \text{Equation 50}$$

$$n_{SO_3^{2-},5passes} = C_{HC} * V_{0src} = 14.58 * 10^3 \frac{\mu mole}{l} * 0.28087\ l = 4093.82\ \mu mole \quad \text{Equation 51}$$

Table 31: calculated production and percentage of oxidation

SO_4^{2-} production	SO_4^{2-} production total	rate of SO_4^{2-} production	rate of SO_4^{2-} production	percentage of oxidation
n_p	n_{ptot}	n_p/Ω	n_p/t	-
µmole	µmole	µmole/pass	µmole/s	%
3442.98	4089.56	688.60	6.24	54.26
216.79		21.68	0.21	
93.22		9.32	0.10	
336.56		33.66	0.39	

[26] see Measuring method for samples in 4.2.2.6

5.2.1.2 SO_4^{2-} - production

The SO_4^{2-} production after certain passes and after 35 passes is calculated with Equation 52 and Equation 53. The different rates of SO_4^{2-} production are calculated the same way as described in 5.1.1.15 for the liberation of iodine.

$$n_p = n_{SO_3^{2-},initial} - n_{SO_3^{2-},5passes} \qquad \text{Equation 52}$$
$$= 7536.81\ \mu mole - 4093.82\ \mu mole$$
$$= 3442.98\ \mu mole$$

$$n_{ptot} = n_{SO_3^{2-},initial} - n_{SO_3^{2-},35passes} \qquad \text{Equation 53}$$
$$= 7536.81\ \mu mole - 3447.25\ \mu mole$$
$$= 4089.56\ \mu mole$$

After 35 passes 4089.56 µmole sulfate are created through cavitation.

5.2.1.3 Percentage of oxidation

The percentage of oxidation examines the question of how much of the initial moles of sulfite are oxidized to sulfate through HC. There are two possibilities to calculate the percentage (Equation 54 and Equation 55).

$$percentage\ of\ oxidation = \frac{100}{n_{SO_3^{2-},initial}} * n_{ptot} \qquad \text{Equation 54}$$
$$= \frac{100}{7536.81\ \mu mole} * 4089.56\ \mu mole = 54.26\%$$

$$percentage\ of\ oxidation = 100 - \frac{100}{n_{SO_3^{2-},initial}} * n_{SO_3^{2-},35passes}$$
$$= 100 - \frac{100}{7536.81\ \mu mole} * 3447.25\ \mu mole \qquad \text{Equation 55}$$
$$= 54.26\%$$

More than 50 % of the initial sulfite is oxidized to sulfate over the range of 35 passes at the given pressure of 5000 psi and the temperature of 20°C.

Table 32: calculated power and energy demand and oxidation efficiency

flow rate	power consumption P=$\dot{Q}$*Δp	power consumption total	energy density	energy	energy costs	oxidation efficiency	oxidation efficiency total
$\dot{Q}$	P	P_{tot}	ρ_e	-	11.2 ¢/kWh	O_e	O_{etot}
m³/s	W	W	J/ml	kWh	¢	µmole/J	µmole/J
2.73E-06	94.12	376.47	172.375	0.36	3.99	6.63E-02	3.19E-03
	94.12		344.75			2.24E-03	
	94.12		344.75			1.04E-03	
	94.12		344.75			4.10E-03	

5.2.1.4 Oxidation efficiency

The parameter “oxidation efficiency” in Table 32 is calculated the same way as described for the “liberation efficiency” in 5.1.1.18. It shows how many µmole are oxidized per Joule.

5.2.2 Oxidation of sulfite: Calculation scheme UC

The parameters and values for the sulfite oxidation caused by UC are calculated the same way as for the liberation of iodine in 5.1.2. The relevant differences referring to the experimental setup are the same as for the HC system.[27]

5.2.3 Oxidation of sulfite: Results

Table 33 shows the used pressure, orifice dimensions and temperatures for all tests. The test with an applied pressure of 1000 psi is executed with two different temperatures. An oxidation is an exothermic reaction (ΔH_R is negative) and a temperature increase shifts the equilibrium to the left side. To investigate the performance of the oxidation at higher temperature, 42 °C has been chosen (Figure 28). The temperature T1 in Table 33 is the temperature in the hopper.[28] To get more volume per stroke of the plunger pump through the cavitation unit, orifice dimension 6/8 is used for 2500, 5000 and 15000 psi and dimension 8/12 is used for 1000 psi.

Table 33: settings for HC tests

pressure	orifice dimension	temperature
p_i	-	T1
psi	thousandths of an inch	°C
15000	6/8	20
5000	6/8	20
2500	6/8	20
1000	8/12	20/42

[27] see 4.3.2.2 and the paragraph below 5.2

[28] see flow chart in 4.3.1

The results of the HC tests with different pressures at 20°C are given in Figure 25. At very high pressure (red line, 15000 psi) the system produces about 4000 µmole of SO_4^{2-} after five passes. Lower pressure like 1000, 2500 and 5000 psi causes a total SO_4^{2-} production of about 3500 µmole after 5 passes. After the first 5 passes the cavitation unit produces enough free radicals respectively H_2O_2 to oxidize sulfite to sulfate. It is apparent that in all cases, the production is the highest after 5 passes and drops afterwards. It can be found that after 15, 25 and 35 passes the production is constant for all pressures. The data points at 15 and 35 passes for the tests with 15000 and 2500 psi are missing because of measurement inaccuracy but the general trend is nevertheless warranted.

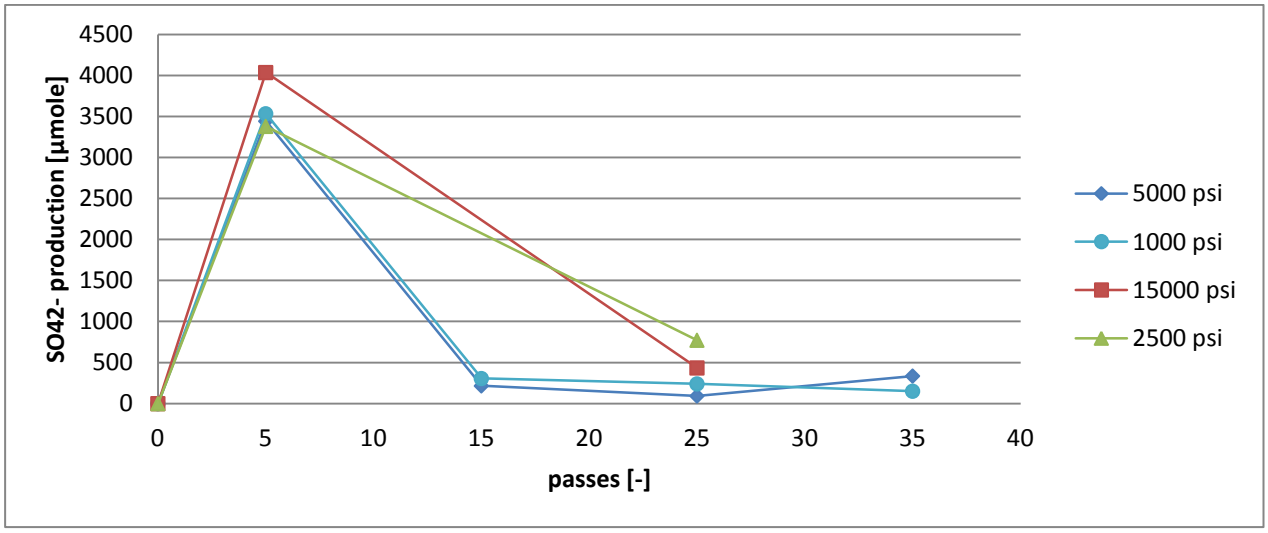

Figure 25: 25 mmole/l; different pressure; 20°C;

It can be observed from Figure 25 that the production or oxidation is the highest at high pressure but the gap between the test with 1000 and 15000 psi is only about 500 µmole[29]. This applied high pressure causes a high electrical input. As predicted and according to Figure 26, the efficiency for 15000 psi is very low. Comparing the data for 15000, 5000 and 2500 psi with 1000 psi from an economical point of view, it is clear that only the lower pressure is acceptable (red line, 1000 psi).

[29] see High pressure and low pressure in 3.2.3

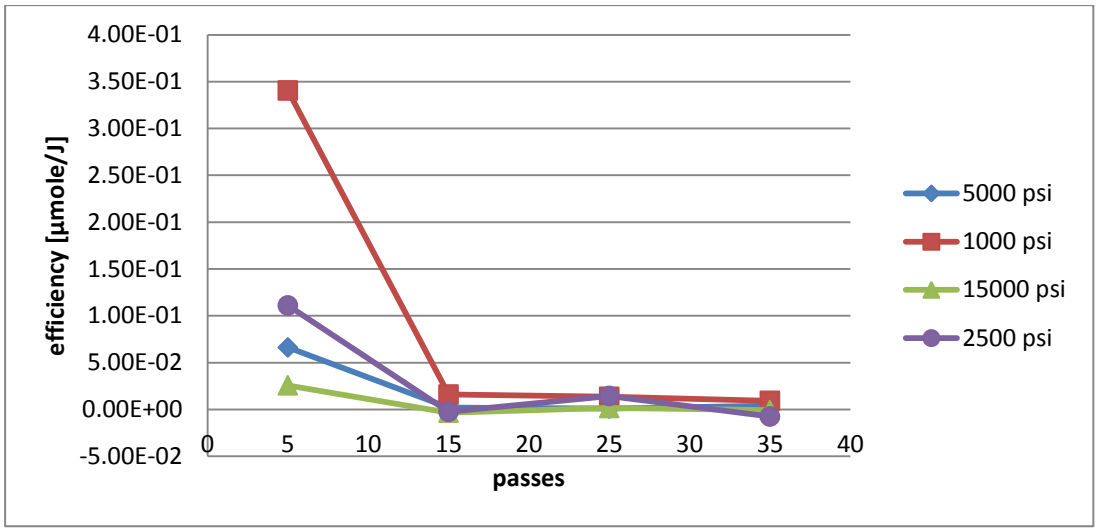

Figure 26: 25 mmole/l; different pressure; 20°C;

The data in Figure 25 and Figure 26 suggest stopping the treatment after 5 passes. For industrial applications, where huge waste water volumes have to be treated, every circulation creates costs. It is useful to take a closer look at the performance of the treatment after the first, second, third, fourth and fifth pass. The results of this investigation are given in Figure 27. The efficiency after 1 pass is higher than the efficiency after 5 passes because of the very low electrical power input. The three points in the diagram (blue diamond, grey cross and orange dot) represent one experiment. In this test a sample is taken after every pass of the initial volume and stopped after the fifth pass. Two data points are missing because of measurement inaccuracy. The red line in Figure 27 presents an independent test with the same parameters. For both tests the efficiency after 5 passes matches within the measurement uncertainty. Generally speaking, a treatment with more than 5 passes can be excluded for future investigations.

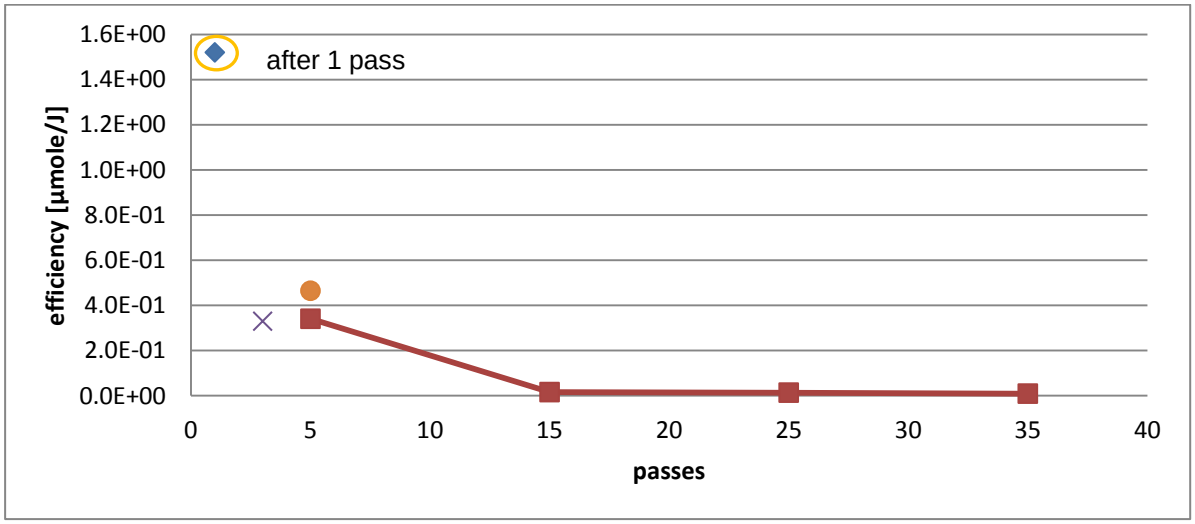

Figure 27: 25 mmol/l; 1000 psi; 20°C

A certain amount of energy has to be supplied for a successful homolytic dissociation of water and further for the oxidation from sulfite to sulfate[30]. The required electrical energy input and the output as percentage of oxidation of the initial amount can be observed in Figure 28. At a pressure of 1000 psi and 20°C the oxidation has the highest value because at low inlet pressure the cavities have more time to generate free radicals[31]. A temperature increase from 20 to 42°C leads to no improvement of the reaction which is in good agreement with Le Chatelier's principle. On the whole, low pressure (5000, 2500 and 1000 psi) shows better results than high pressure. In consideration of the energy aspect, the application of high pressure, respectively 15000 psi can be excluded without any concerns.

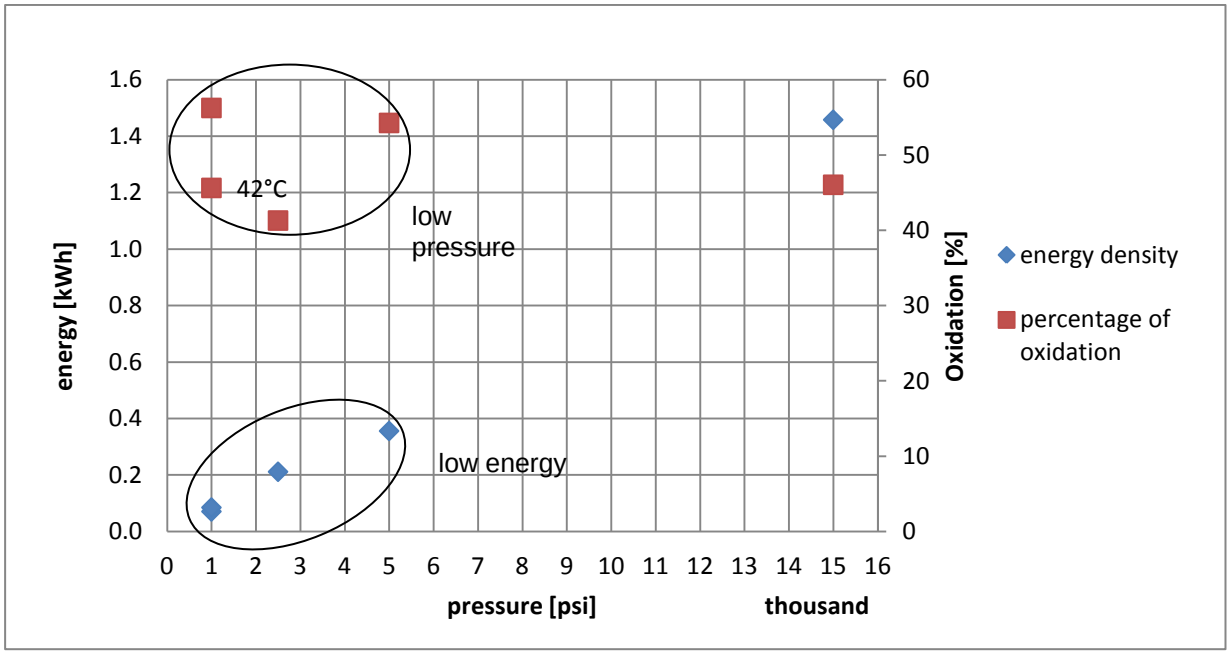

Figure 28: 25 mmol/l; different pressure; 20°C (except one test with 42°C); ; number of passes for the HC data points is converted to treatment time acc. to explanation in section 5.1.1;

[30] see 4.1.1.2 for more information about the oxidation

[31] see 0 for more information about the different impacts on cavitation of high and low pressure

The findings in Figure 28 are confirmed through Figure 29. The test with 1000 psi shows the best efficiency and simultaneously lowest energy consumption.

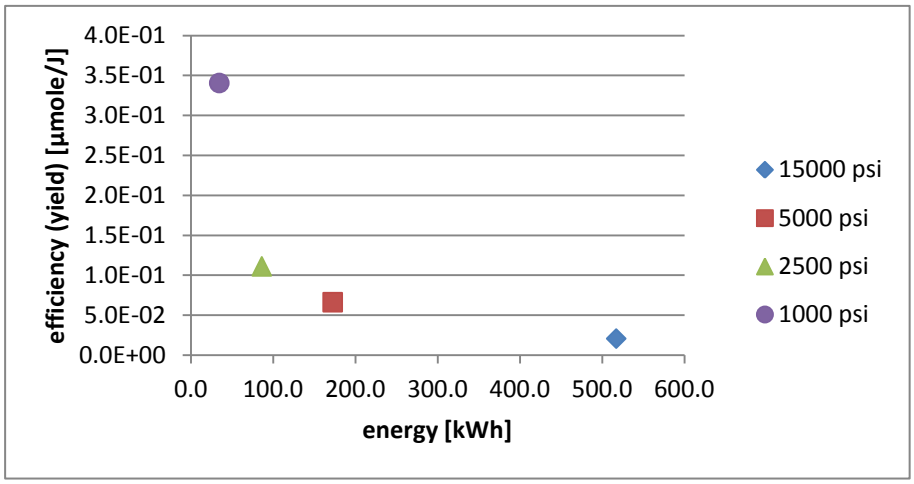

Figure 29: different pressure; 25 mmol/l; 20°C

Additionally to the efficiency and related energy, the rate of the SO_4^{2-} production is of interest. As it can be seen from Figure 25, all tests show the highest number of produced µmole after the first 5 passes. According to this fact, Table 34 shows very high rates after 5 passes comparing to the other rates after more passes. A few cells are empty because of the measurement inaccuracy but the tendency is still the same in every test. The highest rate is presented by the test with 15000 psi. The application of this high pressure for further tests can be excluded because of the small additional gain between this test and the one with 1000 psi (approx. 45 µmole per pass) and the very high energy consumption.

Table 34: rate of SO_4^{2-} - production

passes	rate of SO_4^{2-} production	rate of SO_4^{2-} production	rate of SO_4^{2-} production	rate of SO_4^{2-} production
Ω	n_p/Ω	n_p/Ω	n_p/Ω	n_p/Ω
-	µmole/pass	µmole/pass	µmole/pass	µmole/pass
5	751.36	688.60	675.99	706.70
15	-	21.68	-	30.65
25	51.12	9.32	77.28	24.08
35	-	33.66	-	15.16

Referring to several literature references like Morison, K. and Hutchinson, C. 2009, p. 182 or Chakinala et al. 2008, p. 166 , the more common way to describe the generation rate is in µmole per time unit, as illustrated by Figure 30. The graphs show the same courses as the values in Table 34 because µmole per seconds is just a different representation method for µmole per passes. Comparison of Figure 29 with Figure 30 shows that the generation rate is approx. 2 µmoles per second increased with the pressure of 15000 psi.

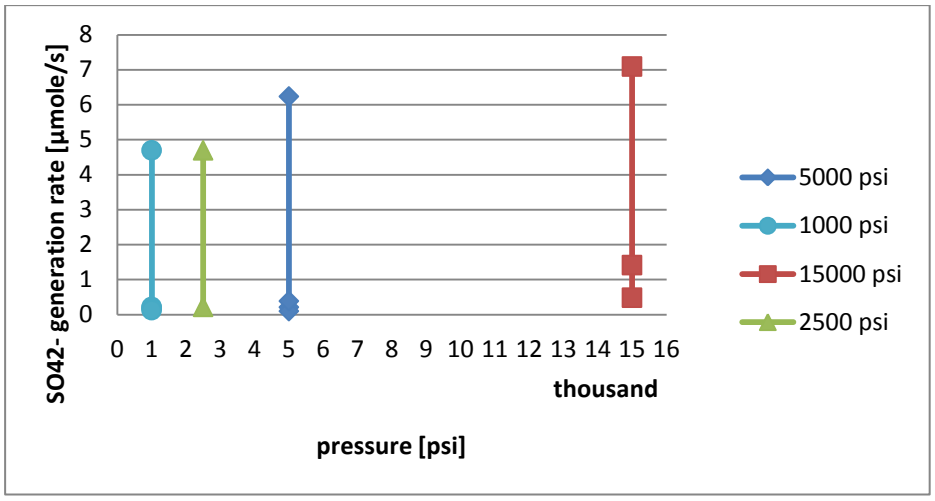

Figure 30: SO_4^{2-} generation rate; 25 mmole/l; different pressure; 20 °C

5.2.4 Oxidation of sulfite: Comparison HC and UC

In this section, the two used cavitation systems are compared and the results of the UC tests are added (Figure 31).

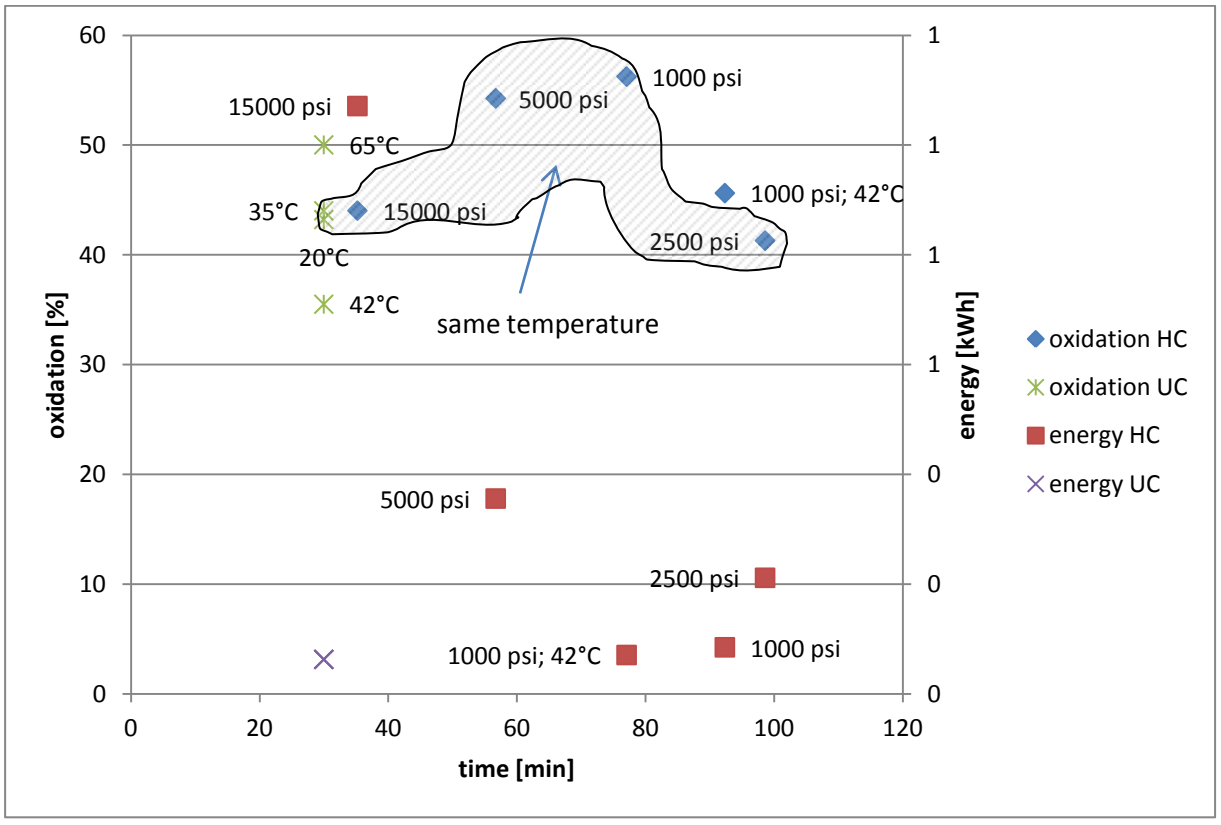

Figure 31: 25 mmole/l; HC tests with different pressure at 20°C; UC tests with different temperature

The data points within the marked area in Figure 31 allow a comparison of the oxidation performance of the HC - system with the UC - system under the same temperature conditions. Inspection of Figure 31 indicates a further improvement of the oxidation

performance of the UC tests by increasing the temperature from 35 to 65°C and deterioration with a temperature of 42°C. Under HC conditions the tendency occurs to be the opposite. Even the UC test with 65°C is not able to reach the performance of the HC test with 1000 psi at 20°C. The energy for all UC tests is the same because of the constant treatment settings. The energy for the HC system follows the already known course - high pressure causes a high energy demand.

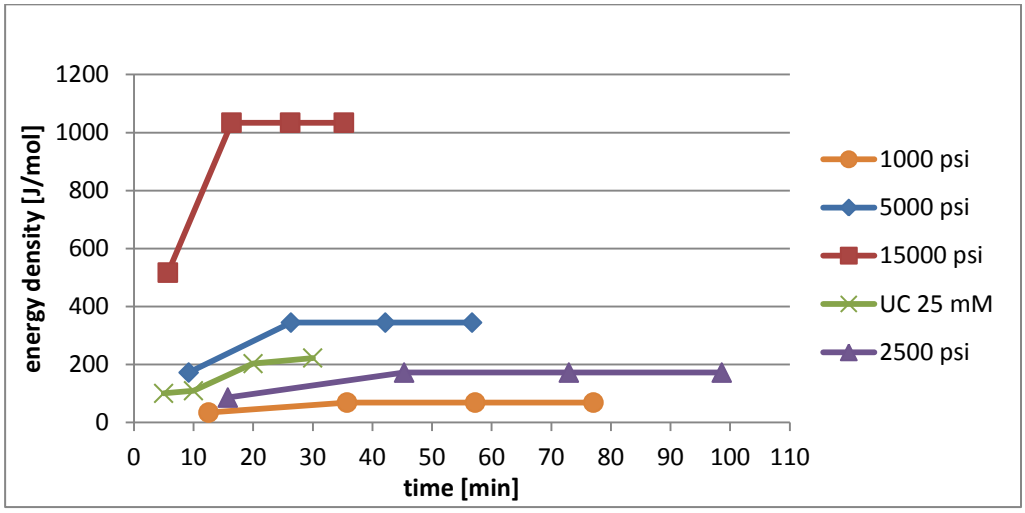

Figure 32: 25 mmole/l; HC with different pressure and UC at 20°C

The UC test with 20 °C can be found, referring to energy density, between the HC tests with high and low pressure.

5.3 Degradation of PNP

The UV/VIS measures the PNP concentration and the difference between the initial mole of PNP and the mole of PNP after the treatment, based on passes or time, are the removed or metabolized mole of PNP respectively the oxidation output. The data of the different parameters is given below (Table 35 - Table 39) for the example series 1.5 - 4.5.

5.3.1 Degradation of PNP: Calculation scheme HC

The parameters and values are calculated the same way as for the liberation of iodine in 5.1.1. Explanations for new parameters can be found below each specific table.

Table 35: settings

number .series	initial concentration				passes	inlet pressure	orifice dimension	min/ pass	time	time real	time accumulated
	C_0	sample m_{0s}	sample real m_{0Sr}	sample real corr. V_{0src}	Ω	p_i	-	t/Ω	t	t_r	t_{acc}
	µmole/l	g	g	ml	-	psi	thousandths of an inch	min/ pass	min	h:mm:ss	min
1.5	25	400	400	401.4	5	1000	8/12	3.34	16.7	00:16:43	16.72
2.5		350	350.8	352	15			2.93	29.3	00:29:20	46.06
3.5		300	300	301	25			2.51	25.1	00:25:05	71.14
4.5		250	247	247.8	35			2.07	20.7	00:20:39	91.79

Table 36: measured temperature and concentration

T1 (vessel)	T2 (vessel skin)	T3 (after cav. unit)	T4 (after heat ex)	sample taken at Arisdyne	pH1	pH2	extinction	concentration of PNP	PNP left in the samples
T11/T12	T21/T22	T31/T32	T41/T42	m_{sAr}	-	-	ζ_{HX}	C_{HC}	n_{PNP}
°C	°C	°C	°C	g	-	-	-	µmole/l	µmole
20.8	21.1	23.1	chiller 20°C	49.2	6.9	11.1	0.4327	23.41	8.24
20.4	20.9	23		50.8	7	11.1	0.4347	23.52	7.08
20.3	20.8	22.7		53	6.9	11.1	0.434	23.48	5.82
20.3	20.8	22.7		50	6.9	11.1	0.4323	23.39	4.63

As mentioned in 4.1.2.1, PNP is very sensitive when the pH changes. The absorbance at a wavelength of 400 nm is measured with a UV/VIS.[32] Kalumuck (2000, p. 467) reports that the pH of the solution has to be set to 11 and refers to the study of Hua et al. (1995, p. 2336). In their study they prefer a pH of approx. 12. In this study the pH is set between 11 and 12. The

[32] see Measuring with the UV/VIS in 4.2.3.4

parameters “pH1” and “pH2” in Table 36 describe the pH directly after the treatment and after adding NaOH to increase the pH.

5.3.1.1 PNP - left in the samples

The column “PNP left” in Table 36 describes the amount of mole which stays in each sample after certain passes (Equation 56). The variable $n_{PNP,5passes}$ examines the question of how many µmole are left in the solution after for example 5 passes. The volume $V_{0src,2.5}$ is the solution volume after 5 passes and also after the sample was taken. The number 2.5 is the name of the series (Table 35).

$$n_{pNP,5passes} = C_{HC} * V_{0src,2.5} = 23.41 \frac{\mu mole}{l} * 0.352\ l = 8.24\ \mu mole \qquad \text{Equation 56}$$

To review the initial concentration, a random sample from one of the initial solutions was taken. The result is listed in Table 37 and they confirm the calibration chart (Figure 8 in 4.2.3.5). The little deviation of the calculated and measured concentration is because of the measurement uncertainty of the UV/VIS (~0.4 %).

Table 37: 25 µmole/l; control of the initial solution

calculated concentration	pH1	pH2	extinction	measured concentration
C_0	-	-	ζ_{HC}	$C_{HC,initial}$
µmole/l	-	-	-	µmole/l
25	6.25	11.00	0.464	25.0967

Table 38: calculated PNP degradation and percentage of degradation

PNP degradation	PNP degradation total	rate of PNP degradation	rate of PNP degradation	percentage of degradation	percentage of degradation total
n_{deg}	n_{degtot}	n_{deg}/t	n_{deg}/Ω	-	-
µmole	µmole	µmole/s	µmole/pass	%	%
1.83	5.44	1.83E-03	3.66E-01	18.18	54.06
1.16		6.60E-04	1.16E-01	29.71	
1.26		8.37E-04	1.26E-01	42.22	
1.19		9.62E-04	1.19E-01	54.06	

5.3.1.2 PNP degradation

The PNP degradation after the first five passes is calculated with Equation 57. $n_{PNP,initial}$ bases on the values from Table 37 and is used as reference for every series respectively for the degradation after certain passes. Equation 57 implies the procedure for the other passes. 1.83 µmole and 1.16 µmole are the amount of µmole which are removed or metabolized after 5 and 15 passes. The different rates of PNP production are calculated identically as described in 5.1.1.15 for the liberation of iodine.

$$n_{deg,5\ passes} = n_{pNP,initial} - n_{pNP,5\ passes}$$
$$= (C_{HC,initial} * V_{0src,1.5}) - n_{pNP,5\ passes}$$
$$= \left(25.0967\ \frac{\mu mole}{l} * 401.4 * 10^{-3} l\right) - 8.24\ \mu mole$$
$$= 1.83\ \mu mole$$

Equation 57

$$n_{deg,15\ passes} = n_{pNP,5passes} - n_{pNP,15passes}$$
$$= 8.24\ \mu mole - 7.08 \mu mole = 1.16\ \mu mole$$

Equation 58

After 35 passes 5.44 µmole PNP are removed in total through HC (n_{degtot}).

5.3.1.3 Percentage of degradation

The initial amount of µmole PNP is the same within one series. In this case (1.5 - 4.5) it is 401.4 ml multiplied with the reference concentration (Table 37). With Equation 59 the degradation regarding to the initial amount after 5 passes is calculated.

$$percentage\ of\ degradation\ after\ 5\ passes$$
$$= \frac{100}{n_{pNP,initial}} * n_{deg,5\ passes}$$
$$= \frac{100}{\left(25.0967 \frac{\mu mole}{l} * 401.4 * 10^{-3} l\right)} * 1.83\ \mu mole$$
$$= 18.18\%$$

Equation 59

The total percentage of degradation describes how much of the initial mole of PNP are removed through cavitation (Equation 60).

$$percentage\ of\ degradation\ total = \frac{100}{n_{pNP,initial}} * n_{degtot}$$
$$= \frac{100}{\left(25.0967 \frac{\mu mole}{l} * 401.4 * 10^{-3} l\right)} * 5.44\ \mu mole$$
$$= 54.06\%$$

Equation 60

More than 50 % of the initial PNP is removed or metabolized after 35 passes at the given pressure of 1000 psi and the temperature of 20°C.

Table 39: calculated power demand, energy costs and efficiency of degradation

flow rate	power consumption P=$\dot{Q}$*∆p	power consumption total	energy density	energy	energy costs	degradation efficiency	degradation efficiency total
$\dot{Q}$	P	P_{tot}	ρ_e	-	11.2 ¢/kWh	D_e	D_{etot}
m³/s	W	W	J/ml	kWh	¢	µmole/J	µmole/J
2.00E-06	13.79	117.22	34.475	0.18	2.01	1.32E-04	8.43E-06
3.00E-06	20.69		103.425			3.19E-05	
5.00E-06	34.48		172.375			2.43E-05	
7.00E-06	48.27		241.325			1.99E-05	

5.3.1.4 Degradation efficiency

The parameter "degradation efficiency" D_e in Table 39 is calculated with Equation 61. It shows how many µmole are removed per Joule.

$$D_e = \frac{n_{deg,5\ passes}}{P * t} = \frac{1.83\ \mu mole}{13.79\ W * 16.72 * 60\ s} = 1.32 * 10^{-4}\ \frac{\mu mole}{J}$$ Equation 61

5.3.2 Degradation of PNP: Calculation scheme UC

The results for the PNP degradation caused by UC are calculated the same way as in Liberation of iodine: Calculation scheme UC in 5.1.2. The relevant differences are explained in Liberation of iodine and degradation of PNP in 4.3.2.1.

5.3.3 Degradation of PNP: Results HC

This chapter shows the results of the HC tests and discuses their meaning. Operating parameters are pressure, pH and temperature.

5.3.3.1 Different pressure at 20°C

In this stage of the study tests with the already known range of different pressures are performed to find out the optimal operating pressure. The first aim was to select the one sample which shows the highest yellow intensity[33] through simple optical inspection. The inspection outlined the samples at 2500 psi and 1000 psi as the two relevant candidates.

[33] see Para - Nitrophenol in 4.1.2.1

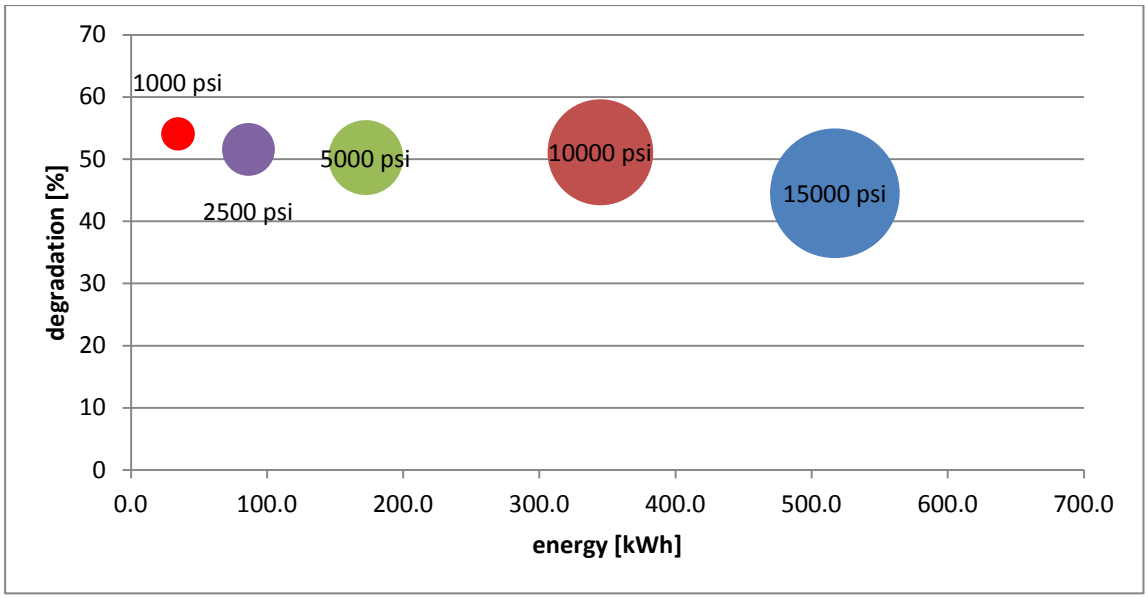

Figure 33: 25 µmole/l; different pressure; 20°C;

After considering the energetic aspect, a decision was made in favor of the sample with 1000 psi. The confirmation that the decision was the right one is given in Figure 33 and Figure 34. As explained in the theory section low pressure causes an increased production of free radicals.[34] The test with an applied pressure of 1000 psi shows a degradation of approx. 54 % and the best degradation efficiency. This result strongly confirms the theory in 0 (see also the explanation below Figure 36).

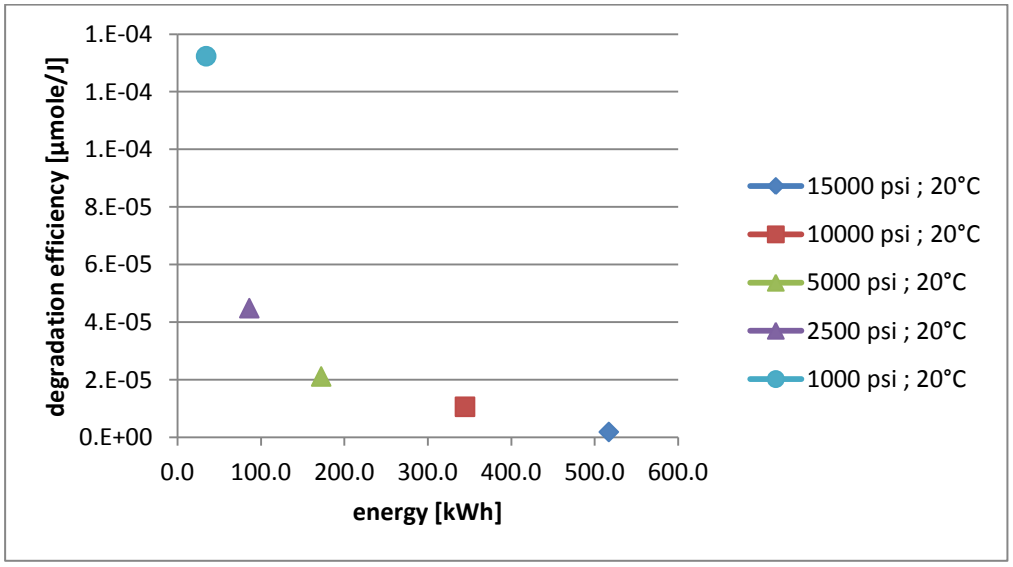

Figure 34: 25 µmole/l; different pressures; 20°C

[34] see chapter 3 for more details and explanations

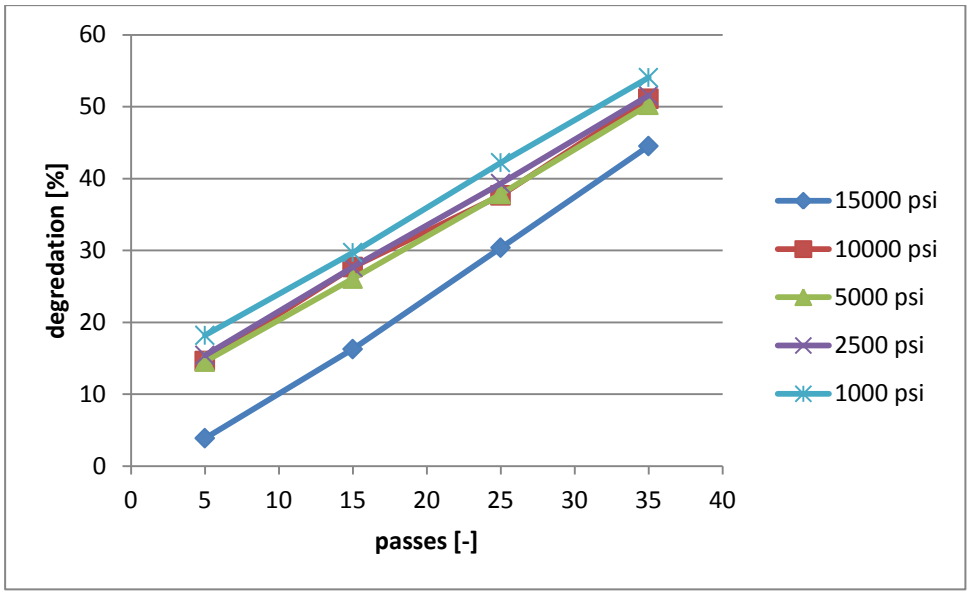

Figure 35: 25 µmole/l; different pressures; 20°C;

In all cases the degradation increases linear from 5 to 35 passes (Figure 35). As reported in chapter 4, the splitting of water through cavitation forms free radicals which attack the benzene ring. The more often the volume runs through the HC loop (Figure 10) the more radicals attack and form intermediate products[35].

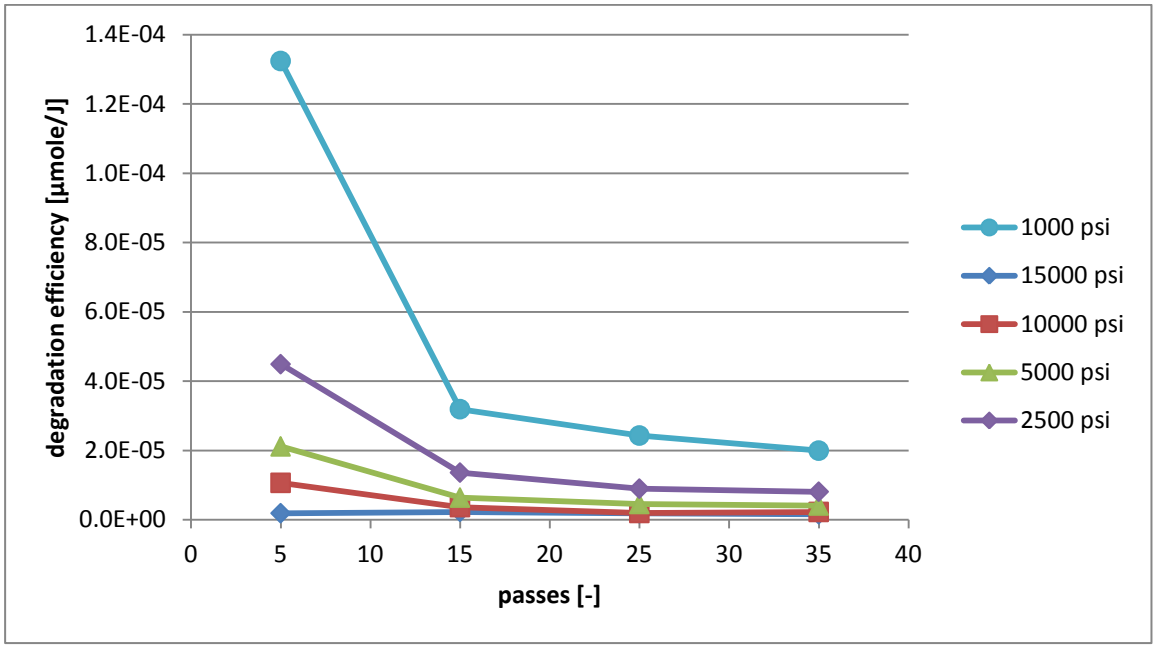

Figure 36: 25 µmole/l; different pressures; 20°C

It is important to reiterate that high pressure means high energy input. It can be identified from Figure 36 and Figure 34 that the test with 1000 psi has the best efficiency. On the whole the efficiency decreases strongly from 5 to 15 passes and flattens from 15 to 35 passes.

[35] see Para - Nitrophenol in 4.1.2.1 for more details about the metabolism of PNP

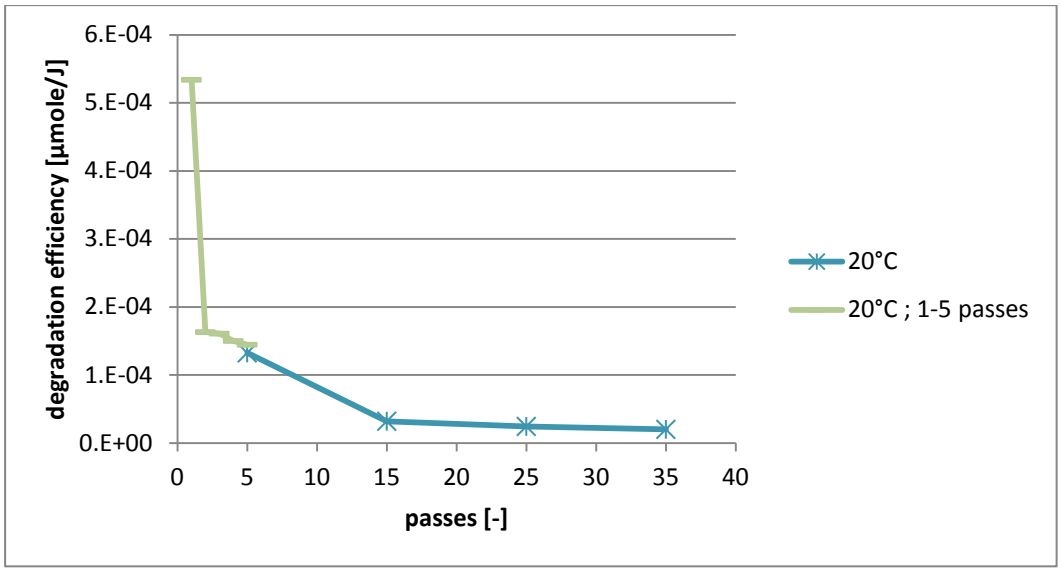

Figure 37: 25 µmole/l; 1000 psi; 20°C; closer look at the first 5 passes;

As already discussed it is very important to minimize the required passes of the volume through the system because a high number of passes of huge volumes causes a high energy demand and therefore creates high costs. Figure 37 shows a closer look at the performance of the cavitation system within the first five passes. It can be observed that the graph peaks after one pass and drops afterwards. After the first pass the cavitation metabolizes more PNP - molecules per Joule as after every following pass. One logical result of this statement would be to stop the treatment after one pass of the volume, which is true if only the energy aspect is considered. By considering the degradation aspect and comparing Figure 35 with Figure 36, it is clear that a longer treatment time means on the one hand a better removal of PNP but on the other hand an increased energy demand.

5.3.3.2 Variable temperature and pH at 1000 psi: degradation efficiency

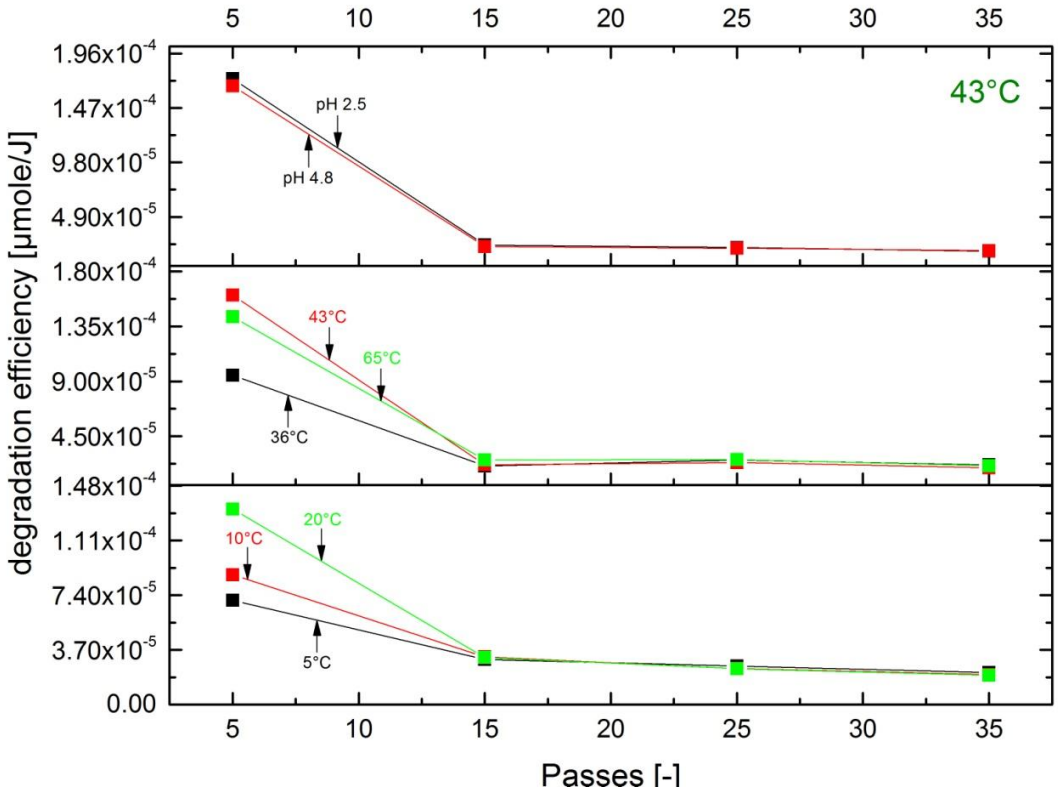

Figure 38: 25 µmole/l; low and high temperature; efficiency at different pH;

All results regarding to degradation efficiency within the predefined passes range can be found in Figure 38. The best results can be observed from layer one with an operating temperature of 43°C and pH of 2.5 or 4.8. Both tests show an efficiency of approx. $1.7 * 10^{-4}$ µmole per Joule. This finding is in good agreement with the work of Kalumuck (2000). At high temperature the test with 43°C in layer two shows a higher efficiency compared to the tests with 36°C and 65°C. At low temperature the test with 20°C in layer three shows better results than the lower temperatures 10°C and 5°C. If the additional energy for heating or cooling is considered, the favorite test is the one with 20°C.

5.3.3.3 Variable temperature and pH at 1000 psi: degradation

The discussion is about the comparison of how many µmole are metabolized after certain passes. From Figure 39 it can be seen that within one test the number of removed PNP molecules is the highest after 5 passes. The number drops to its minimum after 15 passes and slightly increases from 15 to 25 passes and is stable for the last ten passes. This course demonstrates that there is still a removal or degradation of molecules after 35 passes because of the ongoing production of free radicals. The remarkable results in Figure 39 are divided into two parts as follows: Part one contains the tests with 43 °C and pH 2.5 (first layer), 43°C (second layer) and 20°C (third layer). The results from part one are promising if industrial applications are considered (explanation below Figure 37). This investigation found evidence to suggest that the value for the ideal operating temperature is between 20 and

43°C. Compared to the results for the UC tests in 5.3.4, this tendency is quite the opposite and suggests that the metabolization reaction shows a different reaction pattern if the degradation is caused by HC. Further investigations are required to find out more details about the potential metabolization path ways (cf. section 4.1.2.1). Part two contains the rest of the results whereas these tests, performed at higher and lower temperature, can be excluded for further considerations. The tests with a pH of 2.5 and 4.8 are also excluded because compared to the test with 43°C these tests show only an increased degradation of approx. 10 % and the adding of chemicals and additional heating energy decreases the efficiency.

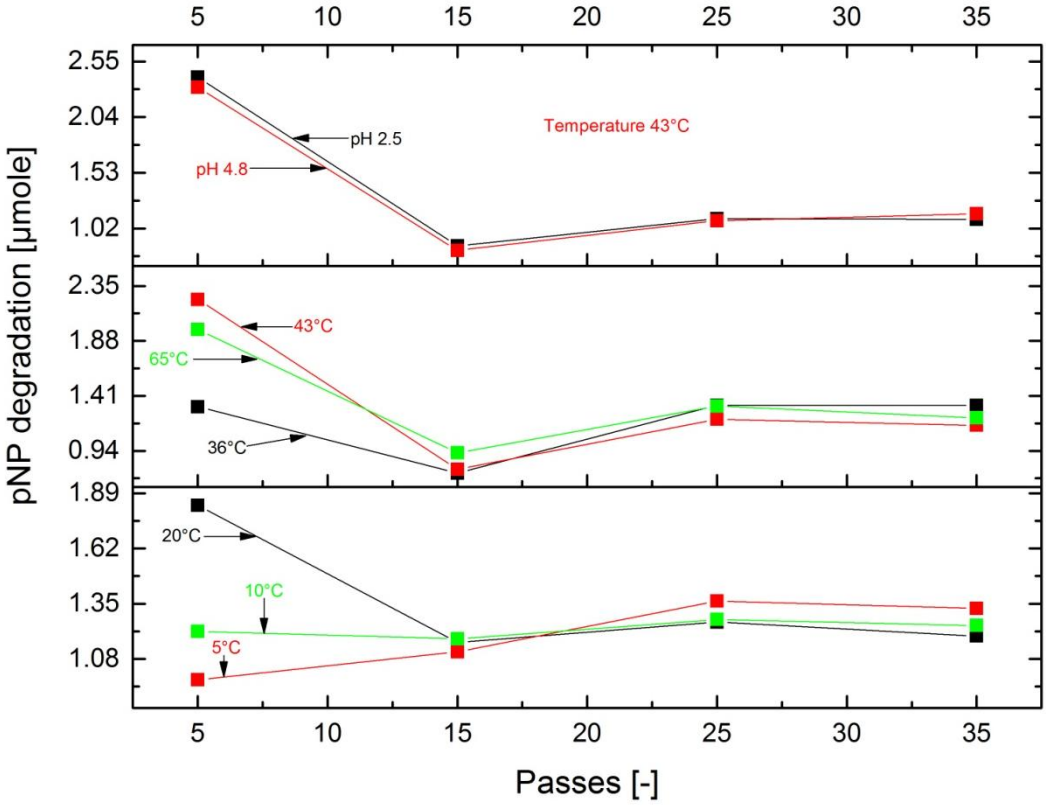

Figure 39: 25 µmole/l; different temperatures and pH

It is apparent that in the majority of cases, HC is able to remove or metabolize more than 40 % of the initial PNP molecules (Figure 40) after 35 passes. This is more than reported by Capocelli et al. (2014a, p. 2571) who reached a removal percentage of 24% with an applied pressure of approx. 65 psi (approx. 0.45 MPa). This is due to the fact that the efficiency and intensity of cavitation strongly depends on the experimental setup and the geometry of the cavitation unit (Gogate (2002, p. 347) and Capocelli et al. (2014a, p. 2566) as well as the operating pressure.

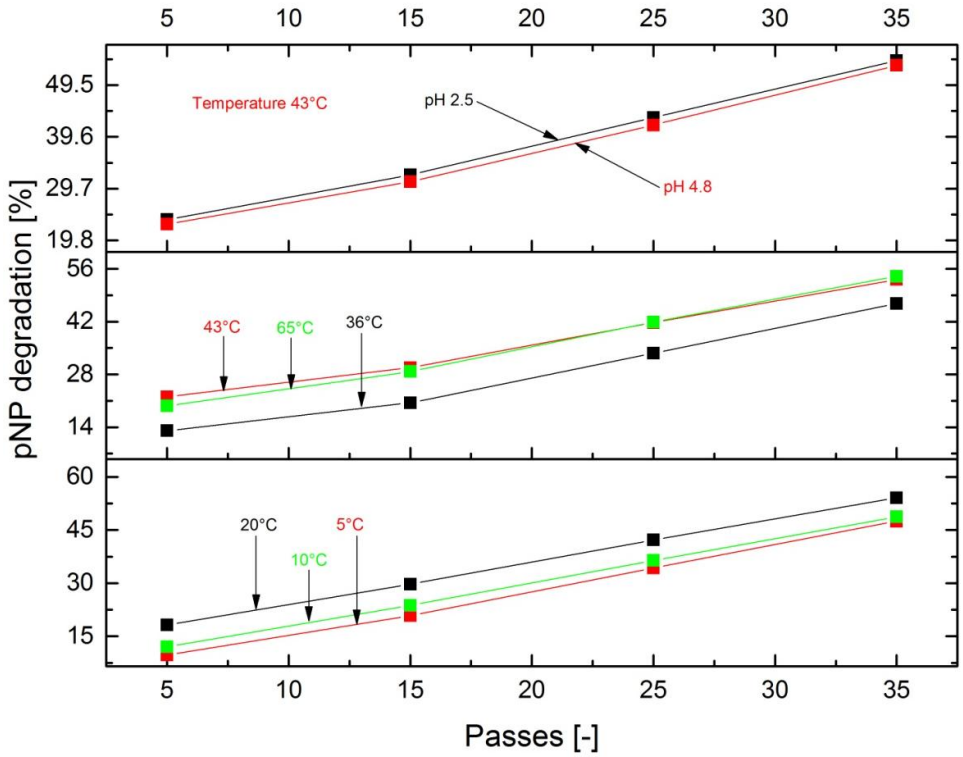

Figure 40: 25 µmole/l; different temperatures and pH

Both tests (Figure 40 - test from layer one with 43°C and pH 2.5 and test from layer three with 20°C) have the same degradation percentage of approx. 50% if the measurement uncertainty and inaccuracy are considered.

5.3.4 Degradation of PNP: Results UC

The results of the tests with the UC system are shown in Figure 41 and Figure 42. The graphs in both figures need further explanation: The first graph in each layer on the left side shows the result of the test for a runtime of 10 minutes. Afterwards a second solution with the same volume for the test with a runtime of 30 minutes is used (second graph on the right side).

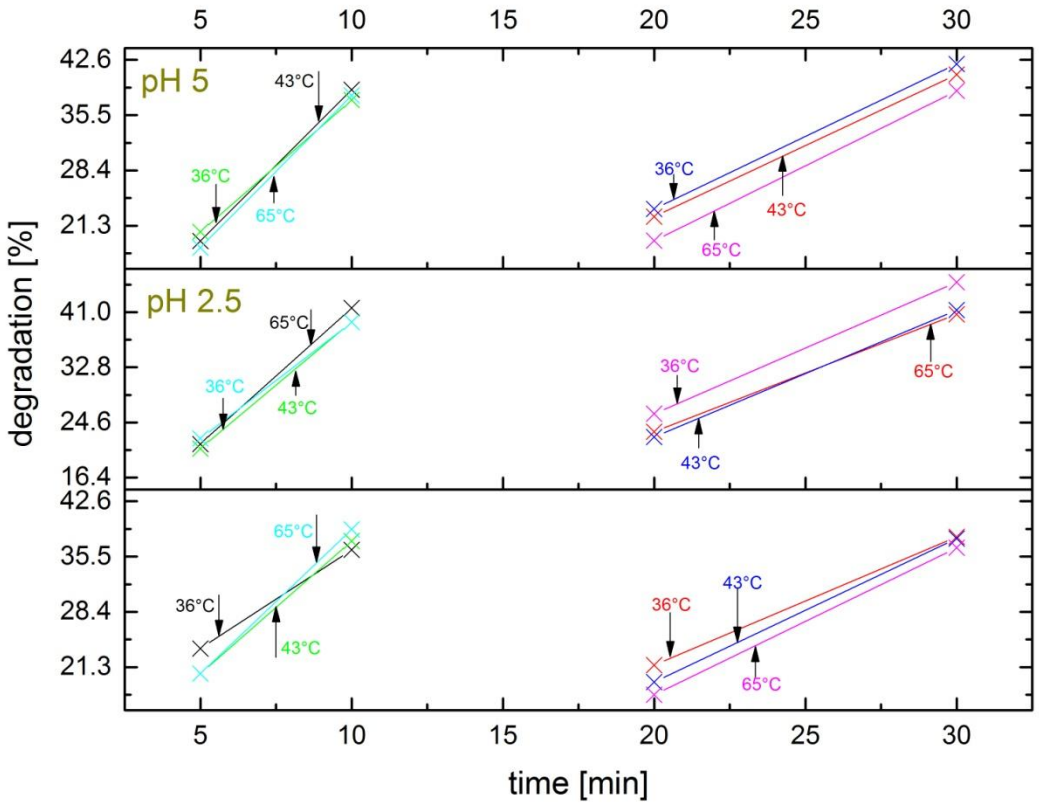

Figure 41: 25 µmole/l; high temperature and different pH

Figure 41 belongs to high temperature conditions and two different pH values. Citric acid (10%) is used to set the pH. Generally speaking there is a strong increase of the degradation over time. Within the period of the first ten minutes approx. 40% are metabolized. Further investigations are needed to explain the fact that in some cases (for example 65°C) the UC is able to remove more of the PNP after ten minutes then after 20 minutes. Measurement uncertainty is only one possibility. With a treatment time of 30 minutes the degradation is in most of the cases higher (approx. 2%) than with a treatment time of 10 minutes. The longer the treatment time, the more PNP molecules are metabolized. Zhang et al. (2003, p. 793) reported that more than 98 % of PNP are removed after 12 minutes by adding hydrogen peroxide into the solution.

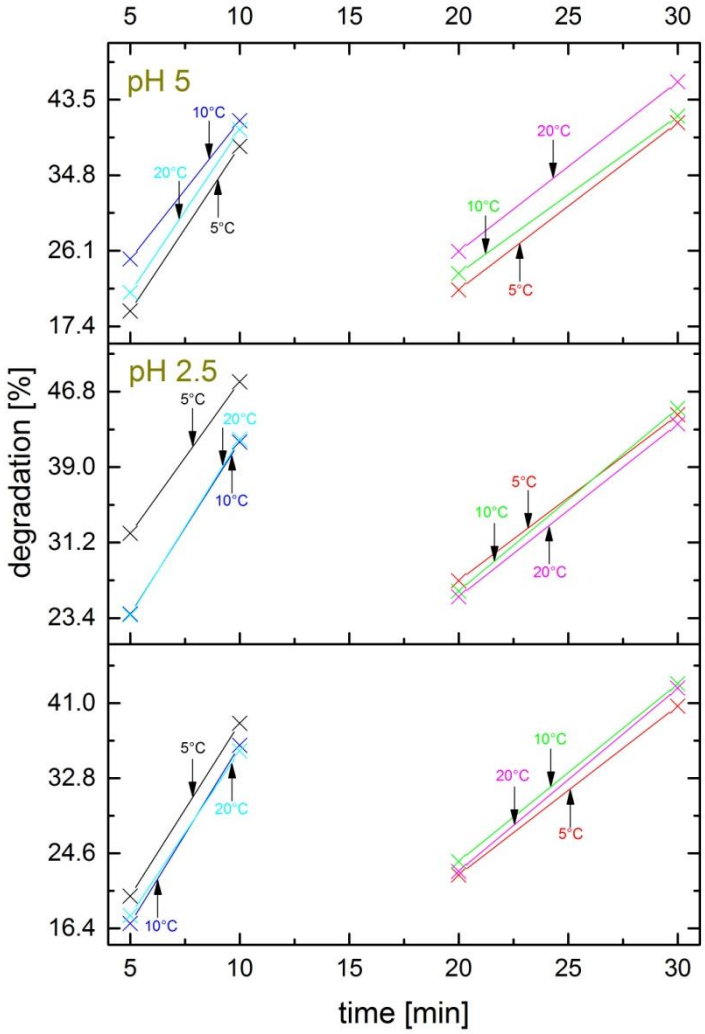

Figure 42: 25 µmole/l; low temperature and different pH

From the labeling in Figure 42 it can be observed that they belong to low temperature conditions and also two different pH values. The required energy for UC is 0.08 kWh for all tests. Comparing Figure 41 and Figure 42 shows that a higher degradation percentage (approx. 45%) is reached at low pH and low temperature because an oxidation is an exothermic reaction and a temperature decrease shifts the equilibrium of the reaction to the products. It is evident from the results that the ultrasonic system shows good results after a short runtime with normal temperature (20°C) conditions and a low pH value.

5.3.5 Degradation of PNP: Comparison HC and UC

For further applications it is important to know which system leads to a better removal of PNP. Energy input and degradation output are the main parameters. The UC system creates a “static” treatment respectively the liquid is not in motion and the only motion comes from the induced ultrasound. In principle the ultrasonic treatment time is equal to the retention time. For the hydrodynamic system the situation is not that transparent. The liquid is always in motion by pumping it through the cavitation unit or the loop. However, the true retention

time, defining the time the liquid actually is under the action of cavitation, is very short.[36] This fact should be always kept in mind when comparing the results of the two systems (Figure 43 - Figure 47).

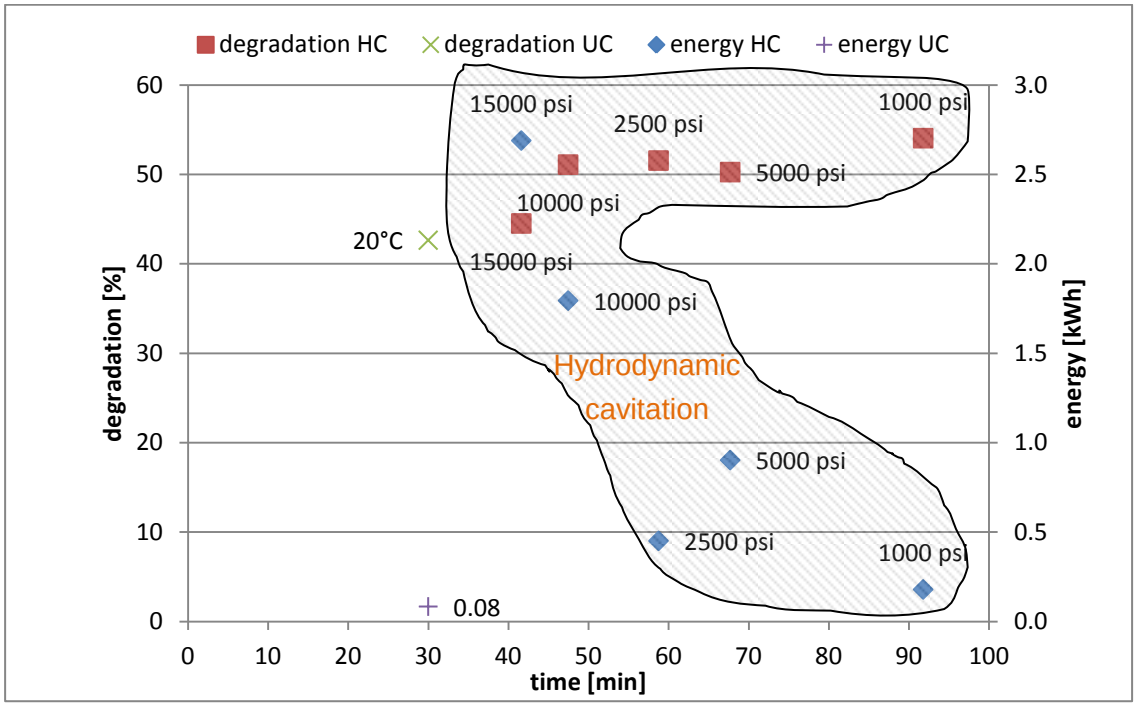

Figure 43: 25 µmole/l; different pressure; 20°C; HC vs. UC

Figure 43 illustrates the comparison of the HC system with different pressures with the UC system at 20°C. Referring to percentage of degradation, the experiment with 1000 psi (54 %) shows approx. a 12 % better degradation than the UC test. As mentioned before the total runtime is 3 times longer with the HC system than with the UC. From the energetically point of view the HC systems follows the already known linear pressure law: High pressure means high electrical power input.

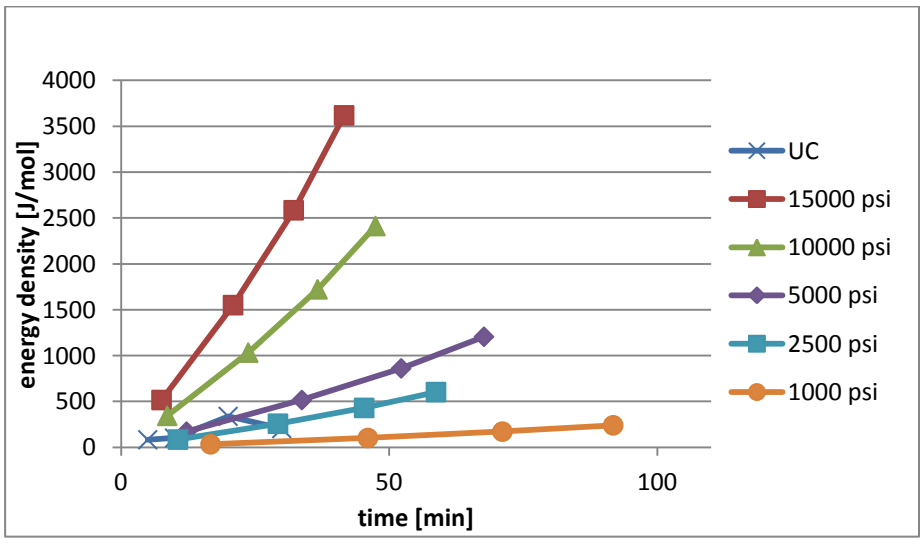

Figure 44: 25 µmole/l; 20°C; HC vs. UC

[36] see also Cavitation unit and retention time in 3.2.1

One of the most important questions to answer is how big is the energy demand of the two systems to remove a certain amount of PNP. Figure 44 displays a comparison between the systems and it is apparent that the UC test has a higher energy density than the HC tests with 2500 and 1000 psi. On the one hand the UC system is able to metabolize about 40 - 45 % of the initial PNP molecules after a short treatment time (30 minutes) but on the other hand it requires a high energy input. At 1000 psi the HC system reaches a degradation of approx. 50% and compared to the UC test energy density is still lower after a treatment time of approx. 90 minutes.
Figure 45, Figure 46 and Figure 47 correspond to different operating parameters which have been tested on both systems. The black dotted line is explained below Figure 47.

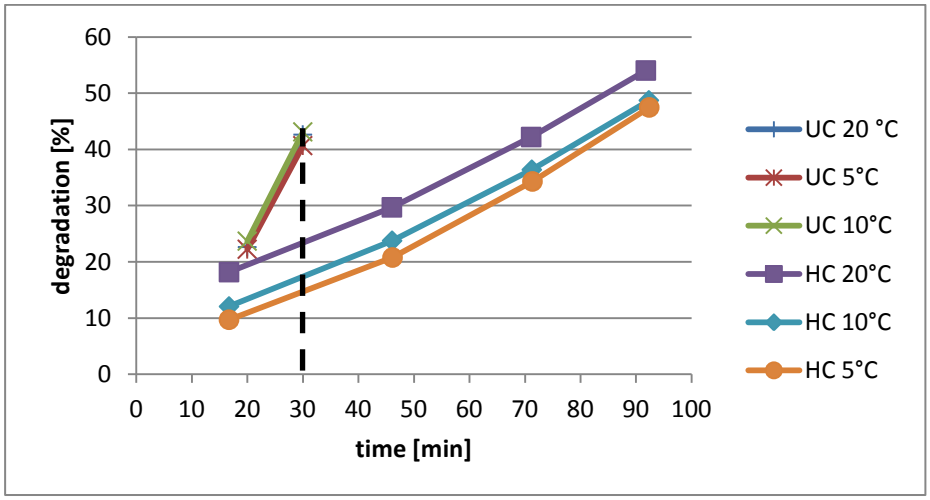

Figure 45: 25 µmole/l; comparison of degradation at low temperature;

Comparing Figure 45 (low temperature) and Figure 46 (high temperature) shows that the UC system works better at low temperatures. The temperature influence in case of HC is negligible because the majority of the experiments show a percentage of degradation of approx. 50 % after 35 passes (displayed as time).

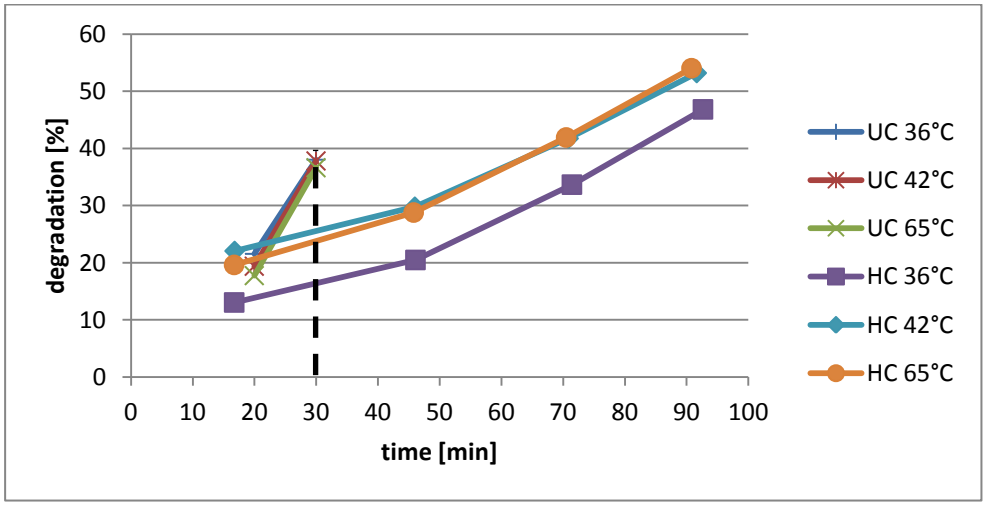

Figure 46: 25 µmole/l; comparison of degradation at high temperature;

For constant temperature conditions an additional aggregate is required. High or low temperature is realized through a heater or a chiller.

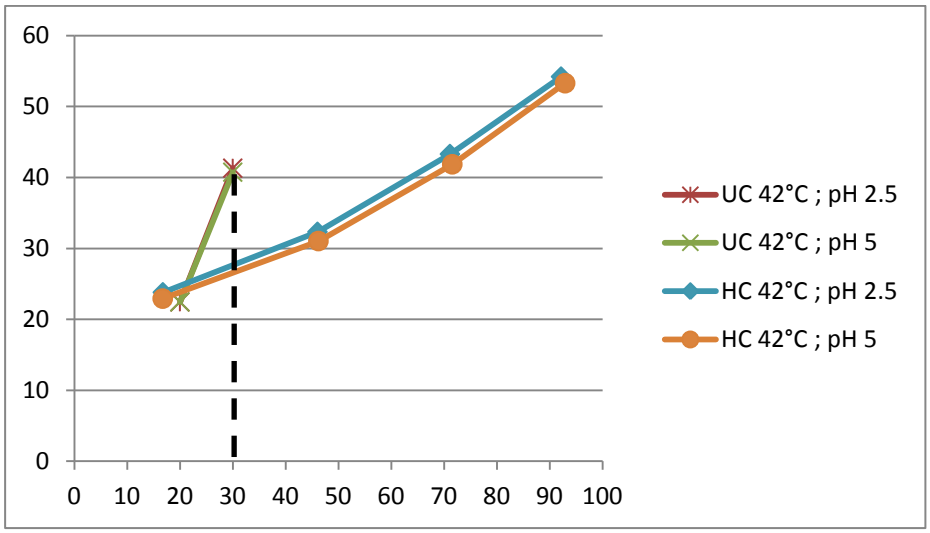

Figure 47: 25 µmole/l; 42°C; different pH;

The black dotted line in all three figures (Figure 45, Figure 46 and Figure 47) should highlight the fact that all UC tests show a much better (approx. 20 %) percentage of degradation after 30 minutes than the HC experiments. This could be caused on the one hand by the short retention time (“true” treatment time) in case of HC and on the other hand by the high energy input through the ultrasonic horn.

Kalumuck (2000) reported a big difference between the application of a pH of 2.5 and 5. In his work the oxidation efficiency is 5 times higher for the test with a pH of 2.5 compared to a pH of 5. Inspection of Figure 38 and Figure 47 indicates that the influence of the pH is not that strong in both of our systems. As mentioned before it is difficult to compare systems which do not have the identically experimental setup.

6 Conclusion

This study confirms the predicted generation of cavitation induced hot spots. Three model reactants, the liberation of iodine (Weissler reaction), the oxidation of sulfite to sulfate and the degradation of PNP are used in two different cavitation systems. The first system generates HC through the patented cavitation unit from Arisdyne systems Inc. which is fully implemented into a closed loop. The second system creates UC through an ultrasonic horn (source of ultrasound) which immerses into a flow cell. Similar setups can be found in pertinent literature (Kumar, P.S. and Pandit, A.B. 1999; Capocelli et al. 2014a, p. 2566). In their studies researchers often used different devices like orifices, high speed homogenizer or venturi pipes to create cavitation. In this study ideal operating conditions within the predefined range are developed through varying parameters like pressure and passes for the HC system and temperature and pH for the UC system. The performed tests on both systems are compared under the same conditions. By comparing the two systems it should be noticed that there is a difference between the treatment and retention times. In case of the UC system, the retention time respectively the time the whole liquid volume actually is treated, equals the total runtime. The retention time in case of HC is much shorter because the HC takes place at a very specific point inside the cavitation unit and only a small fluid volume is affected by cavitation per pass. Beside the retention time the energy aspect has to be considered. The costs rise and the energy efficiency decrease rapidly when a higher pressure or additional heating or cooling is used. The main task is to find a trade - off between additional chemicals, operational energy costs for heating or cooling and reaction output. Further it should be noticed that the total runtime of the HC tests is always higher than of the UC tests. After a total runtime of 30 minutes, the UC tests show a better enhancement, percentage of oxidation[37] and degradation than the HC tests after the same time. As confirmed through previous literature and the results of this study, the energy input is much higher in case of UC. The key results of the three model reactants and the associated reactions are listed in three sections as follows:

Liberation of iodine. The HC tests show better results referring to liberation than the UC tests. The adding of citric acid or in general a decrease of the pH seems to be a very promising application. An 11-fold increase of I_3^- production at a pressure of 2500 psi and a 9.5-fold increase at 1000 psi are reached at 20°C with a pH of 3.3. The adding of any additional chemical to contaminated waste water, as well as probably heating or cooling, creates additional costs. Without any additional supply the HC system reaches a 3.5-fold increase in I_3^- - production at an applied pressure of 2500 psi and an operating temperature of 20°C. Under the same circumstances the UC system reaches only a 2-fold increase.

Oxidation of sulfite. To our knowledge, the data of all this tests are the first of its kind. No reference has been found that describes a sulfite oxidation forced by UC or HC under different conditions (temperature and pressure). Because of the N_2 purge in both systems the experimental setup is unaffected by atmospheric oxygen. This indicates that the oxidation occurs because of the formation of free radicals through cavitation induced hot spots. The

[37] Further tests are required to confirm that statement

main statement of the results is that approx. 50 % of the initial sulfite is oxidized to sulfate at low pressure (1000 psi), room temperature (20°C) and after the first five passes. This finding is promising in terms of developing and investigating possible industrial applications.

Degradation of PNP. The data show that good results (percentage of degradation approx. 50%) can be achieved under economical temperature and pressure conditions like 20°C and 1000 psi. Considering pressure level, it must be indicated however, that comparing the 1000 psi in this study with the pressure used in previous work ((Capocelli et al. 2014a, p. 2568), (Chakinala et al. 2008, p. 167)), 1000 psi is indeed very high. The optimal operating conditions in terms of degradation efficiency are 43°C and a pH between 2.5 and 4.8. The results are in general agreement with previous studies (Capocelli et al. (2014a, p. 2571), Kalumuck (2000)) but the pH influence in the findings is far less sensitive. The study of Zhang et al. (2003, p. 788) outlined that the pH should be in an acidic range.

At 1000 psi the retention time has the highest number (Table 1). This information, the information from 3.2.2, together with the explanations in 0 and 3.3 confirm the results in this study. Future work should focus on the performance at pressure below 1000 psi and long - term tests regarding to time (UC system) and passes (HC system). The maximum possible percentage of liberation, oxidation and degradation should be explored. It is known from the literature ((Gogate et al. 2011, p. 1067; Morison, K. and Hutchinson, C., p. 182) and an accepted fact that there are differences referring to chemism between the upscaling sizes from the lab - scale over the pilot - scale to the operating plant. It is recommended for future work to perform tests on pilot-scale plants to investigate possible deviations to the lab - scale. The findings in this study make it possible to treat water contaminants with controlled cavitation induced hot spots generated by the investigated technology from Arisdyne. The application of HC in the chemical industry has great potential. Future investigations will show if the energy created through cavitation induced hot spots is strong enough to enhance new and emerging fields of application, e.g. the cracking of long-chained hydrocarbons in oil residues.[38]

Some of the aforementioned topics, exemplary the carbon precipitation and the potential interaction of activated carbon with radicals formed by the cavitation still have the status of a current working hypothesis. Further tests are required to investigate the impacts of this effect on possible water treatment applications.

[38] ExxonMobil Research and Engineering Company (EMRE) signed a Joint Development Agreement with Arisdyne Systems Inc. - http://www.businesswire.com/news/home/20150107005688/en/Arisdyne-ExxonMobil-Research-Engineering-Company-Sign-Agreement

7 Directories

7.1 Literature

Publication bibliography

Agency for Toxic Substances and Disease Registry U.S. Public Health Service (1992): Toxicological Profile for Nitrophenols: 2-Nitrophenol and 4-Nitrophenol.

Arisdyne Systems (2015): Technologies. Edited by Arisdyne Systems. Ohio, Cleveland. Available online at http://www.arisdyne.com, updated on 12/8/2015, checked on 12/8/2015.

Avila, Kerstin; Moxey, David; Lozar, Alberto de; Avila, Marc; Barkley, Dwight; and Hof, Björn (2011): The Onset of Turbulence in Pipe Flow. In *Science* 333 (6039), pp. 192–196.

Billinge, B.H.M.; Docherty, Josephine B.; and Bevan, M. J. (1984): The Desorption of Chemisorbed Oxygen from Activated Carbons and its Relationship to Ageing and Methyl Iodide Retention Efficiency. In *Carbon* 22 (1), pp. 83–89.

Boehm, H. P. (2012): Free radicals and graphite. In *Carbon* 50 (9), pp. 3154–3157. DOI: 10.1016/j.carbon.2011.10.013.

Capocelli, Mauro; Musmarra, Dino; Prisciandaro, Marina; Lancia, Amedeo (2014a): Chemical effect of hydrodynamic cavitation: Simulation and experimental comparison. In *AIChE J.* 60 (7), pp. 2566–2572. DOI: 10.1002/aic.14472.

Capocelli, Mauro; Prisciandaro, Marina; Lancia, Amedeo; Dino Musmarra (2014b): Comparison Between Hydrodynamic and Acoustic Cavitation in Microbial Cell Disruption. In *Chemical Engineering Transactions* 38, pp. 13–18. DOI: 10.3303/CET1438003.

Chakinala, Anand G.; Gogate, Parag R.; Chand, Rashmi; Bremner, David H.; Molina, Raúl; Burgess, Arthur E. (2008): Intensification of oxidation capacity using chloroalkanes as additives in hydrodynamic and acoustic cavitation reactors. In *Ultrasonics Sonochemistry* 15 (3), pp. 164–170. DOI: 10.1016/j.ultsonch.2007.02.008.

Chand, Rashmi; Bremner, David H.; Namkung, Kyu C.; Collier, Phillip J.; Gogate, Parag R. (2007): Water disinfection using the novel approach of ozone and a liquid whistle reactor. In *Biochemical Engineering Journal* 35 (3), pp. 357–364. DOI: 10.1016/j.bej.2007.01.032.

d'Agostino, Luca and Salvetti, Maria Vittoria (2007): Fluid Dynamics of Cavitation and Cavitating Turbopumps: Springer Wien New York.

Ellis, Frank (2002): Paracetamol. A curriculum resource. Cambridge: Royal Society of Chemistry.

Gogate, Parag R. (2002): Cavitation: an auxiliary technique in wastewater treatment schemes. In *Advances in Environmental Research* 6 (3), pp. 335–358. DOI: 10.1016/S1093-0191(01)00067-3.

Gogate, Parag R.; Shirgaonkar, Irfan Z.; Sivakumar, M.; Senthilkumar, P.; Vichare, Nilesh P.; and Pandit, Aniruddha B. (2001): Cavitation reactors: Efficiency assessment using a model reaction. In *AIChE J.* (11), pp. 2526–2538.

Gogate, Parag R.; Sutkar, Vinayak S.; Pandit, Aniruddha B. (2011): Sonochemical reactors: Important design and scale up considerations with a special emphasis on heterogeneous systems. In *Chemical Engineering Journal* 166 (3), pp. 1066–1082. DOI: 10.1016/j.cej.2010.11.069.

Gogate, Parag R. and Pandit, Aniruddha B. (2000): Engineering design methods for cavitation reactors II: Hydrodynamic cavitation. In *AIChE J.* Volume 46 (Issue 8), pp. 1642–1649.

Hua, Inez; Höchemer, Ralf H.; Hoffmann, Michael R. (1995): Sonolytic Hydrolysis of p-Nitrophenyl Acetate: The Role of Supercritical Water. In *J. Phys. Chem.* (99), pp. 2335–2342.

Kalumuck, K. M. (2000): The use of cavitating jets to oxidize organic compounds in water. In *Journal of Fluids Engineering (ASME)* (122), pp. 465–470.

Koh, Li Ling A.; Chandrapala, Jayani; Zisu, Bogdan; Martin, Gregory J. O.; Kentish, Sandra E.; Ashokkumar, Muthupandian (2014): A Comparison of the Effectiveness of Sonication, High Shear Mixing and Homogenisation on Improving the Heat Stability of Whey Protein Solutions. In *Food Bioprocess Technol* 7 (2), pp. 556–566. DOI: 10.1007/s11947-013-1072-1.

Kumar, P.S. and Pandit, A.B. (1999): Modeling Hydrodynamic Cavitation. In *Chem. Eng. Technol.* (22), pp. 1017–1027.

Lau, A. C.; Furlong, D. N.; Healy, T. W.; and Grieser, F. (1986): The Electrokinetic Properties of Carbon Black and Graphitized Carbon Black Aqueous Colloids. In *Colloids and Surfaces* (18), pp. 93–104.

Leighton, T.G (1995): Bubble population phenomena in acoustic cavitation. In *Ultrasonics Sonochemistry* 2 (2), pp. S123-S136. DOI: 10.1016/1350-4177(95)00021-W.

Li, Pan; Song, Yuan; Yu, Shuili (2014): Removal of Microcystis aeruginosa using hydrodynamic cavitation: Performance and mechanisms. In *Water Research* 62, pp. 241–248. DOI: 10.1016/j.watres.2014.05.052.

Li, Pan; Song, Yuan; Yu, Shuili; Park, Hee-Deung (2015): The effect of hydrodynamic cavitation on Microcystis aeruginosa: Physical and chemical factors. In *Chemosphere* 136, pp. 245–251. DOI: 10.1016/j.chemosphere.2015.05.017.

Morison, K. and Hutchinson, C. (2009): Limitations of the Weissler reaction as a model reaction for measuring the efficiency of hydrodynamic cavitation. In *Ultrasonics Sonochemistry* 16 (1), pp. 176–183. DOI: 10.1016/j.ultsonch.2008.07.001.

Novikov, A. N. (2014): Heat capacity and density of potassium iodide solutions in mixed N-methylpyrrolidone-water solvent at 298.15 K. In *Russ. J. Phys. Chem.* 88 (10), pp. 1621–1625. DOI: 10.1134/S0036024414100252.

Parag R. Gogate and Abhijeet M. Kabadi (2009): A review of applications of cavitation in biochemical engineering/biotechnology. In *Biochemical Engineering Journal* (Volume 44), pp. 60–72.

Patek, S. N.; Korff, W. L.; Caldwell, R. L. (2004): Biomechanics: deadly strike mechanism of a mantis shrimp. In *Nature* 428 (6985), pp. 819–820. DOI: 10.1038/428819a.

Saharan, Virendra Kumar; Pandit, Aniruddha B.; Satish Kumar, Panneer Selvam; Anandan, Sambandam (2012): Hydrodynamic Cavitation as an Advanced Oxidation Technique for the Degradation of Acid Red 88 Dye. In *Ind. Eng. Chem. Res.* 51 (4), pp. 1981–1989. DOI: 10.1021/ie200249k.

Schlögl, R. and Boehm, H.P. (1988): Photochemical Intercalation in Graphite. In *Synthetic Metals* (23), pp. 407–413.

Suslick, Kenneth S. (1990): Sonochemistry. In *Science* 247 (4949), pp. 1439–1450.

Suslick, Kenneth S.; M. mdleleni, Millan and T. Ries, Jeffrey (1997): Chemistry Induced by Hydrodynamic Cavitation. In *Journal American Chemical Sosiety* (119), pp. 9303–9304.

VDI Heat Atlas (Ed.) (2010). VDI-Gesellschaft Verfahrenstechnik und Chemieingenieurwesen. 2nd ed. Berlin Heidelberg: Springer Verlag.

Wu, Zhilin; Shen, Haifeng; Ondruschka, Bernd; Zhang, Yongchun; Wang, Weimin; Bremner, David H. (2012): Removal of blue-green algae using the hybrid method of hydrodynamic cavitation and ozonation. In *Journal of Hazardous Materials* 235-236, pp. 152–158. DOI: 10.1016/j.jhazmat.2012.07.034.

Xu, S. C.; Irle, S.; Musaev, D. G.; Lin, M. C. (2007): Quantum Chemical Study of the Dissociative Adsorption of OH and H 2 O on Pristine and Defective Graphite (0001) Surfaces. Reaction Mechanisms and Kinetics. In *J. Phys. Chem. C* 111 (3), pp. 1355–1365. DOI: 10.1021/jp066142i.

Zhang, Wenbing; Xiao, Xianming; An, Taicheng; Song, Zhiguang; Fu, Jiamo; Sheng, Guoying; Cui, Mingchao (2003): Kinetics, degradation pathway and reaction mechanism of advanced oxidation of 4-nitrophenol in water by a UV/H2O2 process. In *J. Chem. Technol. Biotechnol.* 78 (7), pp. 788–794. DOI: 10.1002/jctb.864.

7.2 Tables

7.3 Figures